INFORMATION TO USERS

This manuscript has been reproduced from the microfilm master. UMI films the text directly from the original or copy submitted. Thus, some thesis and dissertation copies are in typewriter face, while others may be from any type of computer printer.

The quality of this reproduction is dependent upon the quality of the copy submitted. Broken or indistinct print, colored or poor quality illustrations and photographs, print bleedthrough, substandard margins, and improper alignment can adversely affect reproduction.

In the unlikely event that the author did not send UMI a complete manuscript and there are missing pages, these will be noted. Also, if unauthorized copyright material had to be removed, a note will indicate the deletion.

Oversize materials (e.g., maps, drawings, charts) are reproduced by sectioning the original, beginning at the upper left-hand corner and continuing from left to right in equal sections with small overlaps.

ProQuest Information and Learning
300 North Zeeb Road, Ann Arbor, MI 48106-1346 USA
800-521-0600

S

IONIC INTERACTIONS AND SOLVENT-STRUCTURE EFFECTS IN ADSORPTION AT THE MERCURY ELECTRODE / WATER INTERFACE

by

François Rocheleau

A thesis submitted to the School of Graduate Studies in partial fulfillment of the requirements for the degree of M.Sc. in Chemistry

UNIVERSITY OF OTTAWA
OTTAWA, CANADA, 1978

PREFACE

Since the very schematic model of Von Helmholtz, given in 1861, studies of the double-layer have led to more realistic representations e.g. that by Watts-Tobin and Mott where the ion distribution and solvent orientation at a charged interface was considered in detail. These workers were the first to consider a specific model for the role of solvent (in their case, water) in determining double-layer properties in terms of solvent dipole orientation and the related question of solvent structure.

It has therefore been of interest to study the urea-water system, since urea is known as a "structure breaker", i.e. it modifies the structural and H-bonding equilibria in water. Furthermore, it is of interest to compare the adsorption of urea at Hg with that of the more strongly adsorbed S-analogue, thiourea.

On the other hand, the substitution of water by an organic solvent could, by contrast with water, lead to a better understanding of interfacial

electrochemical phenomena by providing information on solvent adsorption and orientation using a simple, non H-bonded but polar solvent such as acetonitrile.

Finally, studies of adsorption of organic ions such as those of tetraalkylammonium salts can lead to a better understanding of steric and hydrophobic effects in adsorption and hydration at the Hg/water interface. For this purpose, the series of alkylammonium ions, $Pr_nN^+H_{4-n}$, was chosen since it allows the effects of progressive change of hydration, accessibility of charge and hydrophobicity to be studied as n is increased. The adsorption behavior observed can be related to the known hydration properties of this series of ions in aqueous solutions.

ACKNOWLEDGEMENT

The author would like to express his most sincere thanks and gratitude to his research supervisor, Professor B.E. Conway, who directed with generosity and perseverance this research project. Professor Conway was always encouraging and most understanding. It has been an unforgettable experience to work with him, not only because he possesses both great personal knowledge in electrochemistry and ability to supervise research, but also because of his example of perseverance and constant work.

Grateful thanks are also due to J. Currie, H.P. Dhar, J. Klinger (who was of great help in setting up the computer programmes for curve-fitting), D.M. Novak, S. Sharp and other colleagues of the electrochemistry group for their helpful discussions and advice on various occasions.

Technical assistance received from Mr. E. Kristof (in making the drop-time cell) and other workshop staff is also acknowledged with gratitude.

The work of Mrs. Szabo in taking the photographs and preparing some of the diagrams for publication, and of Mrs. M. Storto in typing the thesis, is also gratefully acknowledged.

TABLE OF CONTENTS

LIST OF FIGURES

LIST OF TABLES

ABSTRACT

Studies of the structure and properties of the double-layer at the Hg electrode interface by measurements of the adsorption of urea and of a series of n-propylammonium salts in water, have been carried out by means of electrocapillary measurements using a drop-time tensiometer.

Since the adsorption of surface-active substances at charged interfaces involves solvent displacement, an appropriate adsorption isotherm is chosen in which the relative size ratio x, of adsorbate and solvent is taken into account. The following isotherm was applied to the results obtained in the present work: $Kc = \theta/\exp(x-1)(1-\theta)^x$ or a corresponding one with a lateral interaction term $\exp(-2a\theta)$ included.

Electrocapillary curves were obtained for urea adsorption but did not exhibit the striking adsorption behaviour found experimentally with thiourea in previous work, where a strong Hg-S interaction predominates. Urea was found to adsorb in a more or less perpendicular

orientation to the surface with its C=O group oriented towards the solvent. The Esin and Markov coefficients and the surface pressure behavior were evaluated for urea and tend to confirm the proposed orientation. It is determined by the H-bonding between the C=O function in urea and surrounding urea molecules as well as with other surrounding water molecules in the interphase.

The experimental results for the series of n-propyl-ammonium perchlorates, $(n\text{-}Pr)_n N^+ H_{4-n} ClO_4^-$, show that all the organic cations tend to adsorb more strongly when q_M is negative, as expected on electrostatic grounds. The increase of adsorbability with increasing number of propyl chains corresponds to increasing hydrophobicity and decreasing accessibility of the N^+ charge-center to the H_2O dipoles of the solvent. Evaluation of the standard free energies of adsorption for this series of cations shows that, in a general way, the ΔG^o_{ads} becomes more negative with increasing surface excess, Γ, suggesting that apparent attractive interactions take place among the adsorbed cations in the interphase. At first sight, this is unexpected since repulsion between

ions of the same sign in an ad-layer would be the more expected behavior. These results suggest, however, that the interaction effects amongst hydrated ions must be considered not only in terms of the electrostatic interactions involved but also in terms of interactions between overlapping hydration co-spheres of the ions in the sense of Gurney. The co-sphere overlap of R_4N^+ ions, as in regular solutions of R_4N^+ salts, gives an attractive interaction which accounts for the unusual behavior of ΔG^o_{ads} with increasing surface coverage.

Attempts to study the structure of the mercury-electrolyte solution interphase in acetonitrile was unsuccessful. This unfortunate situation was apparently caused by the presence of traces of water and oxygen in the solvent resulting in the hydrolysis of acetonitrile to acetamide which in turn becomes the predominantly adsorbed species at the mercury surface. This difficulty, noted in other work, prevented any reliable results being obtained in this solvent.

CHAPTER I

INTRODUCTION

PREAMBLE

In recent years, much interest has arisen concerning solutions of alkylammonium ions in water in which the interactions exhibit unusual behavior. Correspondingly, the factors that influence their adsorption are of similar interest, e.g. the balance of hydrophobicity and hydrophilicity, and accessibility of the positive charge to (a) the solvent and (b) charged interfaces.

The work to be described in this thesis involves studies of organic ammonium-type ions in relation to: (a) factors which determine adsorption of such ions and corresponding molecules in the double-layer, especially ionic solvation and water orientation at charged interfaces; and (b) how these factors determine the structure of the double-layer at charged electrode interfaces in the presence of organic ions and molecules. First, a brief review of

the development of theories and models of the double-layer will be given together with an outline of treatment of experimental results in this field of research.

A. Adsorption of Ions at Charged Interfaces: Historical Aspects of Double-Layer Theories

1. Electrostatic Theories of the Double-Layer

The development of theories of the double-layer has extended over a long period of time since the representation proposed by von Helmholtz in 1861. The Helmholtz model[1] was based on the supposition that there are two fixed layers of charges of opposite sign at each side of the interface between the two phases in contact, thus forming a double-layer which could be compared to a parallel-plate condenser of measurable capacity and across which an electric p.d. could exist (Fig. 1a).

Gouy[2,3] recognized that the model of Helmholtz could not be realistic since thermal perturbation, which would give a distribution of adsorbed ions, was not considered. In Gouy's model

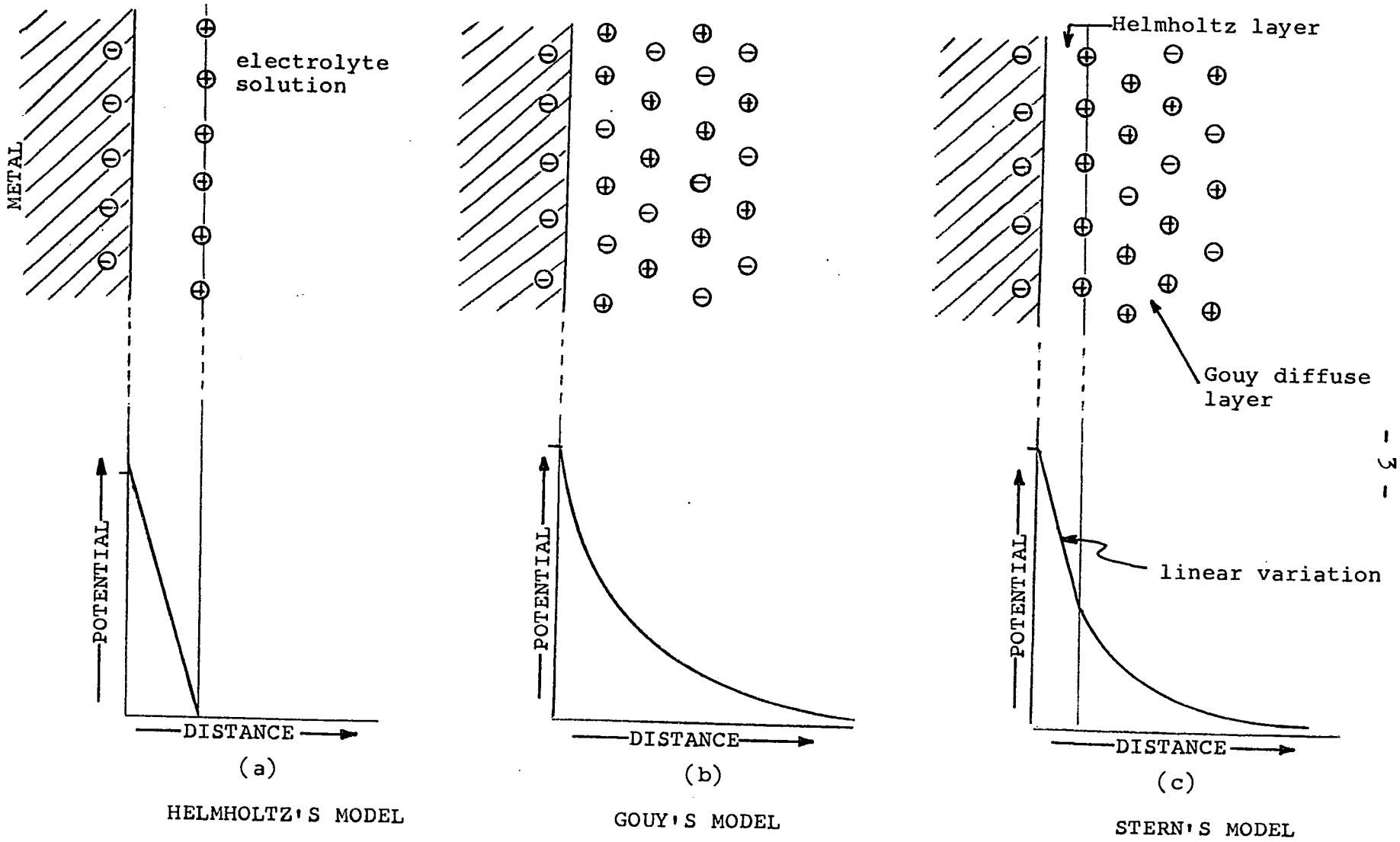

Fig. 1 Adsorption models of the double-layer.

(Fig. 1b), a so-called "diffuse layer" or ionic atmosphere, is set up where an equilibrium distribution of charges arises because of the opposition of the forces due to the electric field and the thermal fluctuations in the solution at finite temperatures. Gouy's model was extended by Chapman[4] who quantitatively evaluated the distribution of ions in the diffuse layer and the corresponding variation of electrical potential using Poisson's equation and the Boltzmann distribution law, as in the Debye - Hückel theory later (1923).

Due to neglect of the finite size of ions, Gouy's theory gave much too large a capacitance for the double-layer, except near the potential of zero charge (p.z.c.).

The basis of modern theories of the double-layer originated with Stern[5] who improved the Gouy-Chapman model: (a) by taking into account the finite size of ions and (b) by thus supposing that there is some minimal contact distance between the ions closest to the electrode surface and the electrode itself, so that the double-layer could be divided into two regions (Fig. 1c): a compact layer as in Helmholtz's model

and a diffuse-layer as in the Gouy-Chapman model. Stern's theory thus combines the models of Helmholtz and Gouy but avoids the erroneous aspects of both. Stern also recognized that chemisorption (so-called "specific adsorption") of ions occurs in addition to the long-range attraction (or repulsion) of ions to the charged interface due to the electrostatic (coulombic) forces. Thus, Stern introduced the Langmuir isotherm into the mathematical description of the properties of the double-layer and recognized that specific adsorption of ions on the metal surface could be an important factor in double-layer behavior. In fact, it is a major feature of most interfacial systems both at electrode and colloid surfaces.

Later, a major advance was made by Grahame[6] in the treatment of the double-layer proposed by Stern. In particular, Grahame took into account the different degrees of solvation of anions and cations by recognizing that specifically adsorbed (an)ions could draw nearer to the electrode than non-specifically adsorbed (cat)ions. He thus divided the compact (Helmholtz) layer in the Stern model into two

planes corresponding to different distances of closest approach of anions and cations to the surface: (a) an "inner Helmholtz plane" (I.H.P.), where the potential is ϕ_1, being the locus of centres of specifically adsorbed ions (usually anions) at closest approach to the metal where they have lost, at least on the side nearest to the electrode, some solvating solvent molecules; and (b) the "outer Helmholtz plane" (O.H.P.) or "Gouy plane", where the potential is ϕ_2, being the locus of centres of non-specifically adsorbed ions (usually cations) which are separated from the electrode by at least the first layer of their hydration shells (Fig. 1d). It is from this layer (out towards the solution) that the diffuse-layer (as in the Stern theory) begins.

A proper, correct and thermodynamically rigorous treatment of the double-layer was not given until 1947 when Grahame[6] published his important general review, referred to in (6) above. An important feature of the double-layer remained neglected, however, and was also little considered in the earlier theories[1-8]; it is the role of <u>solvent</u>

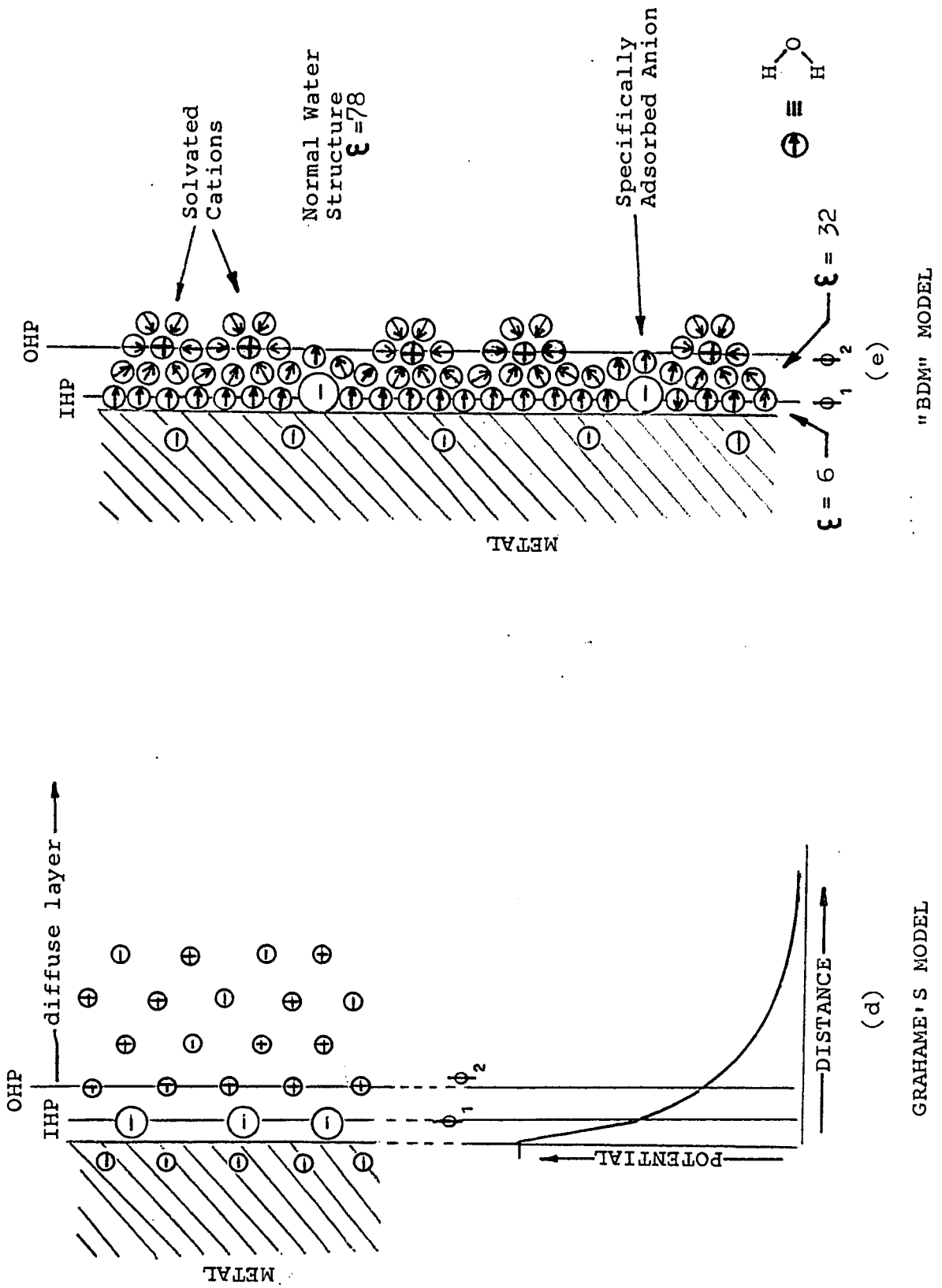

Fig. 1 Adsorption models of the double-layer.

at the interface in determining double-layer properties and ionic adsorption.

2. Solvent Adsorption and Orientation in the Treatment of the Double-Layer

(i) Role of Solvent in Electrostatic Theories of Adsorption

The electrostatic theories of the double-layer, including that of Grahame, gave no account of the role of solvent in the behavior and properties of the double-layer. Only implicitly in the theories of Frumkin[9,10] and of Butler[11] on adsorption of organic substances was the presence of solvent at the charged interface recognized: adsorption of an organic substance requires displacement of a corresponding "area" of electrostatically polarized and oriented water previously present in the interphase.

The first treatment of water adsorption and orientation in the double-layer was given by Mott and Watts-Tobin[12,13,14] and applied to substitutional adsorption in the double-layer by Bockris, Devanathan and Müller[15]. The model involved is shown in Fig. 1e and envisages two states of orientation of water, "up"

and "down", in the field across the inner Helmholtz region. This is undoubtedly an over-simplification since a distribution of water orientations will arise but in comparison with the previous neglect[9,10,11] of the behavior of the solvent in the double-layer, or its treatment in terms of a continuum, this approach [12,13,14,15] was a major advance.

(ii) Theory of Watts-Tobin and Mott on Water Orientation in the Double-Layer

In a series of publications[12,13,14], around 1961, Watts-Tobin and Mott gave a new kind of theoretical treatment of double-layer capacity behavior at Hg in aqueous solutions. An explanation of the sharp increase of capacitance at potentials positive to the p.z.c. was proposed; indeed, somewhat to the positive side of the electrocapillary maximum, where the mercury is uncharged, there is a hump in most plots of capacitance against potential or charge. Watts-Tobin[12] suggested that the hump may be due to the high polarizibility of the water layer between the metal and the O.H.P., i.e. this effect could be caused by an increase in the effective dielectric constant of the layer at the point where the average

dipole moment of the assembly of water molecules in this layer changes sign. Appreciable orientation of a water molecule with dipole moment μ can arise if an average field $|E| > kT/\mu$ is provided, with the direction of orientation being determined by the sign of E. At 300 K, this field E is ca. 6.6×10^6 V cm^{-1} whereas the electrode-solution field which characterizes the double-layer capacity behavior can be greater than 10^7 V cm^{-1}, depending on electrode surface charge. Watts-Tobin then considered in some detail the orientation behavior of the water molecules in contact with the mercury and concluded, probably incorrectly, that the influence of the bulk water was negligible.

The water molecules were regarded as distributed in two limiting orientations, with or against the field, thus in opposite directions; water molecules oriented with their oxygen atom towards the metal were called[15] "down" dipoles (number $N_{\downarrow}$), whereas those oriented with their hydrogen atoms towards the electrode would be called "up" dipoles (number $N_{\uparrow}$); the relative population per cm^2 of "up" and "down" dipoles in a total

N_t ($=N\uparrow + N\downarrow$) depends on the field and on the lateral repulsion between the oriented dipoles[15]. The latter interaction depends on the relative numbers oriented, $N\uparrow/N_t$ and $N\downarrow/N_t$.

The equilibrium between water dipoles in "up" or "down" states can be derived from kinetic relations for adsorption at equilibrium or from application of Boltzmann's law[15]. The distribution function for orientation in the two states is expressed by the following equation:

$$\frac{N\uparrow - N\downarrow}{N_t} = B = \tanh \left[\frac{\mu E}{kT} - \frac{Uc}{kT} \left(\frac{N\uparrow - N\downarrow}{N_t} \right) \right] \quad (1)$$

where c is the coordination number in the interphase, U is the lateral interaction energy between a pair of adjacent dipoles and, E, the field in the inner or outer Helmholtz layer, depending on sign of q_M.

In order to interpret the behavior of a thin film of water molecules in the strong field present in the surface layer, Mott and Watts-Tobin[13] proposed the following relation between q_M, the surface

charge, and ϕ_m, the potential between the metal and the electrolyte, in the absence of specific adsorption:

$$q_M = \frac{K_o}{4\pi \ell_o} \phi_m + \frac{N_t \mu}{\ell_o} \tanh \left(\frac{\mu E}{kT}\right) \qquad (2)$$

where K_o is the dielectric constant of the oriented water molecules, ℓ_o, the distance between the metal and the O.H.P., N_t, the number of water molecules per unit area, μ, the dipole moment of water and E the field across the double-layer.

They were able to reproduce quite well the capacitance hump with the above $q_M - \phi_m$ relationship by plotting the capacity $-dq_M/d\phi_m$ against the potential ϕ_m.

Improvements to the solvent dipole treatment of double-layer capacitance were made by Frumkin and Damaskin[43] and by Parsons[44] using models in which the orientation of water dipole clusters, rather than single molecules, was considered. A better account of the shape of capacitance (C) - potential (V) curves for Hg resulted but a fuller theory in which H-bonding in orientation of elements of the water structure near to a charged interface

yet remains to be developed. Also, the treatments of Watts-Tobin and Mott[12,13,14], Frumkin and Damaskin[43], and of Parsons[44] give no attention to the ion-specific shape of C-V profiles which is an important feature of the experimental behavior in various electrolyte solutions.

B. Adsorption of Neutral Molecules at Charged Interfaces:

(1) Competitive Adsorption Involving Solvent Displacement

Treatments of adsorption of electrically neutral species at electrodes were given by Gouy[2] for the case of electrocapillary data and by Frumkin[10] and Butler[11] for electrocapillary and capacity data. Since the electrode is normally completely covered with water dipoles, each organic molecule which becomes adsorbed on the metal surface must displace a certain number, x, of water molecules from the interface; x depends on the effective projected area of the organic molecule on the metal surface compared with that of a water molecule in the interphase; this process is referred to as

"competitive adsorption". Various viewpoints have been given concerning the mechanism of water displacement upon adsorption of an organic molecule. First Damaskin and co-workers[16], then Giomini and others[17] and Parsons[18] considered the possibility that water molecules could be grouped in clusters and that each cluster would be displaced as a single entity when a neutral molecule becomes adsorbed. Later, Parsons[19] and others[20,21,22] gave more importance to the role of discrete water molecules at the interface. Conway and Dhar[30] argued that the thermodynamic interpretation of adsorption would be independent of whether cluster displacement occurred or not.

(2) Treatment of Experimental Results in Terms of Adsorption Isotherms

(i) Simple Isotherms

From electrocapillary data, Frumkin elaborated methods which allowed the type of adsorption isotherm applicable to a given system to be determined, e.g. the Langmuir or the Frumkin isotherm[9] allowing

for interaction effects. The forms of adsorption isotherms for competitive adsorption involving molecules of different sizes are, however, different and will now be discussed here and in Chapter IV since they are involved in important ways in the evaluation of the present experimental results.

(ii) Isotherms for Competitive Adsorption Involving Solvent Displacement

Solvent displacement was implicit in the early dielectric treatments of Frumkin[10] and Butler[11]. Bockris, Devanathan and Muller ("BDM"),[15] however, treated the isotherm for this type of adsorption in the following, much more specific, molecular terms:

(a) an organic molecule has some specific tendency to become adsorbed due to electrostatic and/or "chemical" interactions with the surface. However, in order to do so, it is necessary that it displace water molecules. These water molecules are oriented [eqn. (1)] and held electrostatically in the double-layer with an energy μE modified by

a lateral interaction energy Uc/kT, as in eqn. (3) below. Hence the energy of adsorption of an organic substance is determined, amongst other factors, by the energy of displacing a certain number, x, of water molecules oriented in the double-layer and themselves having an energy proportional to field or surface charge.

(b) the water molecules, in becoming oriented, suffer lateral repulsion with a pairwise interaction energy U. This opposes their orientation and also makes them relatively more easily displaced by an organic molecule since this interaction diminishes the main interaction with the electrode field E. H-bond interaction, although not specifically considered by BDM in ref. 15, will be involved in U.

Taking into account factors (a) and (b) gave[15] the equation:

$$\frac{\theta_{org}}{1-\theta_{org}} = \frac{C_{org}}{C_w} \exp\left[\frac{-\Delta G^{o}_{chem}}{RT}\right] \exp Bx \left[\frac{Uc}{kT} - \frac{\mu E}{kT}\right] \quad (3)$$

The "BDM" theory provided good agreement

between theory and the general experimental behavior in neutral molecule adsorption but, like other electrostatic models, it failed to explain the experimentally observed maximum adsorption of neutral molecules between -2 to -4 μC cm^{-2} opposed to that expected at the p.z.c. However, it is easy to introduce a factor which will reproduce such behavior: if water dipoles have themselves some tendency for specific adsorption in a preferred orientation, viz. with O facing the Hg, then a small net negative q_M must be established to achieve zero net orientation, and hence maximum adsorption of neutral organic molecules. Experimentally, this occurs at q_M = -2 to -4 μC cm^{-2}. Therefore H_2O dipoles are preferentially oriented with their O atoms towards Hg in the absence of external field effects, corresponding to interaction of lone-pair O orbitals with the Hg surface.

C. Basis of Electrochemical Measurements at Mercury

1. Main Relations Established for Experimental Analysis of Double-Layer Properties

It will be convenient to define the typical parameters of the double-layer and to recall the principal operations by which these parameters are derived in the analysis of experimental data.

When a system involving two immiscible phases in planar contact is in equilibrium, the thermodynamic analysis of the interfacial properties is based on the Gibbs adsorption equation:

$$d\gamma = -S_\sigma \, dT - \sum_i \Gamma_i d\mu_i \qquad (4)$$

at constant pressure, where γ is the surface tension between the two immiscible phases, S_σ the surface excess entropy, T the absolute temperature, Γ_i the surface excess concentration and μ_i the chemical potential of each species i in solution.

Considering the particular case of an "ideally polarizable" interface, i.e. where an electrostatic equilibrium exists between the charged surface and adsorbed ions and molecules, but no charge-transfer processes are occurring, Grahame and Whitney[23] and Grahame[6] showed that, for an electrolytic system containing two types of ions, a cation M^{z+} and an anion A^{z-}, neutral adsorbable species (n) and a solvent, the following general relation can be obtained for an electrolyte of stoichiometry defined by $z_+\nu_+ = |z_-|\nu_-$:

$$-d\gamma = q_M dE_{\pm} + \frac{\Gamma_{\mp}}{\nu_{\mp}} d\mu_{\pm} + \Gamma_n d\mu_n \qquad (5)$$

q_M being the electrode surface charge density; if q_s is the charge density on the solution side of the double-layer at equilibrium, then the electroneutrality condition for the entire interphase requires that $q_M + q_s = 0$. E designates the experimentally defined difference of potential applied between the working electrode and an electrode reversible with respect (E_+) to the cation or (E_-) to the anion of the electrolyte. $\Gamma_{\mp}$ is the anion (Γ_-) or cation (Γ_+) surface excess while μ is the chemical

potential for the salt $M_{\nu_+}^{z+} A_{\nu_-}^{z-}$ in the bulk solution. Γ_n and μ_n are the surface excesses and chemical potentials, respectively, for the neutral components of the solution.

From relation (5), it is possible to obtain the thermodynamic quantities q_M, $\Gamma_\pm$ and Γ_n of the interphase as shown by the following relation called the Lippman equation:

$$\left(\frac{\partial \gamma}{\partial E_\pm}\right)_{p,T,\mu,\mu_n} = \left(\frac{\partial \gamma}{\partial E}\right)_{p,T,\mu,\mu_n} = -q_M \tag{6}$$

Also, since the Gibbs relation is a complete differential equation, the following are easily obtained for ions:

For E_+, μ_n ions,

$$\left(\frac{\partial \gamma}{\partial \mu}\right)_{p,T,E_+,\mu_n} = -\frac{\Gamma_-}{\nu_-} \tag{7}$$

$$\left(\frac{\partial \gamma}{\partial \mu}\right)_{p,T,E_-,\mu_n} = -\frac{\Gamma_+}{\nu_+} \tag{8}$$

and for the neutral species,

$$\left(\frac{\partial \gamma}{\partial \mu_n}\right)_{p,T,E,\mu} = -\Gamma_n \tag{9}$$

It can be seen that eqn. (6) gives the surface charge q_M on the metal if the variation of surface tension with potential is measured under conditions of constant chemical potential of components in the solution phase, constant temperature and pressure. Also, the individual ionic surface excesses, Γ_+ or Γ_-, are obtainable from eqns (7) and (8) (or one of them with the aid of $q_M = -q_s$) without thermodynamic ambiguity. Thus, a very complete view of the structure and properties of the double-layer can be obtained, at least at Hg.

Another important quantity, the double-layer capacitance, C, can be obtained from the Lippman equation (6), (eqn. (5) with constant μ's):

$$C = \left[\frac{\partial q_M}{\partial E}\right]_{p,T,\mu,\mu_n} = -\left[\frac{\partial^2 \gamma}{\partial E^2}\right]_{p,T,\mu,\mu_n} \tag{10}$$

However, C will not be obtainable with very great precision using the electrocapillary method since it requires double differentiation of γ data w.r.t. potential. Normally it is directly measured by means of a.c. impedance[24]. The use of this method has been treated in detail in a number of Grahame's papers (see review ref. 6).

2. Adsorption Isotherms and Evaluation of the Standard Free Energy of Adsorption ΔG^{o}_{ads}

Equations of state of adsorbed species relate surface pressure ϕ_q, for a given charge density, q, to some function of the respective surface excesses Γ_i, Γ_j of the adsorbable species. At a liquid surface, ϕ_q is easily measured as the change of surface tension due to adsorption, viz. $\phi_q = \gamma_b - \gamma$ [20] where γ and γ_b are the surface tensions with and without an adsorbable species (i or j), respectively. The general expression for the equation of state is:

$$\phi_q = f(\Gamma) \qquad (11)$$

For an ideally polarizable electrode, from eqn. (5) at constant temperature, pressure and μ_s (solvent), and with the definition $Ad\phi = d\mu$, where A is the surface area of the interphase,

$$d\phi_q = \Gamma d\mu_i \tag{12}$$

From equations (11) and (12), one can obtain by elimination and integration a relation between one of the three quantities ϕ_q, Γ and μ and the others. We are interested here in the adsorption isotherm relating Γ to the chemical potential μ determined by the activity of the adsorbate in the bulk phase, and the equation of state $\phi_q = f(\Gamma)$.

A number of electrochemical isotherms have been proposed by various investigators; they have been summarized by Damaskin[16] and were grouped into two classes[26]; (i) the non-localized models and (ii) the Langmuir type model for adsorption at localized sites. Only the most commonly used adsorption isotherms[16] will be briefly presented below.

(i) Isotherm for Mobile Species

In this model, the adsorbed species is regarded as being able to move freely on the surface in a non-structured medium and under a uniform field. The adsorbed film behaves like a "two-dimensional" gas[27]. Forms of isotherms, expressed in terms of fractional coverage θ, are as follows:

(a) The Henry's law isotherm [no finite space requirement, no interactions]

$$Kc = \theta \tag{13}$$

(b) The Volmer isotherm [finite space requirement, no interactions]

$$Kc = \frac{\theta}{1-\theta} - \exp\left[\frac{\theta}{1-\theta}\right] \tag{14}$$

(c) The isotherm with a virial coefficient [no finite space requirement, but interactions significant]

$$Kc = \theta \exp(-2a\theta) \tag{15}$$

where a is a parameter characterizing interactions between adsorbed molecules and is less than zero for repulsive interactions.

(ii) The Langmuir Type Isotherm for Fixed-Site Adsorption

(a) The Langmuir isotherm[28] itself

In deduction of the Langmuir isotherm, an homogeneous surface divided into sites that can be occupied by adsorbable particles is considered. The following relation can be obtained either by a kinetic treatment[28] or by statistical mechanics:

$$Kc = \frac{\theta}{1-\theta} \tag{16}$$

where K is an equilibrium constant determined by the standard free energy of adsorption, ΔG^{o}_{ads}. At an electrode, ΔG^{o}_{ads} is usually a function of electrode potential or charge q_M.

(b) The Frumkin isotherm

$$Kc = \frac{\theta}{1-\theta} \exp(-2a\theta) \qquad (17)$$

where a is again a parameter characterizing lateral interactions.

Damaskin[16] used Zhukovitskii's adsorption isotherm[29] which takes into account the fact that x solvent molecules must be displaced from the surface by every organic molecule adsorbed:

$$Kc = \frac{\theta}{x(1-\theta)^x} \qquad (18)$$

or by introducing a correction parameter a for attractive interactions between the adsorbed particles,

$$Kc = \frac{\theta}{(1-\theta)^x} \exp(-2a\theta) \qquad (19)$$

He showed[16] that x was apparently 1 for a number of organic compounds at Hg and interpreted this observation in terms of displacement of groups

of associated water molecules (cf. 17,18) by the organic substance. It is unclear why groups of water molecules should adjust themselves in size to coincide with the area or organic adsorbates of different sizes. The deduction that $x = 1$ for solvent displacement adsorption is probably incorrect.

However, Dhar, Conway and Joshi[30], considering a number of works[31,32,33] where the importance of the size factor was recognized, showed that "the failure to include the size factor in the isotherm leads to serious errors in the evaluation of any interaction effects in the adsorption behavior" and rigorously derived the following adsorption isotherm which will be discussed in more detail in Chapter III:

$$Kc = \frac{\theta}{\exp\ (x-1)\ (1-\theta)^x} \qquad (20)$$

or a corresponding one with an interaction term $\exp\ (-2a\theta)$.

D. Relation to Structure of Liquid Water

The Watts-Tobin and Mott, and the "BDM" theories, and implicitly the discussion of Damaskin and others[16,17,18], introduced questions concerning the state of water in the double-layer. Further, more recent treatments have been given by Conway and Gordon[34] on the entropy of water in the double-layer, by Parsons[18] and by Bockris and Habib[35] who introduced the treatment of clusters of water molecules in multi-state theories of water adsorption and orientation.

In recent years, very many papers[37-42] have appeared in the literature on the structure and properties of liquid water itself. An excellent and complete review is given in the monograph by Eisenberg and Kauzmann[36]. More recently, the state of water and hydrated ions at charged interfaces has been reviewed in detail in an article by Conway[25]. Factors such as changes of H-bonding at the interface, dipole imaging, surface excess entropy and interaction of surface oriented water with hydration spheres of adsorbed ions were considered.

E. Choice of Systems for Study in the Present Work

1. Acetonitrile: Importance of the Solvent in Double-Layer Studies

It must first be noted that the great majority of results obtained so far on interfacial phenomena at electrodes has been for the particular case of water as the solvent. However, by changing the nature of the solvent, e.g., by substitution of an organic solvent for water, and from comparison of data obtained for such a system with that for a corresponding aqueous system, it should be possible to gain a better understanding of the aspects of interfacial electrochemical phenomena which originate specially from the properties of water as the solvent.

Some progress has been made in recent years with regard to studies of this kind in non-aqueous solvents. While the first work on the double-layer at Hg in a non-aqueous solvent was done by Frumkin[10,46] using the electrocapillary technique, detailed studies in this field are only

much more recent and have been directed towards elucidation of adsorption of ions at the mercury electrode or the study of the influence of the solvent dielectric constant ε on the differential capacity behavior, e.g. with methanol (ε= 32.5), dimethylformamide (ε= 36.7), sulpholane (ε= 44), dimethylsulfoxide (ε=46.6), formic acid (ε=57), propylene carbonate (ε=64.4), ethylene carbonate (ε=89), formamide (ε=109) and N-methyl formamide (ε=182).

All previous work in non-aqueous solvents has been concerned with description of the double-layer properties in terms of ionic double-layer capacitance and ion adsorption, including the question of the dependence of the capacity hump on the nature of the solvent. The conclusion is that it is not simply due to solvent reorientation[12,13,14] but rather to specific adsorption of ions in relation to their solvation.

The dependence of inner-layer solvent properties at the electrode interface on the solvent has received virtually no attention. In the present

work, the initial aim was therefore to try to provide information on solvent adsorption and orientation using a simple, non H-bonded solvent by studying solvent displacement adsorption, as was done in water with pyrazine[47]. Acetonitrile is ideal for this purpose since:

(i) it has a simple linear structure involving a small number of atoms which facilitates the eventual description of the state and orientation of the species in the double-layer;

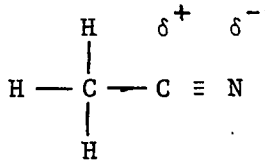

(ii) it is an excellent solvent for organic compounds and also dissolves a number of simple inorganic salts;

(iii) like other nitriles, this solvent is chemically inert towards many other compounds at normal temperatures;

(iv) CH_3CN has a relatively high dielectric constant ($\sim$ 37); and

(v) finally, a large range of potentials is available for electrode polarization without decomposition of this solvent. At the mercury electrode, the

range goes from +0.69 V on the anodic side to -2.0 V on the cathodic side with $LiClO_4$, 0.1M[48] as the supporting electrolyte.

As will be shown later, many serious and unexpected difficulties arose with CH_3CN as solvent which prevented the aims of this part of the work being achieved.

2. Urea: Water Structure Effects and Adsorption in Relation to Solution Properties

One of the most interesting aqueous mixed "solvents" is the urea-water system[50] because urea is known[51-54] to change the structure and H-bonding equilibria in water. For these reasons, many studies have been made on urea-water mixtures in relation to protein denaturation[49]. It was therefore of interest to examine the adsorption of urea at the Hg electrode interface with regard to structural aspects of the water interphase at Hg. Furthermore, it is of interest to compare the adsorption behavior of urea in the double-layer with that of thiourea, previously studied by Frumkin[55],

Parsons[56] and Shapink et al[57]. Thiourea adsorption has been of special interest since its behavior is similar to that familiar with surface-active anions such as iodide rather than that typical of other neutral molecules. This behavior is due to the strong interaction between the sulphur lone-pair orbitals and the mercury surface (cf. 55).

Adsorption of aqueous urea solutions will be discussed in Chapters II and III.

3. $R_nN^+H_{4-n}$ Salts: Steric Effects in Adsorption and Hydration

Adsorption of ions at electrodes is controlled by (a) the extent of hydration of ions and the deformability of the hydration sheath; (b) accessibility and availability of lone-pair donor orbitals and (c) any hydrophobic character the ions may have which may tend to cause them to be expelled from the aqueous phase to any interface. The series of alkylammonium ions, $R_nN^+H_{4-n}$ where $0 \leqslant n \leqslant 4$, provides an interesting class of ions where hydration,

accessibility of charge and hydrophobicity, can be progressively changed as n is increased. This series of ions has also been studied previously in this Laboratory in relation to their hydration and by Everett and Wynne-Jones[58] in relation to their ionization equilibria in water (for n$\geq$3).

The adsorption behavior of ions of this class will depend on: (a) the relative size or number of alkyl chains involved; (b) the geometry of the ion in the double-layer and the minimum distance of approach between the N^+, or hydrated N^+ center, and the metal surface; (c) the degree of hydration for each adsorbed cation.

It would also be interesting to compare the present results with those obtained in parallel with the present work by Bennes and Conway[59] on surface potential measurements for the same compounds at the air/water interface; finally, it will be useful to evaluate the variation of the standard free energy of adsorption as a function of the number of carbon atoms for each adsorbed cation with respect to Traube's rule (see Chapter IV) and the hydrophobicity effects.

CHAPTER II

EXPERIMENTAL

A. Choice of Method

The study of surface-active substances at the dropping mercury electrode (d.m.e.) is of importance in polarography and other electrode processes[60,61,62] as it can lead to a better understanding of the influence of organic compounds, e.g., maxima suppressors, masking agents, complexing agents and inhibitors in some charge-transfer reactions, etc. Double-layer measurements on a stationary mercury electrode in a Lippmann apparatus have been found to be highly reproducible and thermodynamically dependable[63,64].

On the other hand, under some conditions, polarographic drop-time (t) measurements may be more convenient e.g. when investigations of highly surface-active compounds[65,66], or studies in a non-aqueous solvent are to be made (see below). It should be stated that there have been controversial discussions

as to which of the capillary electrometer, the drop-weight or the drop-time methods give the most reliable electrocapillary curves[67] $\left[\gamma \text{ as } f\ (E)\right]$. In fact, only in the last decade has it been possible to obtain very accurate and reliable drop-time measurements[68] with the aid of electronic timers, so that proper comparisons between the methods can be made.

Damaskin[69], amongst others, has indicated that use of the Lippmann electrocapillarometer with a stationary Hg meniscus in a capillary may be preferable to other techniques for study of adsorption, e.g. capacity measurements at a growing drop, or drop-time or drop-weight determinations at successive growing drops. The electrocapillary technique avoids any ambiguity concerning non-attainment of adsorption equilibrium which can arise with some systems, e.g. involving large molecules. However, the objection that the contact angle at the Hg meniscus may be potential-dependent has been often raised but Kimmerle, Menard, Conway and Dhar[70] made a direct comparison of adsorption and surface tension data obtained with the small molecule pyrazine at Hg

using drop-time and electrocapillary measurements and found agreement between the two methods to be quite satisfactory. With pyrazine and pyridine, Dhar[47] recently obtained very satisfactory results using the capillary electrometer in this Laboratory, as reported in a recent thesis.

The conversion of drop-times (t) to surface tensions (γ) remains the main problem: it is necessary to start with the classical Tate relationship[71] in which the drop-weight or drop-time of a d.m.e. is, to a first approximation, expressed as a linear function of surface tension:

$$2 \pi r \gamma = Mg = m t g \qquad (21)$$

where M is the mass of the Hg drop (mg), m, the flow rate of Hg (mg sec^{-1}), r, the radius of the capillary bore (cm), g, the gravitational constant and γ, the surface tension of Hg (dyne cm^{-1}).

From this relation, Corbusier and Gierst[72] were able to make satisfactory conversions of t to γ

using the equation:

$$\frac{\Delta\gamma}{\gamma} = K \frac{\Delta t}{t} \qquad (22)$$

where K, the proportionality constant, tends to unity for a capillary of small bore and a large head of Hg. For a specific experiment, K was obtained as 0.97_3, this being an average value for the range of potentials studied. Sathyanarayana[73], using the function established by Corbusier and Gierst, and employing some correction factors, showed that it was possible to calculate surface tensions accurately and obtain reliable electrocapillary curves from drop-time measurements.

Later, Barradas and Kimmerle[68] were able to clarify and improve Corbusier and Gierst's mathematical treatment; they recognized two main physical factors involved in the calculation of γ from t: (a) the terminal weight of a Hg drop is equal to the net upward force due to surface tension round the circumference of the capillary orifice and (b) the "back pressure" effect due to the curvature

of the drop which opposes the upward force. These factors are expressed in the following equation:

$$2\pi r \gamma - \frac{2 \pi r^2 \gamma}{R} = \frac{D - d}{D} m t g \qquad (23)$$

where R is the radius of the Hg drop, D, the density of Hg, and d, the electrolyte density at constant temperature. By use of computer techniques, they were able to calculate individual values of K for each measured value of t for a specific solution of defined concentration and composition at a constant applied potential; Barradas and Kimmerle clearly showed that the drop-time method was satisfactory and reliable by demonstrating that their results were as good as those obtained by the classical Lippmann electrocapillarometer.

It should also be mentioned that the drop-time method offers the advantage of a periodically renewed mercury surface which diminishes the possibility of contamination, e.g. in the case of non-aqueous solutions where sticking of the meniscus in the Lippmann electrometer is a problem. This is why the

use of a drop-time tensiometer for electrochemical adsorption studies at Hg was chosen for the initially projected work in acetonitrile.

B. Experimental Technique

1. Method and Apparatus

Experimentally the drop-time method consists in applying a controlled and recorded potential over a range of ca. 0.0 to -1.250 V to a mercury electrode and measuring precisely the average time of formation of a mercury drop at a certain potential and temperature, and for a defined concentration and composition of the solution.

The apparatus consists principally of six units: a 1 m mercury column, a glass capillary d.m.e., a thermostatted drop-time cell, a polarization circuit, an optical viewing circuit and an electronic timer capable of recording times with 0.1 msec. accuracy.

2. Mercury Column

The mercury column was contained in a thick-walled, thermostatted glass tube, 1 m long, surmounted by a 200 cc Hg reservoir; the flow of mercury was controlled by a high-vacuum screw-type teflon stopcock; the Hg level in the reservoir was recorded before each run by means of a cathetometer but the variation of Hg level in the reservoir during a single run was negligible. The whole system was suspended from the ceiling by means of a vibration-proof mounting.

3. Capillary d.m.e.

The drop-time measurements were carried out using a Sargent-Welch polarographic glass capillary whose period was 2 - 5 seconds, depending on the head of Hg. The capillary tip was cut with a sharp glass-knife and examined under a magnifying glass to avoid microscopic cracks at its edge[73] and was mounted between the column and the cell by means of a screw union made of teflon. The normal cleaning process consisted in washing the assembly

successively in chromic acid solution for one day, in double distilled water for the same period of time, in 50% aq. nitric acid for one hour, sucking in successively solutions of 50% and 10% aq. nitric acid, followed by doubly-distilled water. The apparatus was finally dried in a vacuum oven at 100°C. Studies in a non-aqueous solvent also involved the use of siliconized and conical capillaries[75].

4. Drop-Time Cell

A thermostatted, double-walled pyrex glass cell was constructed (Fig. 2). It consisted of two main compartments: the dropping Hg electrode and the reference electrode compartments separated by a glass stopcock to minimize diffusion from the reference electrode to the d.m.e. A clean platinum wire, sealed to the bottom of the Hg collecting flask, acted as the counter electrode. The cell was also provided with a bubbler for passing oxygen-free nitrogen into the solution. The drop-times were measured automatically by interruption of a confined beam of light by the falling Hg drops. This method

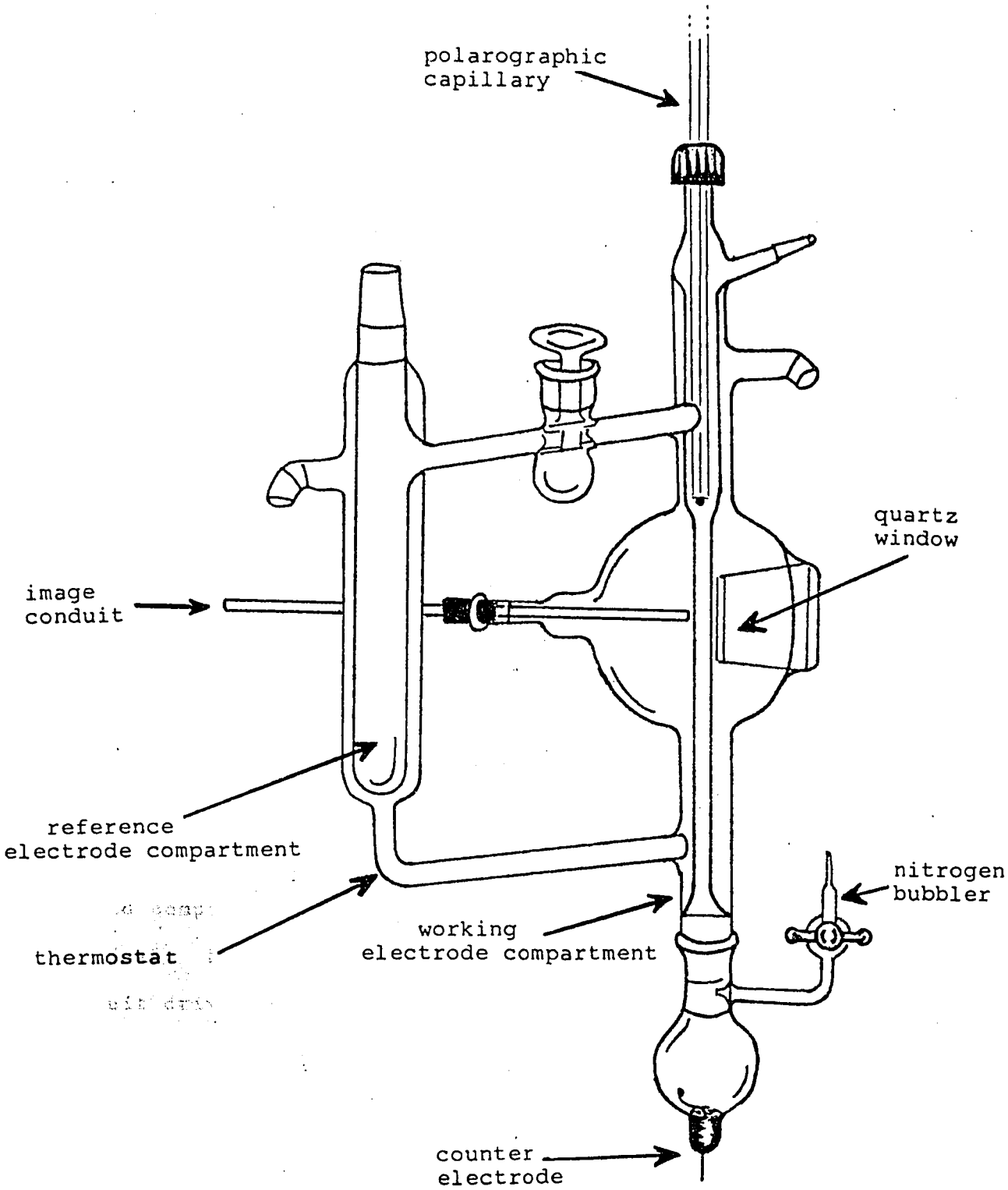

Fig. 2 Drawing of the drop-time cell.

requires the incorporation of a glass window and a quartz light pipe (American Optical Co.) on each side of the inner cylindrical tube the diameter of which was only slightly larger than the outside bore of the capillary (Fig. 4). The design of the cell facilitated manipulation of the capillary since the cell volume was small and required only a small quantity of solution. Recent technical improvements permit measurements in a flowing electrolyte system[76].

5. Polarization Circuit

The electrical circuit[77] (Fig. 3) is comprised of a d.c. potentiostat unit and a Radiometer pH - millivoltmeter for measurement of the potential of the mercury drops with respect to that of a standard reference electrode in the second compartment of the cell. Control of potential could also be made by means of a potentiometer circuit driven from a 12V lead-acid battery with a rheostat (coarse) and a helipot divider for fine adjustment of the applied voltage.

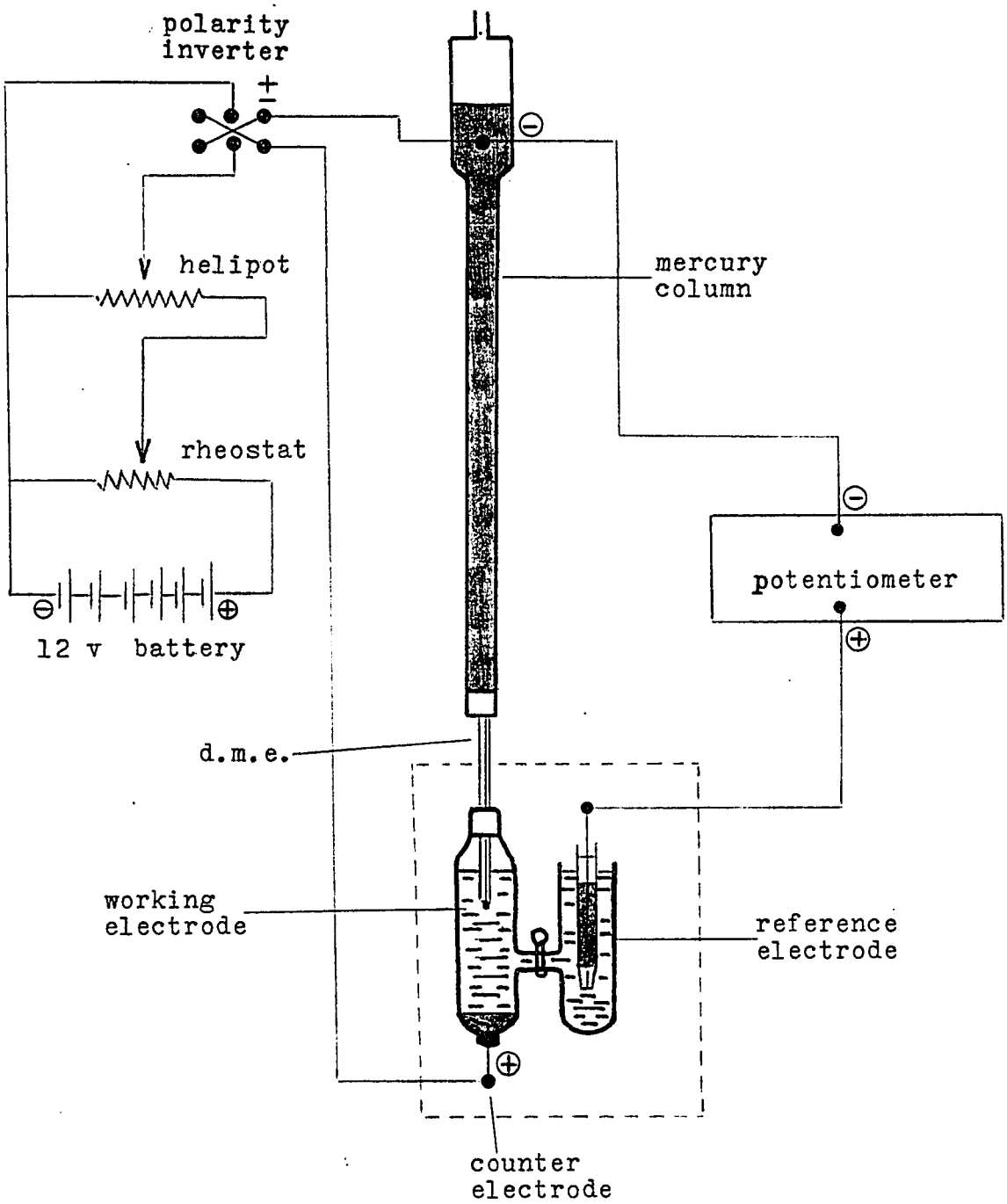

Fig. 3 Electrical circuit.

6. Optical Unit

The optical method of measuring drop-time values has been established as the most accurate procedure by a number of workers[68,72,73,77...]. A drop of mercury, in its fall, intercepts a narrow light beam converging in the middle of an inner cylindrical tube (Fig. 4); two parallel brass plates separated by about 0.3 mm were fixed between a Bausch and Lomb lamp and a quartz window beside the inner tube; this system produces a flat light beam which is focused by the cylindrical tube containing the solution acting as a converging lens. Each drop causes a sudden variation of the light intensity stimulating a photoelectric detector cell. The sensitive surface of the photocell is protected from exterior light by a cylindrical screen in order that it can function under normal ambient conditions. The transient electric signal produced by interruption of the light activating the photo-electric cell is rectified and amplified by a Schmidt-trigger device (photoelectric light switch); the resulting 10 V signal, having a rise time of

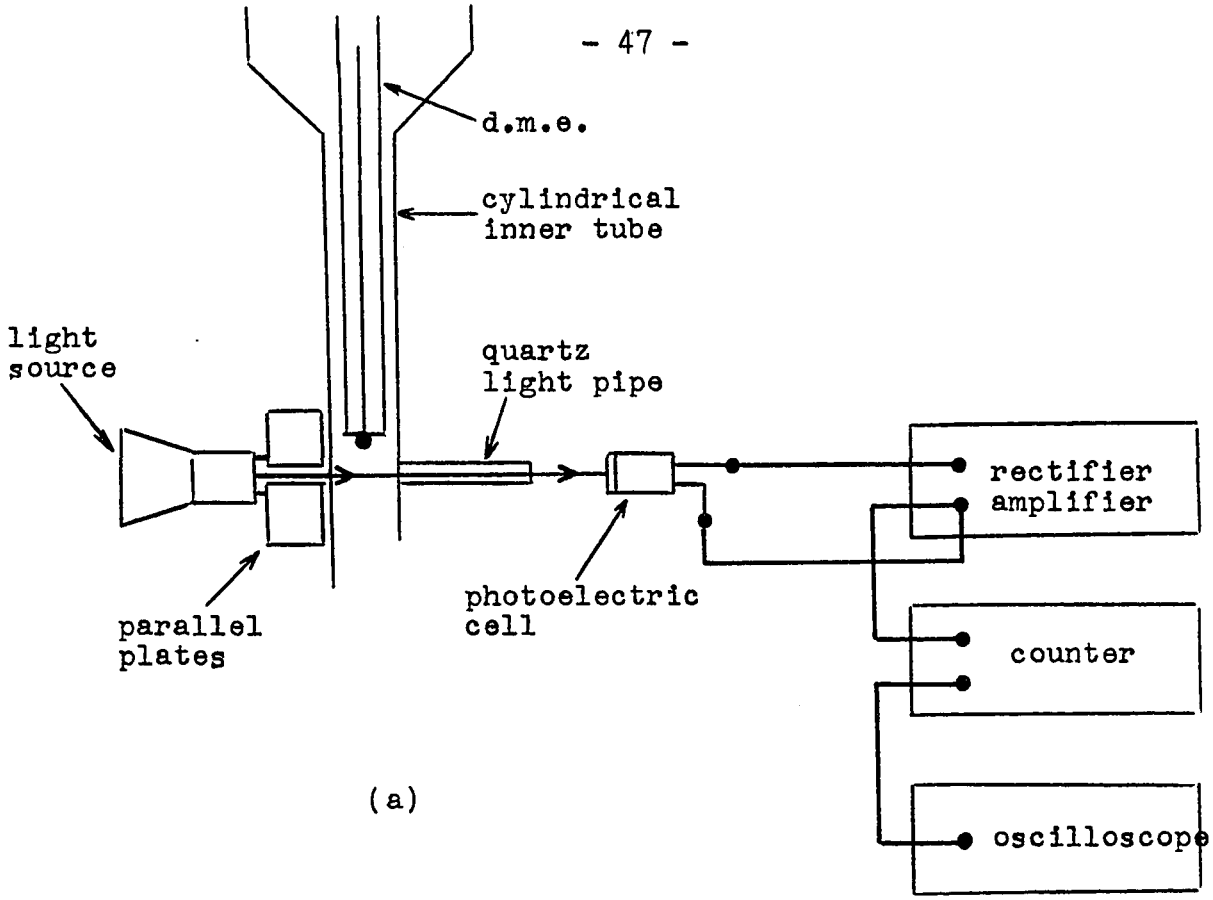

(a)

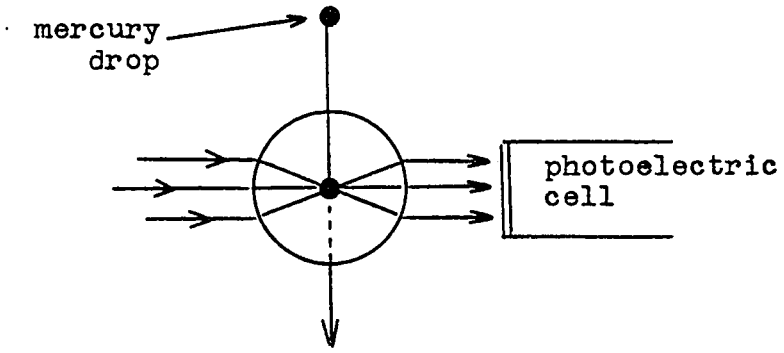

(b)

Fig. 4 Optical unit. a) Optical circuit. b) Cross-section of the cylindrical inner tube.

less than 10 μsec, is used to operate a Hewlett-Packard digital timer from which drop-time values are recorded with a precision of 0.1 msec; the signal is also viewed on an oscilloscope in order to facilitate adjustment of the capillary in the cell since it has to be positioned accurately at the centre of the light-converging glass tube. The optical method is more reliable than the procedure of Corbusier and Gierst[72] based on sudden changes of double-layer capacity when the drop falls since it has uniform sensitivity independent of the potential of the drop.

7. Thermostasis Unit

The working and the reference electrode compartments of the drop-time cell, and the mercury column, were all constructed in an annular fashion with double pyrex glass walls to permit circulation of thermostatted water through the entire system. All measurements were made at 300 ± 0.2K.

C. Accuracy of Drop-Time Measurements

Precision of drop-time measurements

depends largely on keeping the capillary free from mechanical vibrations; in order to minimize vibrations, the cell, the mercury column, the lamp and the photoelectric cell were fixed to a metal framework suspended from the ceiling by means of springs attached to a platform resting on a semi-inflated inner tube[76]. This system proved to be very satisfactory. A first experimental run gave a standard deviation (σ) of ± 0.03% over a range of 10 drop-times for each potential.

Residual vibrations were found to be due only to the water circulation system. They were minimized by using a long connection of plastic tubing between the thermostat and the cell. Under these conditions, runs with water circulation, gave in general, $\sigma = \pm 0.02\%$ or better i.e. ±0.1 dyne cm^{-1} in γ which provided good accuracy for the work. In the absence of water circulation, σ was ±0.01% but then unacceptable systematic shifts of temperature occurred.

Other factors which are important in the accuracy and reproducibility of the results

are as follows: preparation of the capillary requires certain precautions in order for it to function in a reproducible manner over a prolonged period of time. Thus it is desirable to avoid any excessive positive or negative polarization which could bring either an anodic deposit or evolution of hydrogen at the end of the capillary. Use of concentrated electrolyte solution, especially KCl, causes some significant variations of the capillary characteristics, perhaps due to etching. The axis of the capillary must be aligned vertically. Any appreciable ($>1^{\circ}$) deviation of the capillary from the vertical produces a significant diminution of the drop-times. Thus, experiment shows[72] that drop-time values (t) remain almost constant for deviations from the vertical smaller than 1 degree; t diminishes then by ca. 0.1% per degree. Use of an accurately cylindrical capillary free from microscopic cracks is also necessary[73]. Drop-time values are only reproducible if the period of interruption of the light beam by the drop is sufficiently short compared with the drop-time. This condition is realized when the distance between the capillary tip and the light beam axis is larger than 1 cm.

Variation of temperature modifies the geometrical characteristics of the capillary, the viscosity of mercury and its surface tension. The overall temperature coefficient, experimentally determined, is, however, not very significant as long as thermostasis can be maintained to better than $\pm 0.2^{\circ}C$ since only relative changes in surface tension are of interest in the measurements.

D. Experimental Conditions

1. Purification of Materials

(a) Water: Doubly-distilled water was used in all the experiments in which aqueous solutions were employed. The work did not require water having a higher degree of purity.

(b) Mercury: The purification of mercury involved four main steps, as described by Ives and Janz[78]:

1) Commercially available pure-grade mercury is first filtered through a perforated filter

paper for removal of any gross impurities, e.g. dust, on its surface.

2) The mercury is then treated for at least 8 hours with acidified mercurous nitrate solution by agitating it under dilute nitric acid by means of a stream of air drawn through it by means of a water pump; finally the Hg is washed in the same manner using distilled water.

3) The mercury is then passed from a funnel down a column of dilute nitric acid terminated by a u-tube containing CCl_4. This arrangement ensures that the mercury is delivered in a more or less dry state. The chemical oxidation (stages 2 and 3) removes traces of base metals but does not eliminate noble metal impurities. The above procedure is therefore followed by a distillation.

4) The clean mercury, delivered from the column, is then dried overnight in an atmosphere of nitrogen and distilled twice under moderately reduced pressure, with an air leak. This procedure

reduces the total concentration of metallic impurities to much less than one part per million of mercury.

(c) Acetonitrile: Acetonitrile used in part of the work was the Union Carbide grade 99% material; it was purified by the procedure of Mann et al.[79] which first involves distillation under dry nitrogen from potassium permanganate through a short column having ca. 3 theoretical plates. This operation was followed by acidification of the acetonitrile distillate with concentrated sulfuric acid and decantation from any precipitated ammonium sulfate. The acetonitrile was finally distilled from calcium hydride under dry nitrogen through a tall packed column having about 30 theoretical plates. The "middle" fraction was collected and stored in a glove box under a dry atmosphere (b.p. 1 atm = 81.6°C).

(d) Sodium perchlorate: "Anhydrous" sodium perchlorate (Anachemia) was dried under vacuum at 80° C for 24 hours. It was used as the supporting electrolyte for studies in various aqueous solutions

because the perchlorate anion is known for its minimal specific adsorption at the Hg surface.

(e) Potassium chloride: BDH "analytical reagent" grade potassium chloride was dried under vacuum at 60° C for 12 hours and used without further purification since the same results were shown to be obtained when a sample of KCl, doubly-recrystallized from water, was used; potassium chloride was used for standardization of capillaries in terms of the known surface tension of the Hg/aq.KCl interface at various potentials[80].

(f) Perchloric acid: BDH "analytical reagent" grade perchloric acid was used without further purification in the experiments on alkylammonium ion adsorption. Its initial strength was measured by means of a titration with standardized aq. sodium hydroxide.

(g) Hydrochloric acid: BDH "Aristar" grade hydrochloric acid was used without further purification.

(h) Sodium chloride: "analytical reagent" grade 99.9% sodium chloride was dried overnight at 60°C under vacuum.

(i) Urea: Anachemia "purified" grade urea was dried at 80°C under vacuum for 24 hours before use.

(j) n-propylamine*: Matheson Coleman and Bell n-propylamine was purified by distillation under dry nitrogen (B.P.: 47.8°C).

(k) Dipropylamine: Matheson Coleman and Bell dipropylamine was distilled under dry nitrogen at atmospheric pressure (B.P.: 109.4 - 110.4°C).

(l) Tripropylamine: This amine was obtained from Eastman Kodak Co. and distilled at reduced pressure under dry nitrogen (B.P.: 156°C).

(m) Tetrapropyl ammonium hydroxide: This compound (10% in H_2O) from Eastman Kodak Co. was used without further purification to prepare

---

* All the propylamine salts were those involving the straight-chain n-propyl group.

$(n\text{-}Pr)_4N^+ClO_4^-$ solutions by titration with the $HClO_4$ mentioned above.

2. Reference Electrodes

The silver-silver chloride electrode was used as the standard reference electrode in this work because normally potential measurements can be maintained stable to well within 1 mV and because good reproducibility is assured.

For studies in a non-aqueous solvent such as acetonitrile, most workers[81] have used reference electrodes (principally the calomel electrode) in an aqueous medium even though this has some disadvantages such as possible contamination of the solvent by water or difficulties in evaluation of the aq./non-aqueous solution liquid-junction potential.

The silver-silver chloride electrode was prepared as described by Janz[82]: a silver wire, welded to a platinum wire sealed in a glass tube, was soaked in concentrated ammonium hydroxide (16 hrs.),

washed with water for one day and then anodically chloridized in 0.1N hydrochloric acid solution. The electrode was washed in conductance water for 2 days before testing. For testing, the potentials of the new electrodes were measured relative to a previously prepared standard silver-silver chloride electrode and rejected if not satisfactory. Electrical contact with the reference electrode solution was made through a solution-wetted 7/25 ground joint to minimize diffusion of ions out the reference electrode compartment since the supporting electrolytes used in most of the work were aq. $HClO_4$ or $NaClO_4$.

3. Counter-Electrode

A platinum wire sealed to the Hg-collecting flask at the bottom of the working electrode compartment was used as the counter electrode in all the adsorption studies.

E. Measurement Procedure and Calibration of the Capillary

The cleaned dropping Hg cell was first washed several times with the solution under study and then filled with 50 ml of the electrolyte solution. The silver-silver chloride reference electrode was inserted into its compartment and dry nitrogen was bubbled through the solution for at least 30 minutes before the experiment was commenced. Then the cell was fixed to the capillary which was already dropping to avoid any wetting of the inside of the capillary. The optical drop timer unit was turned on and, by means of the oscilloscope, the position of the capillary was adjusted as accurately as possible so that drop-time measurements could be commenced.

The experiment consists in applying successively controlled potentials to the mercury electrode over a range of 0 to -1250 mV at 50 mV intervals after a constant delay of 30 seconds to enable adsorption equilibrium to be attained.

Consecutive drop-time values given by the electronic counter were recorded and an average drop-time was calculated. Each experiment was performed by executing consecutive positive and negative - going changes of potential and repeating each measurement at least twice within a short period of time. By plotting the drop-time (t) against the applied potential (E), typical electrocapillary curves were generated after applying the calibration factor described below.

Grahame, in one of his publications[83], gave accurate values for the surface tension of mercury in aqueous solutions of 0.1N KCl at 25°C for a range of potentials, including those studied in the present work. By repeating the experiment under the same conditions using the drop-time method, it is possible to reproduce the shape of the electrocapillary curve and calculate the capillary constant. The calibration of the capillary was based on equation (22) which gives, after integration,

$$\log \frac{\gamma_1}{\gamma_2} = K \log \frac{t_1}{t_2} \qquad (24)$$

where t_1 and t_2 are drop-times for a specific capillary and γ_1 (e.c.m.) and γ_2, the corresponding surface tensions, taking into account that γ_1 = 426.2 dyne cm^{-1} for 0.1N KCl at 25°C as established by Grahame[83]. Also, Verdier et al.[84], using Barradas and Kimmerle's γ-t relation (eqn. 23), were able, after some approximations, to relate the capillary constant K to the surface tension γ of mercury, as shown by the following equation:

$$\frac{1}{K} = 1 + \frac{20.2\ r^{2/3}}{3\ \gamma^{1/3}} + \frac{0.00912\gamma^{2/3}}{3\ h\ r^{1/3}} \qquad (25)$$

where r is the radius of the capillary bore and h, the pressure of mercury. A graph of K vs γ, based on eqn. (25), is reproduced here in Fig. 5 for various r and h combinations, including one (curve #5) used in the present work. As can be seen, the variation of K is very small ($\sigma = \pm$ 0.01%), for r = 4×10^{-3} cm and h = 100 cm, over the range of surface tension values studied in this work. K can therefore be considered constant. Once K for a specific capillary was determined, drop-time data for the mercury/solution interface under other conditions could be easily

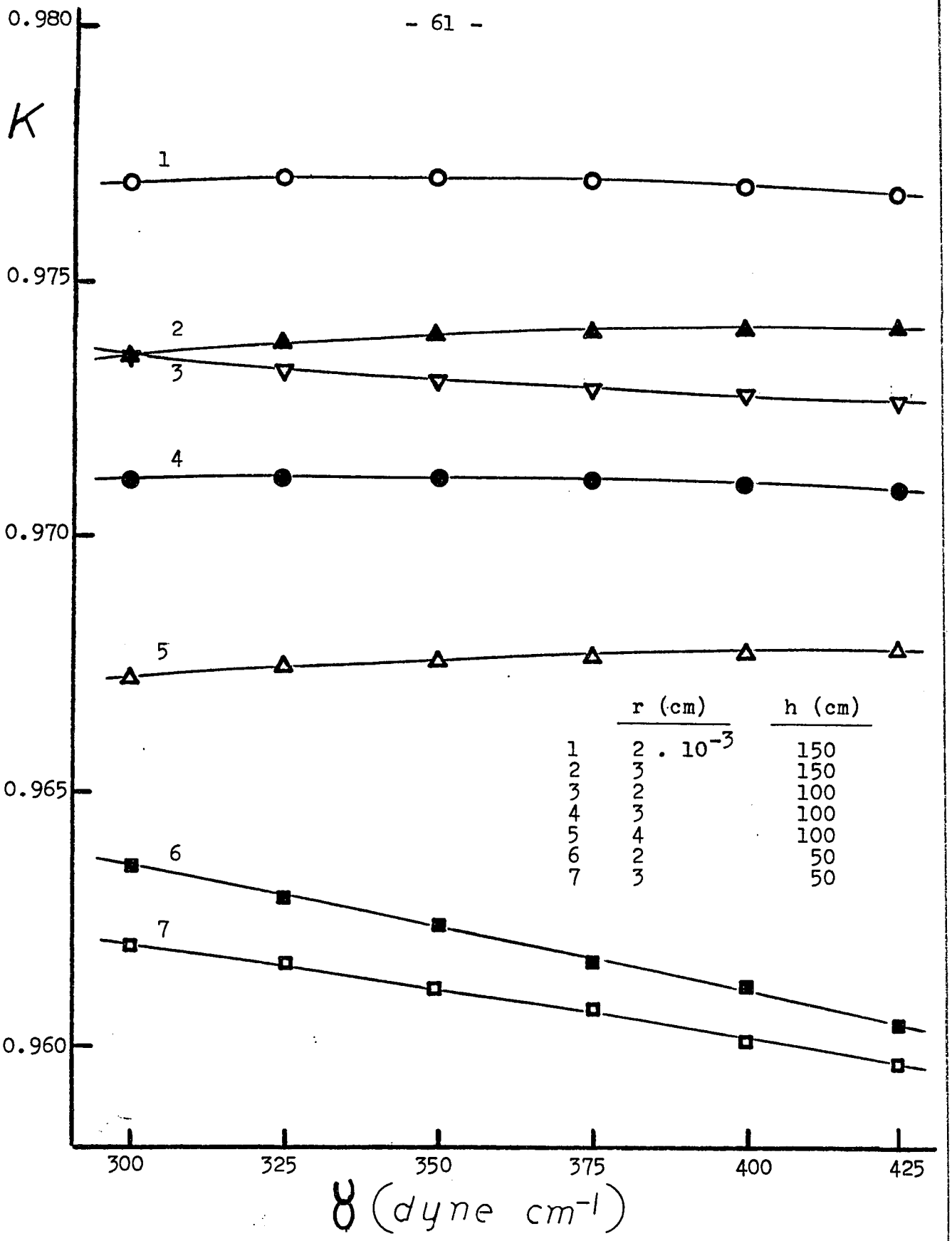

Fig. 5 Variation of the capillary constant K with the surface tension γ, the capillary bore r and the pressure of mercury h.

converted to respective surface tension values. The curves obtained for 0.1N KCl, the calibration solution, were superimposable on the one given by Grahame when coincidence between two points of the curve corresponding to two given potentials was arranged or when the curves were superimposed at the common p.z.c. The agreement with Grahame's results is shown in Table I and proves the reliability of the drop-time method as well as the accuracy of the drop-time tensiometer used and the procedure employed. Relative deviations from Grahame's data are shown as $\Delta\gamma$ in the last column of Table 1.

F. Sources and Estimation of Errors

Errors arise from two main sources: (a) those related to the apparatus and its manipulation and (b) those related to the interpretation and treatment of the experimental results by means of a computer program through curve-fitting approximations involved in the representation of the experimental points.

TABLE 1

Electrocapillary Data for 0.1N KCl at 25°C

E(N calomel)	γ	γ (pzc) $-\gamma$		$\Delta\gamma$
(mV)	(dyne cm^{-1})	calc. (Grahame)	obs.	(dyne cm^{-1})
100	395.6	30.6	29.8	0.8
150	403.3	22.9	22.4	0.5
200	409.4	16.8	16.1	0.7
250	414.6	11.6	11.2	0.4
300	419.0	7.2	6.9	0.3
350	422.3	3.9	3.7	0.2
400	424.4	1.8	1.6	0.2
450	425.7	0.5	0.5	0.0
500	426.2	0.0	0.0	0.0
550	425.8	0.4	0.3	0.1
600	424.9	1.3	1.2	0.1
650	423.5	2.7	2.5	0.2
700	421.4	4.8	4.5	0.3
800	415.7	10.5	10.0	0.5
900	408.3	17.9	17.6	0.3
1000	399.1	27.1	26.9	0.2
1100	388.4	37.8	38.1	0.3
1200	376.3	49.9	50.2	0.3

mean deviation: 0.3

1. Errors Related to Experimental Measurements

As mentioned above, the reproducibility of the drop-time measurements themselves is very satisfactory since a standard deviation of ± 0.02% or ± 0.1 dyne cm^{-1} was found for any individual run.

Following the procedure of Corbusier and Gierst[72] and Verdier et al.[84], the use of an average capillary constant* for the range of potentials studied is quite satisfactory since this constant can be determined precisely and since a standard deviation smaller than ± 0.01% is found. Although this is a high level of accuracy in the γ values, at least this accuracy is needed for reliable

*

Strictly the "capillary constant" is found to be slightly potential-dependent presumably because of variation of the shape of the drop at the moment of its detachment arising from change of γ with potential.

computation of the required derivative quantities based on curve-fitting by polynomial functions.

Another source of error can be the change of potential of the reference electrode in contact with solutions containing organic species. However, the silver-silver chloride electrode was found to be sufficiently stable for investigations in aqueous media. The reference electrode was checked regularly against another standard electrode of the same type in the solution under study. If the difference of potential between the two Ag-AgCl electrodes was larger than 1 mV, a new reference electrode was made.

Electrocapillary curves under given conditions could be reproduced for all the compounds (except those studied in acetonitrile; see below) in the potential range - 50 to -1250 mV to within 0.5 dyne cm^{-1} or better, depending on the potential range.

2. Errors Introduced in Evaluating Results

Knowledge of the activity coefficients of the species in solution is a formal requirement for the evaluation of the surface excess (Γ) quantities from the surface tension results. Activity coefficient data were not available for most of the organic compounds studied. However, for calculations involving urea, molal activity coefficients given by Stokes[85] were used since the range of concentrations was extended up to 2.5M. For all other compounds, activity was replaced by the molar concentration taking into consideration that activity coefficients were probably near to one (the maximum concentration being 0.5M).

The use of a computer program for calculation of double-layer parameters is another possible source of errors; this is why the curve fitting of experimental points must be as precise as possible. For this reason, it is desirable that electrocapillary curves be obtained with points at closely spaced intervals of potential and

concentration (about 6 points were taken per decade of concentration change). A third-order polynomial was found to give the best fit for the experimental curves after comparison with fitting by $n^{\underline{th}}$ order polynomials, with n = 1,2,3,4, using an appropriate computer program. Some third-order fits for several compounds are shown in Fig. 6.

G. Sizes of Molecules

In the interpretation of results, the "sizes" of the various adsorbate molecules are required independently of estimates that may be made from saturation coverages, Γ_m, derived from isotherms. In many cases, such Γ_m values can be ambiguous depending on packing or molecular orientation. Values of Γ_m were therefore calculated from projections of Courtauld space-filling molecular models. (Table 3). The dimensions of these models are based on various considerations concerned with bond-lengths and Van den Waals radii as discussed by Hartley and Robinson[86].

CHAPTER III

RESULTS

A. Computer Evaluation of Drop-Time Results

The essential parameters for the adsorption behavior of various compounds were obtained from the primary surface tension results using a computer program similar to the one described by Lawrence et al.[87] and employed previously by Dhar[47] in this Laboratory. The quantities calculated were, q_M, the surface charge density, Γ the relative surface excess, ϕ_q, the surface pressure and ΔG^o_{ads}, the standard free energy of adsorption.

The surface charge density, q_M, was determined using the following procedure: for a particular electrocapillary curve, Parson's ξ function (eqn. 26 below) was computed for various values of q_M. For a given value of q_M, equation 26 has a maximum at a value of E determined by:

$$\xi = \gamma + q_M E \qquad (26)$$

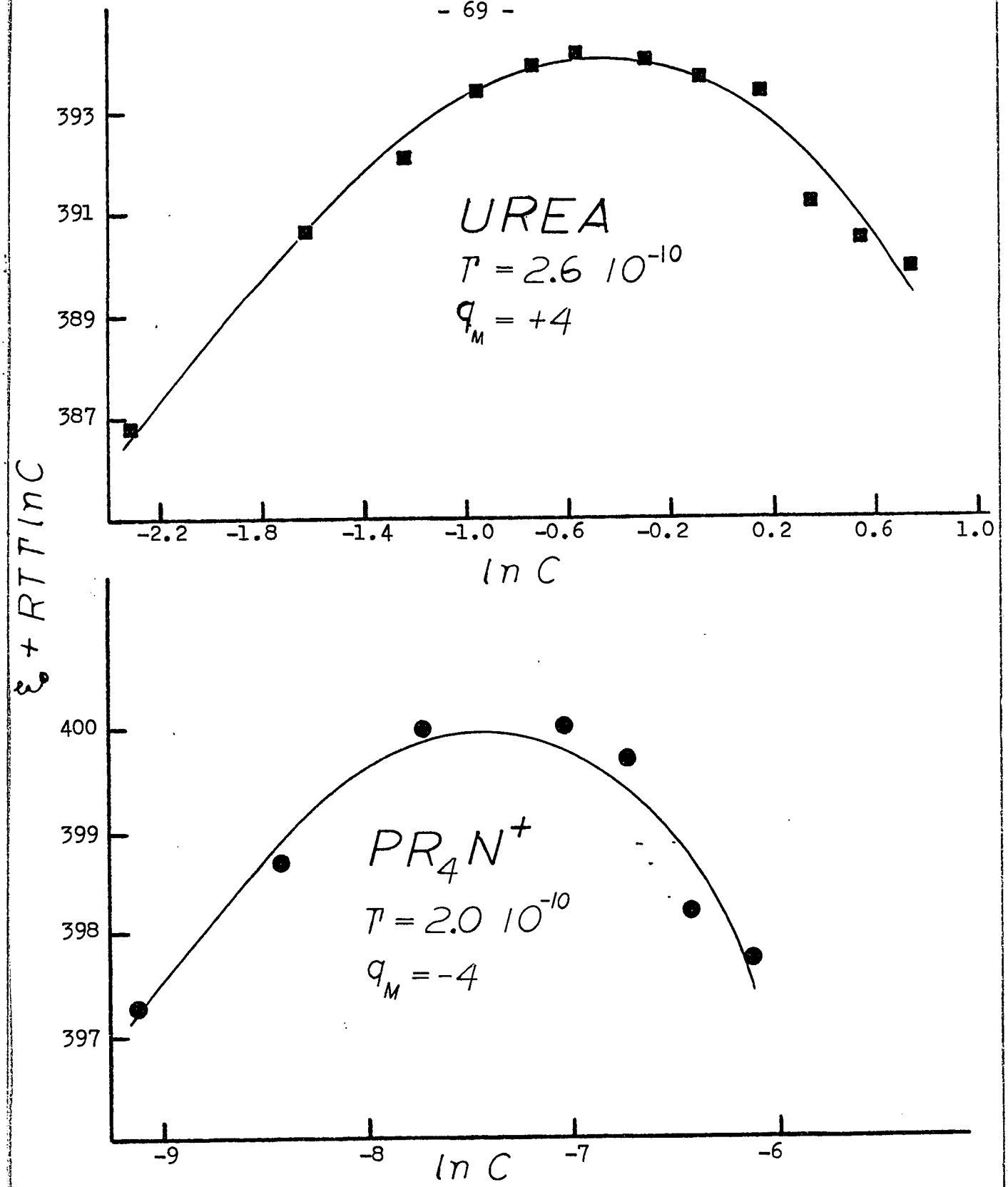

Fig. 6 Plots showing curve-fitting in a 3rd order polynomial for two compounds. ■ and ● are experimental points and —— smooth curves represent best fits through the points.

for which q_M is the slope of the electrocapillary curve. Thus, differentiating $\xi = f(E)$, gives

$$\frac{d\xi}{dE} = \frac{d\gamma}{dE} + q_M = 0 \quad \text{at the maximum} \qquad (27)$$

Hence, $\frac{d\gamma}{dE} = -q_M$

is evaluated.

Then, instead of fixing E and differentiating the electrocapillary curve at that point to obtain the q_M at that value of E, a value of q_M is chosen for which E and γ are determined.

By applying the Gibbs adsorption equation to surface tension measurements, the surface excess Γ of a species is obtained from the plot of interfacial tension versus log activity (or concentration) of the electrolyte, taken under conditions of constant measured electrode potential E as represented by the following equation (29)

$$\Gamma_E = -\left[\frac{\partial\gamma}{RT\ \partial \ln c}\right]_E \qquad (29)$$

When evaluating Γ as a function of q_M, the thermodynamic equation is transformed in the following manner in terms of the ξ function:

$$\Gamma_{q_M} = - \left[\frac{\partial \xi}{RT \; \partial \ln c} \right]_{q_M} \tag{30}$$

In this case, at a constant value of q_M, the maximum of the curve:

$$y = \xi + RT\Gamma \ln c \tag{31}$$

gives the value of c for a chosen value of Γ. Therefore, Γ vs c, or Γ vs $\log c$ relations can be computed at different q_M values.

The surface pressure ϕ_q at constant q_M is defined as $\phi_q = \xi_b - \xi$ where ξ_b refers to zero concentration of adsorbate (supporting electrolyte solution); it is determined by the change of surface tension caused by the adsorbate after allowance for electrical effects in the term "$q_M E$". ϕ_q is a two-dimensional "spreading" pressure of the adsorbate, analogous to that directly measurable with a Langmuir trough at a liquid/vapour interface.

B. Adsorption of Urea

1. Electrocapillary Curves

As established by crystallographic measurements, urea shows a structure identical to that of thiourea, $(NH_2)_2CS$, which is planar, probably including the H atoms; this molecule has a dipole moment of 4.56D compared to 4.89D for thiourea.

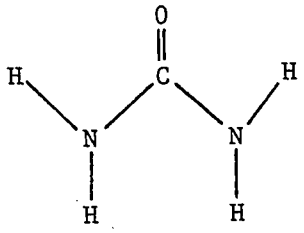

The adsorption of urea was studied from a supporting electrolyte of 0.1M $NaClO_4$ solution. Electrocapillary curves based on 25 electrode potential points were obtained in the potential range -50 to -1250 mV. Measurements were made at 27°C and for the following molar concentrations: 0.1, 0.2, 0.3, 0.4, 0.5, 0.6, 0.8, 1.0, 1.3, 1.6, 2.0, 2.5. A 0.1M NaCl/Ag-AgCl half-cell was used as the reference electrode. The reference and the working electrode compartments were maintained at a constant temperature to avoid any thermal junction potential in the electrolyte.

Experimental electrocapillary curves for this compound are shown in Fig. 7. Inspection of the electrocapillary curves is the first step in the interpretation of the adsorption behavior: even if it is not always easy to interpret quantitatively those curves, one can see that, in a general way, urea is preferentially adsorbed when the Hg surface is negatively charged so that the urea is presumably oriented with its NH_2 groups towards the Hg surface.

Determination of the useful concentration range over which to conduct the experiment is established by a plot of surface tension vs ln a (Fig. 8): the activity coefficient data required for this plot was taken from the work of Stokes[85]. The lower limit corresponds to the concentration where $-\Delta\gamma/\Delta\ln a$ tends toward zero; the upper limit is given by the region where the slope tends toward a constant value, corresponding to saturation coverage. In the case of urea, saturation coverage was not reached, even at a concentration of 2.5 M, but was approached. It was therefore necessary to evaluate the maximum surface excess value, Γ_m, from Courtauld molecular

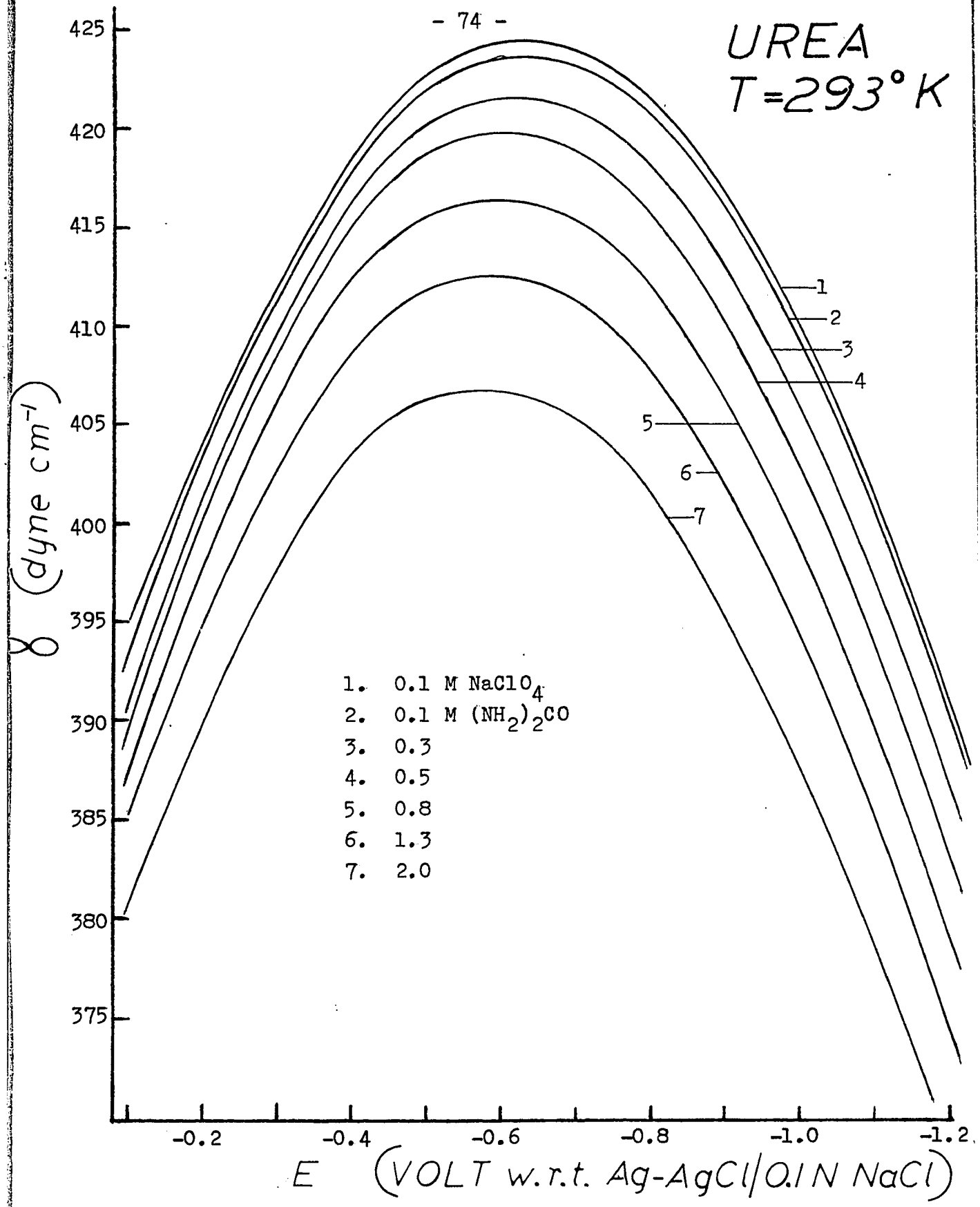

Fig. 7 Electrocapillary curves (based on γ values at 50 mV intervals) for adsorption of urea from aq. 0.1 M $NaClO_4$ solution.

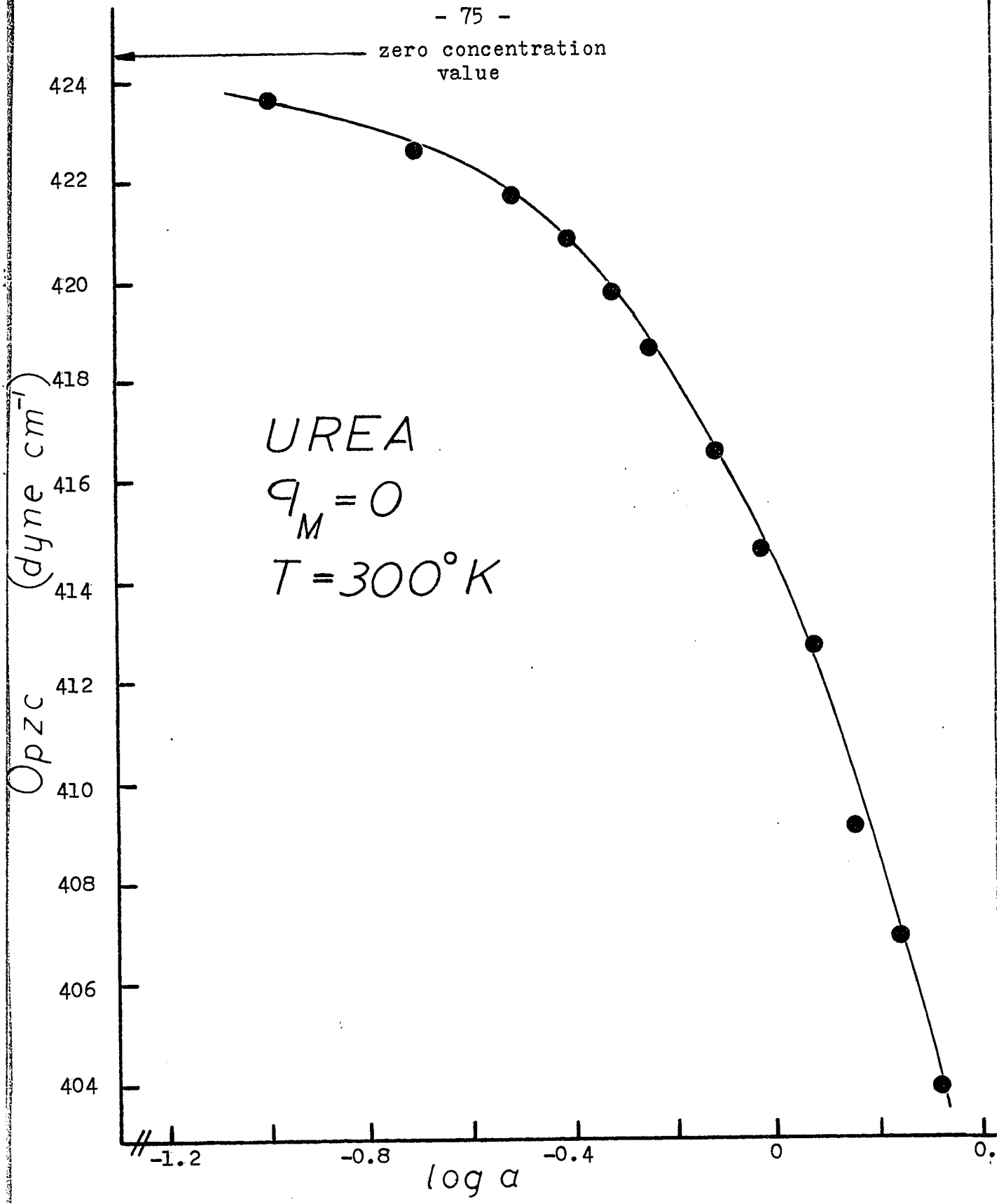

Fig. 8 Surface tension as a function of activity (log a) of urea for zero surface charge density.

models. From an estimate of the Γ_m value approached experimentally, it was possible to come to some conclusion concerning the orientation of urea with respect to the mercury electrode surface.

2. Surface Excess Values

The evaluation of several plots of surface excess (Γ) vs log a (Fig. 9) for urea at various surface charges, q_M, shows that the maximum surface excess value, $\Gamma_m = 9.3\ 10^{-10}$ mole cm^{-2}, corresponds fairly well to the one calculated with the Courtauld molecular models for a molecule of urea oriented perpendicularly with respect to the mercury electrode.

Fig. 10 shows plots of Γ vs q_M for urea at various bulk concentrations (activities). Inspection of these curves shows that the surface coverage increases with increasing negative charge for a given log a, which suggests that the molecule tends to sit with its two NH_2 groups on the surface while the oxygen atom is oriented towards the solvent.

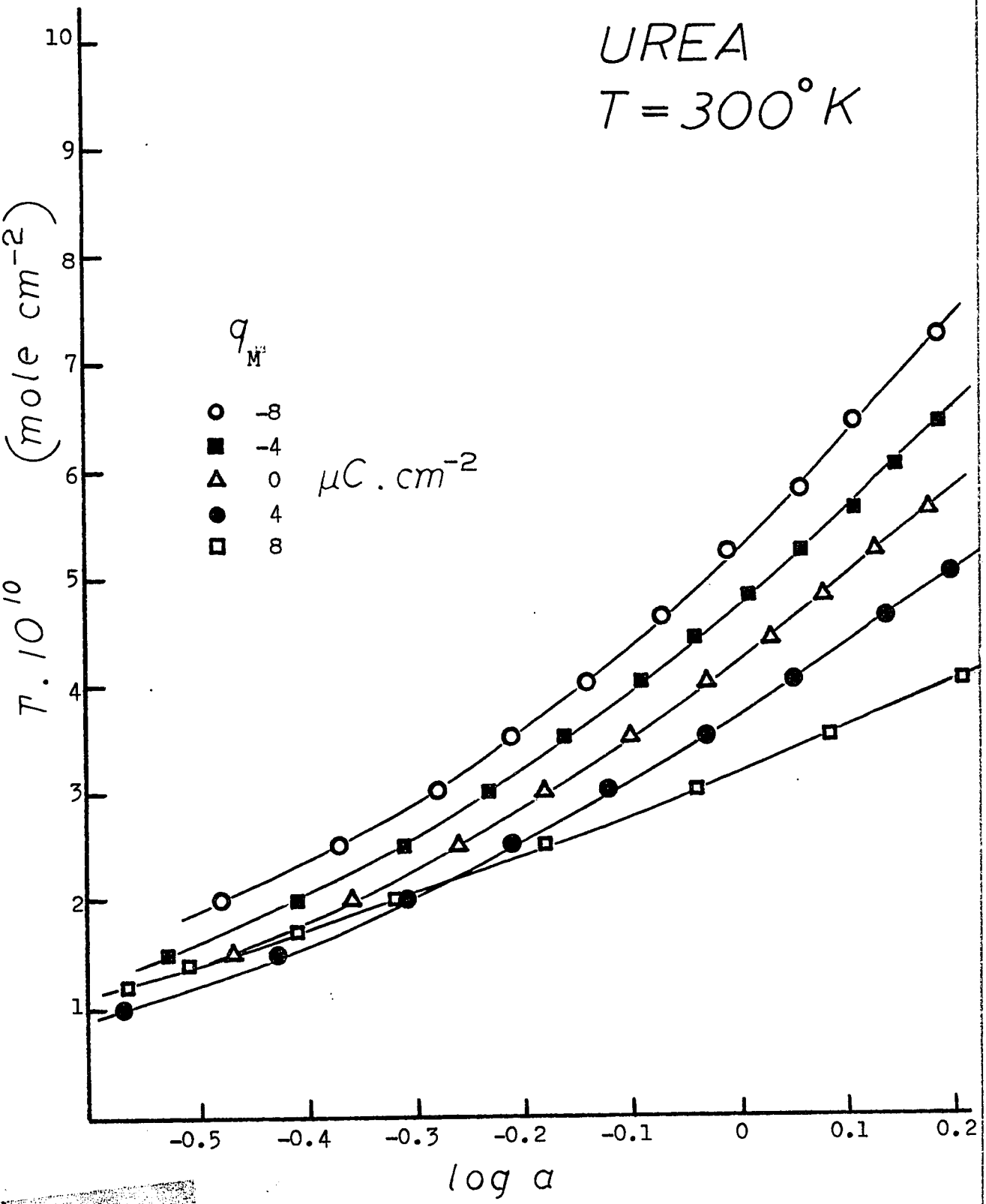

Fig. 19 Plots of Γ versus log a for urea at various values of q_M.

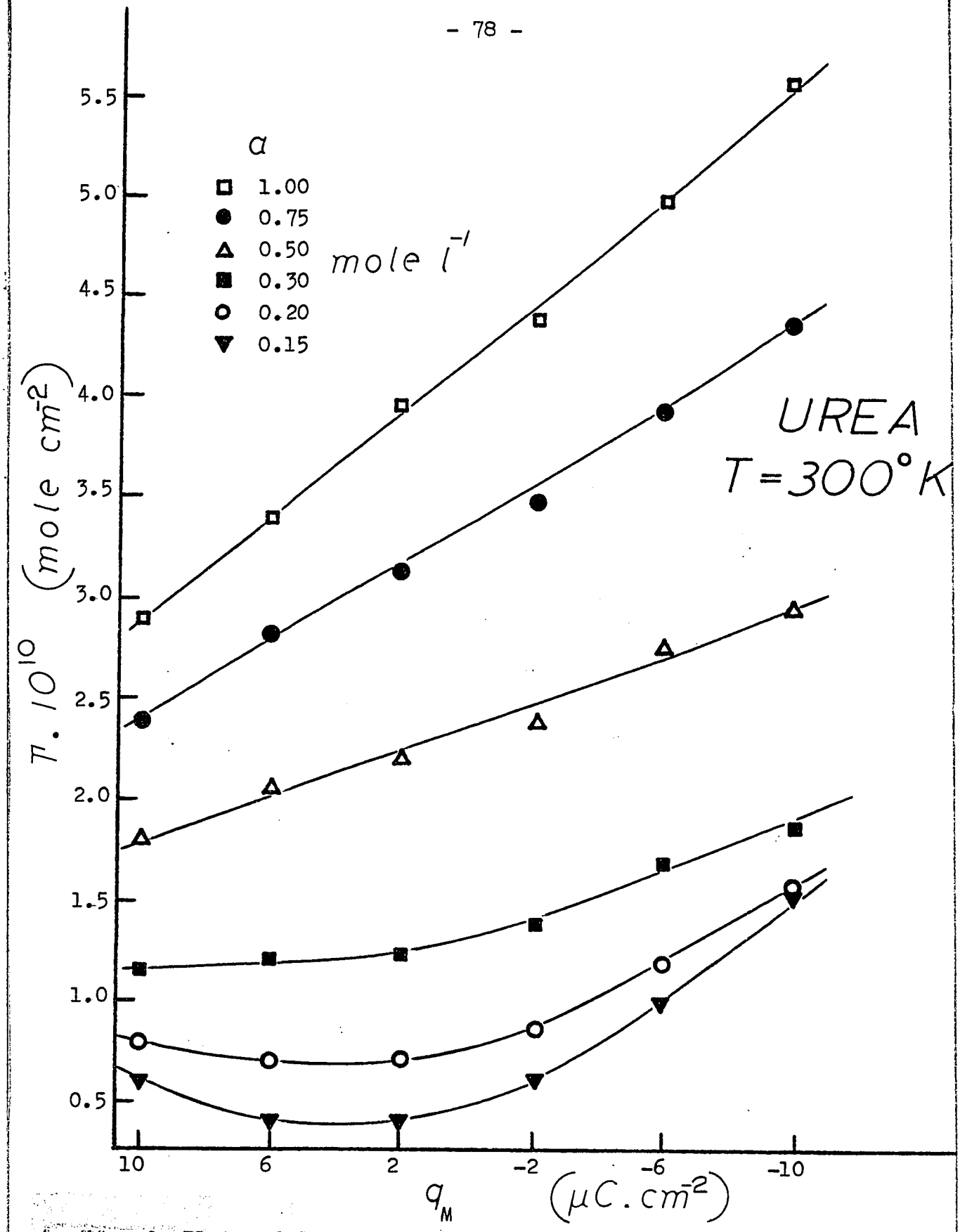

Fig. 10 Plots of Γ versus q_M for various urea bulk activities.

At lower concentrations and for q_M values more positive than +5 $\mu C\ cm^{-2}$, the behaviour becomes more similar to that for thiourea[57] viz, the NH_2 groups become somewhat oriented towards the solvent. However, this behavior disappears rapidly with increasing bulk concentration.

3. Esin and Markov Plots for Urea Adsorption at Hg

In studies on the double-layer and adsorption at Hg electrodes, it is always useful to make "Esin and Markov" plots, i.e. the shift of the potential ΔE_{q_M} for a given q_M value with log c or Γ. Historically, plots for the particular case $q_M = 0$ were made but the procedure can be generalized for any q_M value. For specifically adsorbed molecules or ions, the plots of ΔE_{q_M} vs Γ or log c give information on the change of potential drop in the inner layer due to (a) orientation of adsorbed molecular dipoles; (b) displacement of previously adsorbed and oriented solvent dipoles and (c) changes of adsorption of ions.

A series of Esin and Markov plots for urea adsorption is shown in Fig. 11 for q_M values from + 6 to - 8 $\mu C \cdot cm^{-2}$. The shifts of potential, ΔE_{q_M}, are defined as the difference E_{q_M} (adsorbate solution) - E_{q_M} (base solution). They show two regions similar to those observed with pyridine adsorption[47] where (a) solvent displacement and (b) orientation of adsorbate dipole characterizes the electrical behavior.

C. Adsorption of $Pr_nN^+H_{4-n}$ Perchlorate Salts

1. Protonation Equilibria in Adsorption of Bases and their Ions

Organic aliphatic bases (RN) become almost completely ionized in 1 N aq. $HClO_4$ according to the formal reaction:

$$RN + HClO_4 \longrightarrow RNH^+ + ClO_4^- \qquad (32)$$

i.e.
$$RN + H_3O^+ \longrightarrow RNH^+ + H_2O \qquad (33)$$

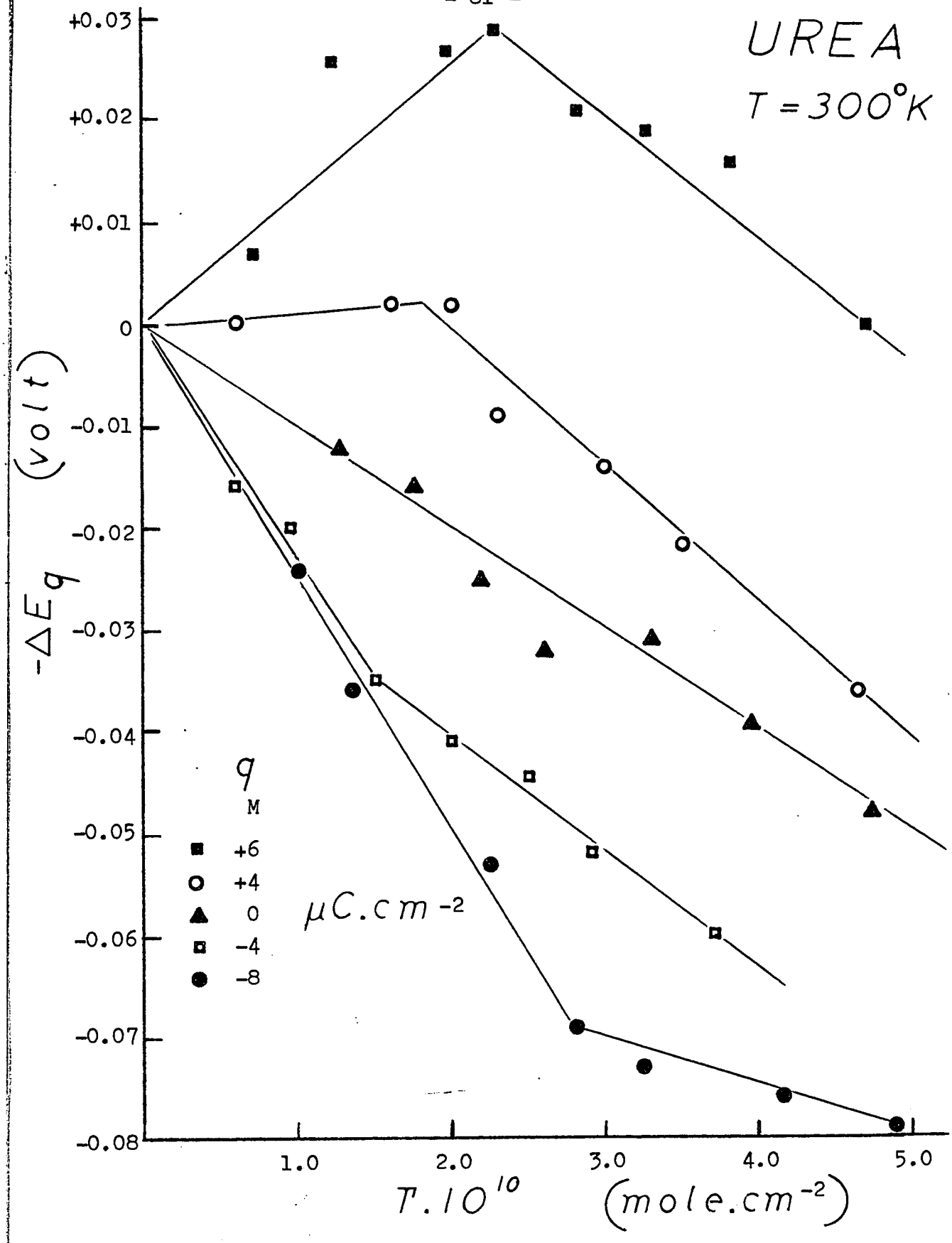

Fig. 11 Esin and Markov plots for urea adsorption at Hg for various q_M values.

Blomgren and Bockris[88] gave a thermodynamic treatment for adsorption from ionized base systems and concluded that the surface excess for amines must be defined strictly as:

$$(\partial\gamma/\partial\mu_{RN})_{q_M} = -(\Gamma_{RN} + \Gamma_{RNH^+}) \qquad (34)$$

due to the simultaneous presence, in principle, of both neutral RN species and protonated molecules RNH^+. Therefore, without knowledge of Γ_{H^+} and $\Gamma_{ClO_4^-}$ one cannot strictly exclude adsorption of the neutral molecule species. However, for amines having high pK_a values and for an excess of $HClO_4$, $C_{RNH^+} \gg C_{RN}$, so that the total surface excess is to a very good approximation equal to that of the protonated amine, Γ_{RNH^+}. Thus, in e.g. 1.0N $HClO_4$ with 0.1N amine solution, the extent to which neutral RN is present is only 10^{-9}M which is entirely negligible in relation to the concentration of RNH^+ ions. In fact, the ratio $[RN]/[RNH^+]$ is obviously defined simply by $K_a/[H^+]$.

The role of ionization in adsorption of organic bases was studied by Conway and Barradas[89]

by comparing the free energies of adsorption of N-compounds in their predominantly neutral or ionized forms.

In the present work, all solutions were prepared by diluting the organic base, αM Pr_nNH_{3-n} (or Pr_4NOH), with 1M $HClO_4$, so that the final solutions contained 1M ClO_4^-, αM (Pr_n N^+H_{4-n}) and $(1-\alpha)M$ H^+, i.e. the ClO_4^- concentration was maintained constant. The advantage of these conditions is that changes of amine concentration in excess $HClO_4$ correspond to changes of the concentration of the ammonium type ion so that the Γ value derived from the changes of γ applies to a good approximation to Γ for the adsorbed cation only.

For each ammonium-type perchlorate salt, electrocapillary curves were obtained in the potential range -50 to -1250 mV at 27° C. A 1M perchloric acid solution was used as the supporting electrolyte. An Ag-AgCl electrode in a solution of 1.0M HCl was used as the reference electrode.

2. Adsorption of n-Propylammonium-Type Ions, $R_nN^+H_{4-n}$ $(1 \leq n \leq 4)$

The structure and properties of a particular alkyl ammonium-type ion are determined by the nature and the number of substituents around the tetrahedral N atom; for four equivalent H atoms or R groups, the structure is tetrahedral with a bond angle of about 109.5^o. However, as soon as an H atom is replaced in NH_4^+ by an R group, the interactions around the N atom are changed so that the previously tetrahedral structure can be somewhat modified; however, the sp^3 hybridization at N is maintained; the nature and the number of alkyl chains will be an important factor determining the distance of closest approach of the N^+ center to the mercury surface and the accessibility of the N^+ center to water with regard to hydration.

In the case of the n-propyl ammonium ion, the molecule has a quasi-linear structure determined by the single propyl chain; therefore this ion can present only two main orientations with respect to the Hg surface, parallel or perpendicular.

The series of three n-propyl ammonium perchlorates ($n = 1,2,3$) were studied in excess $HClO_4$ by adding appropriate quantities of the required alkylamine base to aq. $HClO_4$ to generate the required alkyl ammonium ion for $n = 1,2$ and 3 according to reactions of the form:

$$(n\text{-}Pr)_nNH_{3-n} + H_3O^+ \longrightarrow (n\text{-}Pr)_nN^+H_{4-n} + H_2O \qquad (35)$$

The tetra n-propylammonium salt $(n\text{-}Pr)_4N^+ClO_4^-$ was prepared by addition of the corresponding hydroxide to the aq. $HClO_4$ supporting electrolyte solution.

Various concentration ranges were studied depending on (a) the solubilities of the $(n\text{-}Pr)_nN^+H_{4-n}$ perchlorates in aq. $HClO_4$ and (b) the adsorbabilities of the organic cations since the least adsorbable species (n=1) requires a range of higher concentrations than those for a more adsorbable species if a reasonable range of coverages is to be covered. In all cases, the organic cation tends to be more strongly adsorbed when q_M is negative as

expected on electrostatic grounds.

Various orientations of the four ions of this series can be envisaged depending on the direction of the alkyl chains with respect to the Hg surface. For n=1, the alkyl chain can be parallel or perpendicular to the surface. For n=2, the orientation is difficult to define since the two n-Pr chains can rotate quite freely around the N^+ center and thus adopt various conformations as shown by molecular models. The orientation of the Pr-N-Pr plane with respect to the Hg surface will determine the orientation of the ion.

The experimental results for this series of ions are shown in several families of Figures, as follows:

the electrocapillary curves: Fig. 12.

the Esin and Markov plots (ΔE_q vs log c): Fig. 13.

plots of γ vs log c: Fig. 14.

plots of E_{pzc} vs log c: Fig. 15.

plots of Γ vs log c: Fig. 16.

plots of Γ vs q_M for various bulk concentrations: Fig. 17.

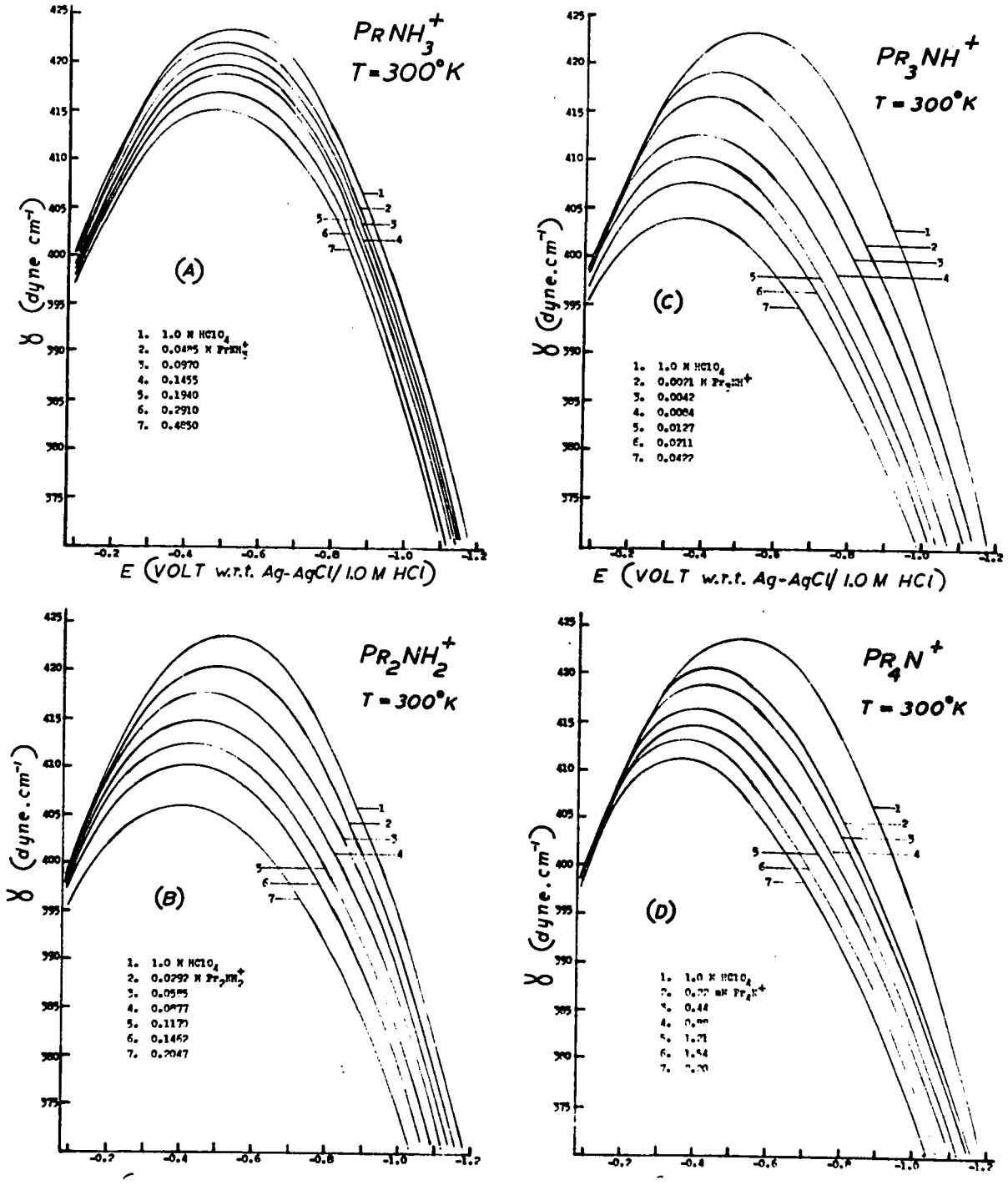

Fig. 12 Electrocapillary curves (based on γ values at 50 mV intervals) for adsorption of n-propylammonium cations from aq. 1M $HClO_4$ solution. (a) $PrNH_3^+$; (b) $Pr_2NH_2^+$; (c) Pr_3NH^+; (d) Pr_4N^+.

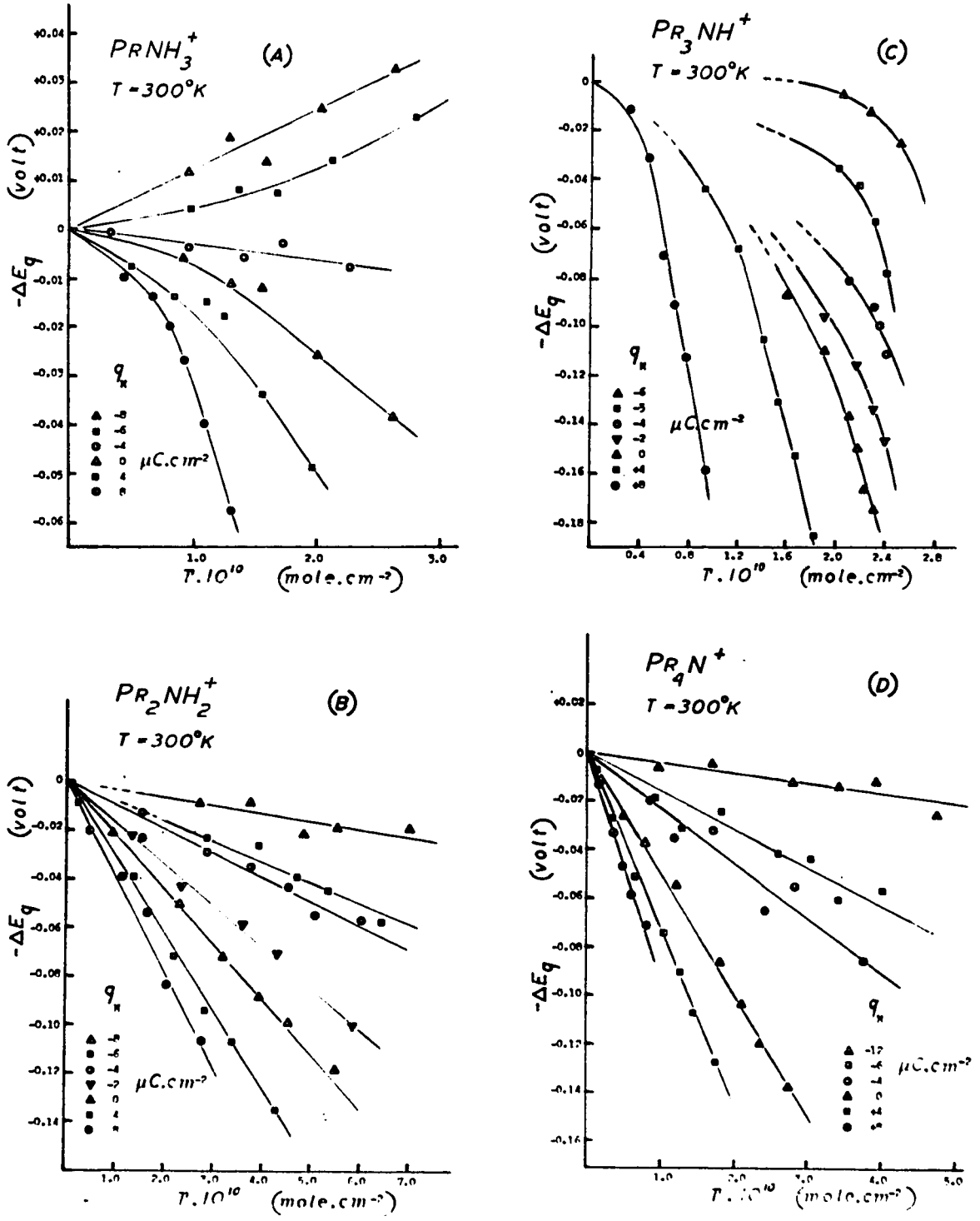

Fig. 13 Esin and Markov plots for n-Pr-ammonium cations adsorption at Hg for various q_M values. (a) $PrNH_3^+$; (b) $Pr_2NH_2^+$; (c) Pr_3NH^+; (d) Pr_4N^+.

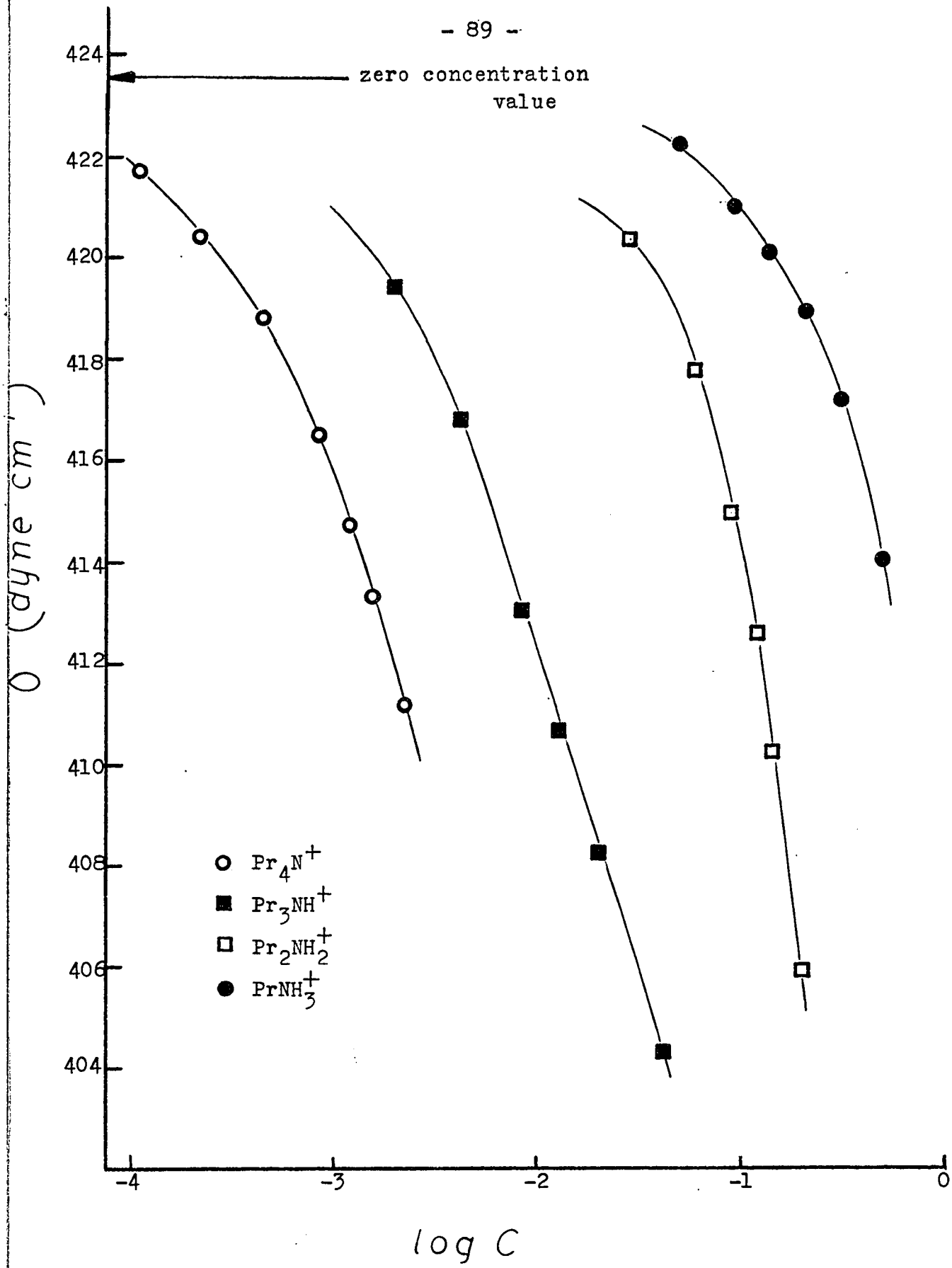

Fig. 14 Surface tension as a function of concentration of alkylamines in 1 M $HClO_4$ for zero surface charge density.

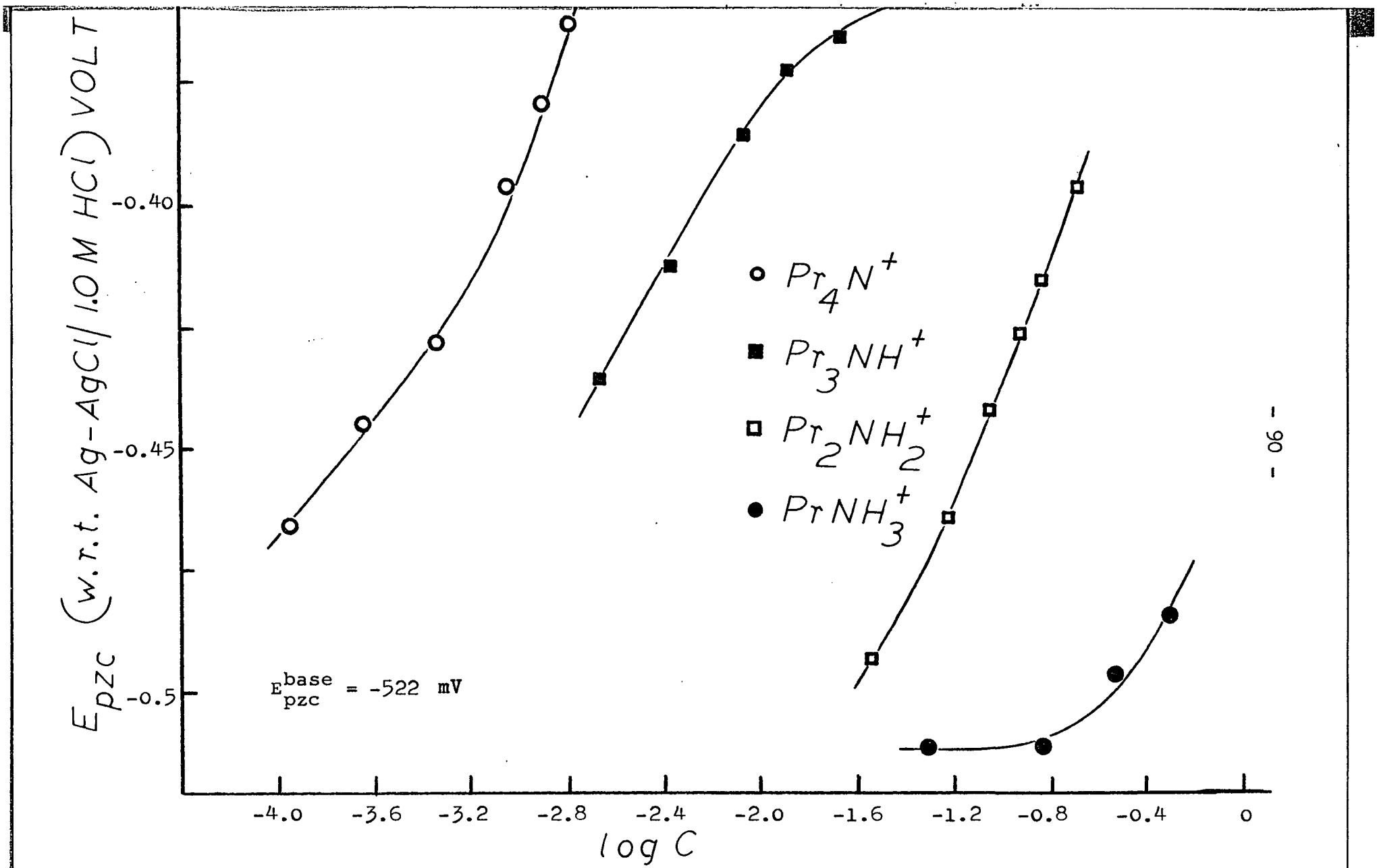

Fig. 15 Shift of the E_{pzc} as a function of concentration of alkylamines in 1M $HClO_4$.

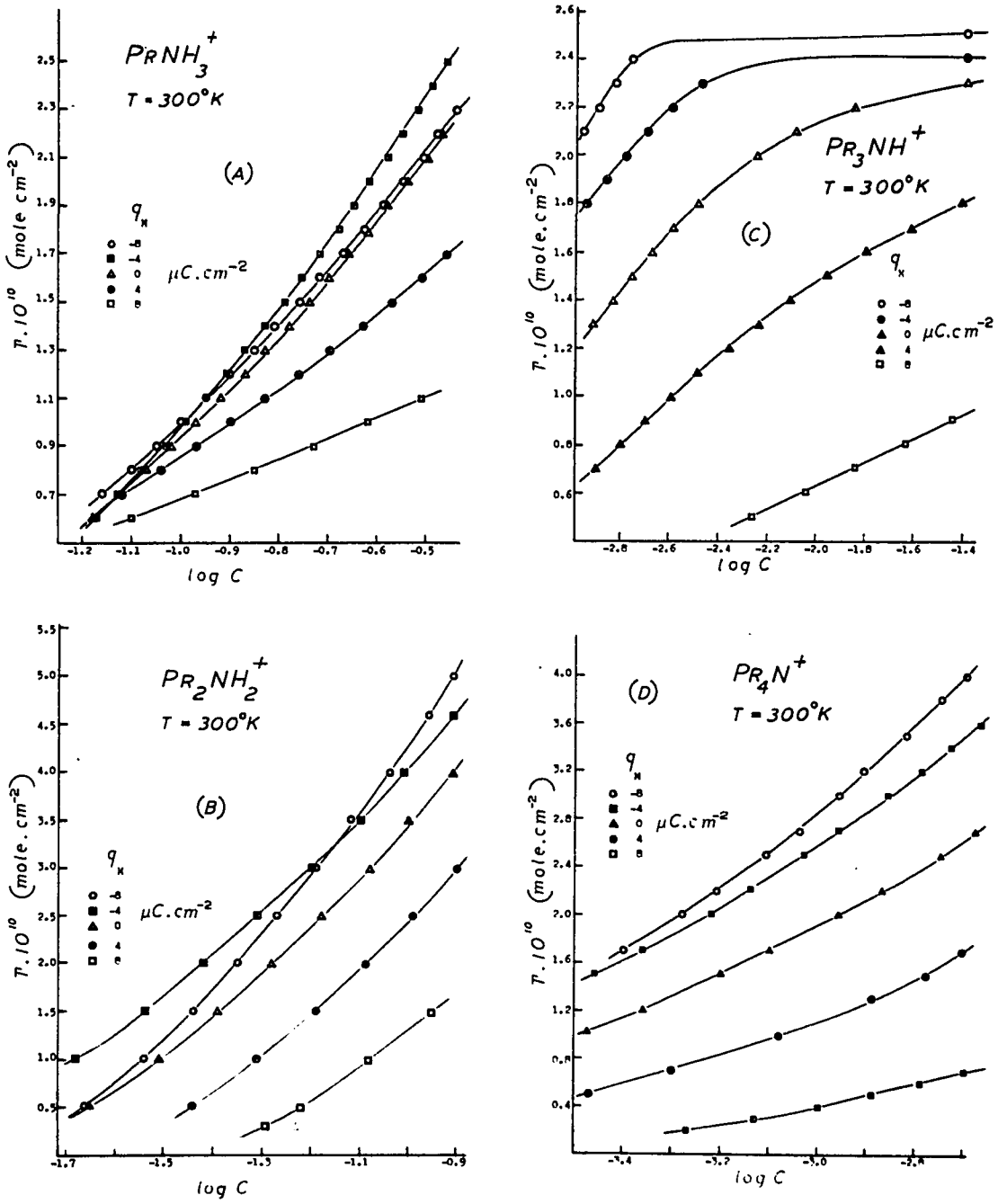

Fig. 16 Plots of Γ versus log c for n-Pr-ammonium cations in 1M $HClO_4$ at various values of q_M. (a) $PrNH_3^+$; (b) $Pr_2NH_2^+$; (c) Pr_3NH^+; (d) Pr_4N^+.

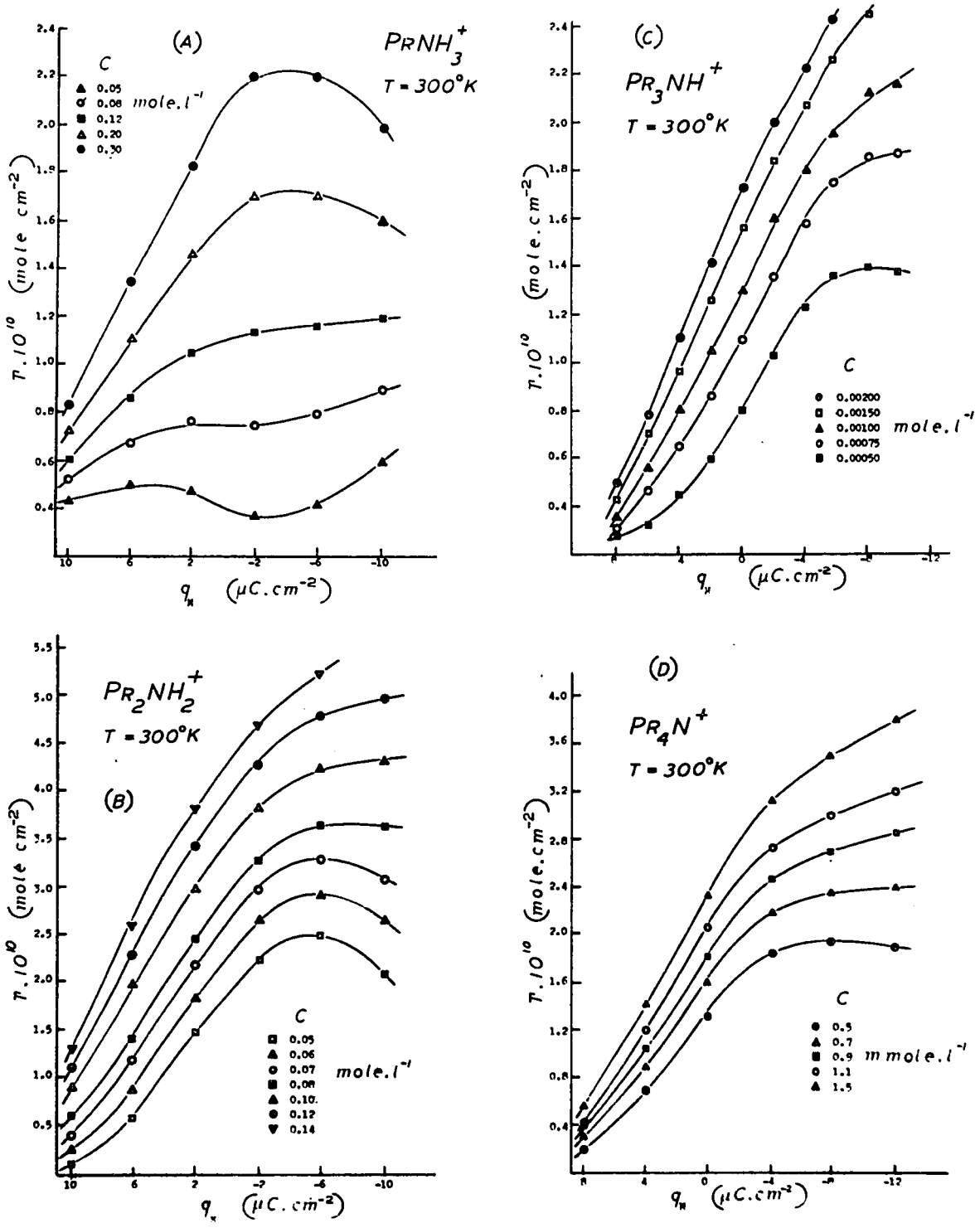

Fig. 17 Plots of Γ versus q_M for various n-Pr-ammonium cations bulk concentrations. (a) $PrNH_3^+$; (b) $Pr_2NH_2^+$; (c) Pr_3NH^+; (d) Pr_4N^+.

The increase of adsorbability in the series of n-Pr-ammonium ions with increasing n is shown in Fig. 14 where several plots of γ at the p.z.c. vs log c are compared. This order corresponds to increasing hydrophobicity and decreasing accessibility of the N^+ charge-center to H_2O dipoles of the solvent.

The increasing adsorbability with increasing numbers of propyl chains is also indicated by the plots of surface charge as a function of applied potential: (a) with regard to the effects of increasing concentration of the ammonium-type ion, Fig. 18 shows q_M vs E curves as a function of concentration of $(n\text{-Pr})_4N^+$; it is seen that the charge for a given potential positive to the "cross-over point" becomes less positive and for a more cathodic potential becomes less negative as the concentration of the ammonium-type ion increases; this is analogous to the Esin and Markov effect $(dE/d\ln c)_{q_M}$; here the quantity is $(dq_M/d\ln c)_E$ and reflects the increase of specifically adsorbed cation charge with log c and with size of the organic ion.

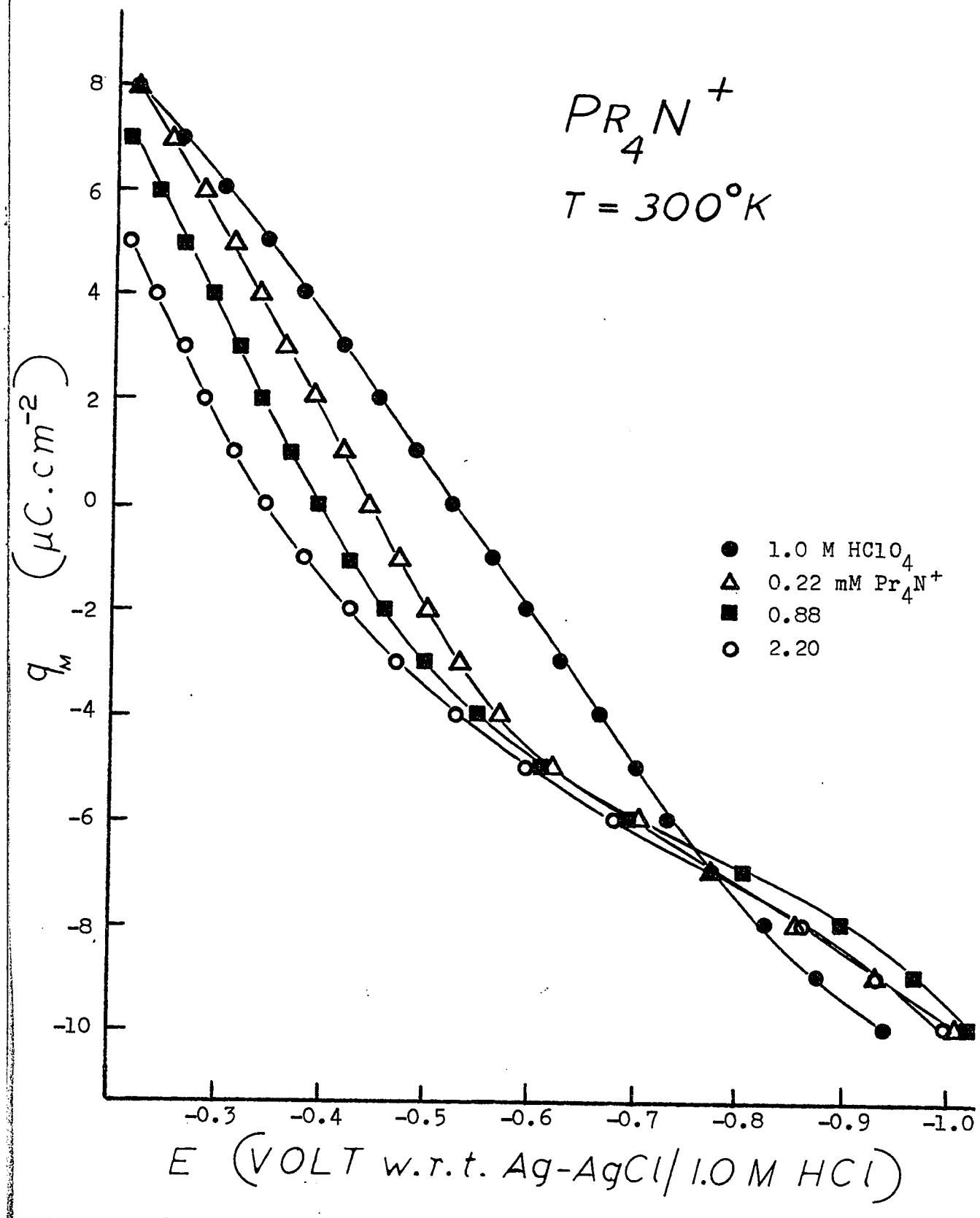

Fig. 18 Surface charge density as a function of applied potential for Pr_4N^+ at various bulk concentrations.

(b) considering the nature of the ammonium-type ion, Fig. 19 shows q_M *vs* E curves as a function of the identity of the species adsorbed: at constant electrode coverage, (Γ/Γ_m), the deviation of q_M values from those for the base electrolyte curve becomes more pronounced as n increases.

Plots of Γ *vs* log c (Fig. 16d) for Pr_4N^+ at various q_M values show that surface coverage for this cation does not reach saturation within the range of concentrations studied because of the problem of the low solubility of Pr_4NClO_4 in $HClO_4$. Fig. 17d shows plots of Γ *vs* q_M for various bulk concentrations: these curves demonstrate that surface coverage increases with increasing negative surface charge until it remains more or less constant as $q_M < -6\ \mu C\ cm^{-2}$ for each concentration but at Γ values less than Γ_m, the saturation surface excess.

3. Comparison of Esin and Markov Plots for Adsorption of the Alkylammonium Cations at Hg

As shown earlier (see section B.3 in this

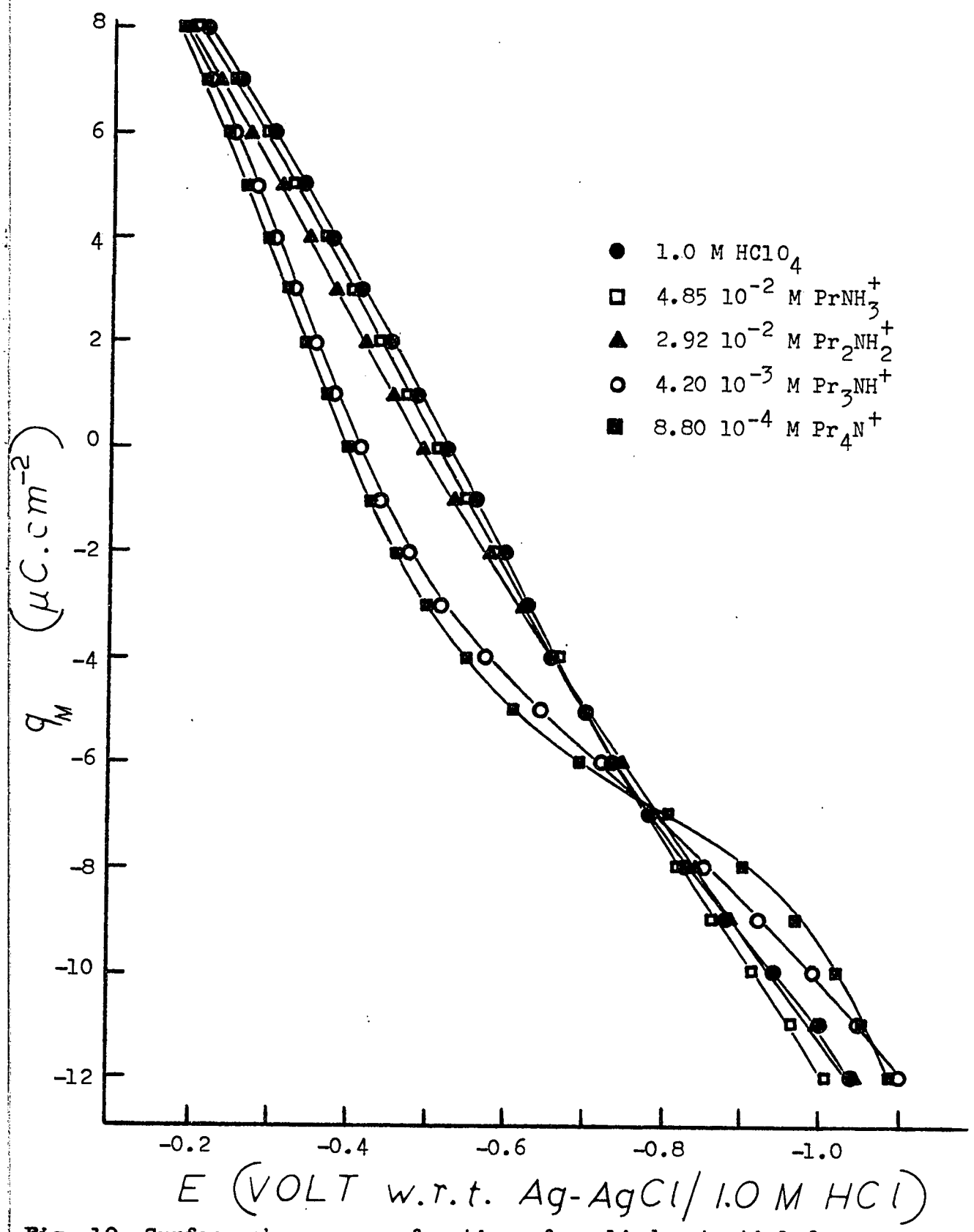

Fig. 19 Surface charge as a function of applied potential for alkylamines at a constant electrode coverage of ca. $\theta = 0.2$

chapter) for the case of urea, it is useful to plot ΔE_{q_M} *vs* log c or Γ for the adsorbed species. A series of such plots for the normal, secondary, tertiary and quaternary propylammonium cations in $HClO_4$ are shown in Fig. 13. The plots cover a range of q_M values from -12 to +8 $\mu C.cm^{-2}$. For $(n\text{-}Pr)NH_3^+$, ΔE_{q_M} takes both positive and negative values as q_M is increased from -8 to 8 $\mu C.cm^{-2}$. This behaviour is analogous to that of pyrazine at Hg. With $(n\text{-}Pr)_2NH_2^+$ and $(n\text{-}Pr)_3NH^+$ (Figs. 13b and 13c) the trend of ΔE_{q_M} is to increasingly positive values, from near zero, as q_M is increased from -8 to +8 $\mu C.cm^{-2}$. With the $(n\text{-}Pr)_4N^+$ salt, the trend of ΔE_{q_M} is similar to that in Fig. 13b for $(n\text{-}Pr)_2NH_2^+$.

The slopes (or initial slopes) of the Esin and Markov lines of Figs. 13a to 13d are tabulated below as a function of q_M.

Table 2

Esin and Markov Slopes as a Function of Surface Charge q_M for the n-Propyl Ammonium Salt Series

$(dE/d\Gamma)_{q_M}$ $\left[\text{Volt cm}^2 \text{ mole}^{-1} \times 10^7\right]$

q_M	$(n\text{-Pr})NH_3^+$	$(n\text{-Pr})_2NH_2^+$	$(n\text{-Pr})_3NH^+$		$(n\text{-Pr})_4N^+$
			Initial(±20%)	Final(±10%)	
-12	———	———	———	———	4.0
- 8	-12.3	3.2	3.9	140	———
- 6	- 5.2	8.4	17.0	150	16.0
- 4	3.3	10.0	39.0	145	22.0
- 2	———	17.0	———	———	———
0	7.6	22.0	47.0	170	50.0
4	15.0(±20%)	31.0	51.0	195	73.0
8	24.6(±20%)	39.0	71.0	265	94.0

All data are for a 1 N aq. $HClO_4$ supporting electrolyte solution.

D. Problems with Studies in Acetonitrile

Initially, the project proposed for this research work was the study of adsorption of some neutral molecules such as pyrazine (that has previously been studied in the water medium) from a non-aqueous non-H-bonded polar solvent of simple structure, such as acetonitrile. In this solvent, the adsorption of water as a solute could hence be studied. The purpose of such work was to be the examination of the substitutional adsorption of a neutral, non-polar rigid molecule in the absence of H-bonding interactions which complicates the behavior of interphases in the aqueous medium. Knowledge of the substitutional adsorption behaviour in a simple, non-H-bonded polar solvent would have been very valuable in the treatment of neutral molecule adsorption at charged interfaces.

An attempt was therefore made to study the structure of the interphase mercury-electrolyte solution ($NaClO_4$) in anhydrous acetonitrile by using the dropping mercury electrode technique since

previous preliminary studies had shown that the capillary electrometer was unsatisfactory in this medium due to sticking of the meniscus in the capillary.

However, it was never found possible to be able to obtain any sufficiently characteristic and reproducible electrocapillary curves in acetonitrile solution despite many attempts at purification of this solvent. By starting from -50 mV and moving toward more negative potentials, an unusual behavior was noticed in going through the electrocapillary maximum. The surface tension values were no longer reproducible and there was a large deviation from the expected curve as shown typically in Fig. 20.

This unfortunate behavior was apparently caused by the presence of traces of water and oxygen in the organic solvent, and the difficulties could never be satisfactorily eliminated to the point where high accuracies of drop-time measurements, required to obtain reliable adsorption data, could be obtained. These problems were also found by Champion[93] who considered the influence of dissolved oxygen and

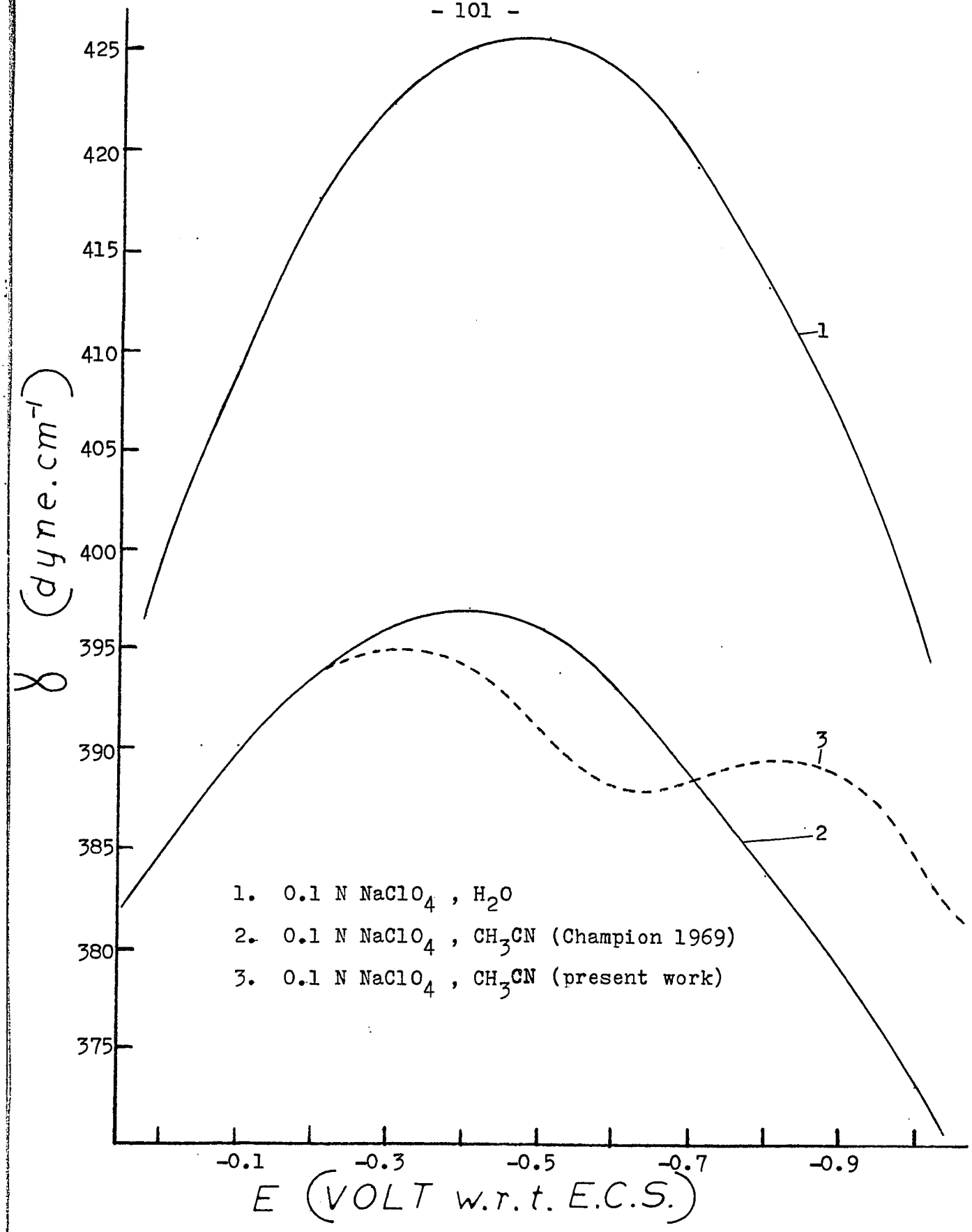

Fig. 20 Electrocapillary curves (based on γ values at 50 mV intervals) for adsorption of sodium perchlorate from acetonitrile solution.

concentration of water [94] in the behaviour of electrolytic solutions of $NaClO_4$ in CH_3CN. From his observations, he came to the conclusion that the difficulties arose from the cathodic reduction of oxygen in acetonitrile at Hg according to the following reaction:

$$O_2 + e \longrightarrow O_2^- \qquad (36)$$

Since he observed that the presence of water amplified the anomalous phenomena, it was proposed that O_2^- formed in reaction (36), because of its basic properties, was acting as a catalyst in the hydrolysis of acetonitrile to acetamide according to the reaction:

$$CH_3CN + \underset{\text{(traces)}}{H_2O} \xrightarrow{O_2^-/Hg} CH_3-\overset{\overset{O}{\|}}{C}-NH_2 \qquad (37)$$

Then it could be acetamide that would be the principal species adsorbed on mercury and would not be desorbed even at more positive potentials. The solution to this problem would be a laborious distillation of acetonitrile (less than 5 p.p.m. of water) and a technique that keeps it subsequently free from

atmospheric contamination by water vapour and oxygen throughout the whole experiment.

Many experiments of this kind were tried over a period of nine months but no satisfactory electrocapillary curves of the required accuracy and reproducibility could be obtained. The aims of the work in this project were therefore revised, as described in the earlier sections of this chapter and thesis.

CHAPTER IV

DISCUSSION

The results reported in the previous section will be discussed in terms of (a) adsorption isotherms and standard free energies of adsorption; (b) surface pressure and equations of state and (c) surface potential changes as revealed by the Esin and Markov coefficients, $(\partial E/\partial \Gamma)_{q_M}$.

A. Isotherms and Introduction of the Standard Free Energy of Adsorption ΔG^{o}_{ads}

1. Method of Approach

In order to provide derived quantities which will provide a basis for some quantitative interpretation of the basic results given above, the following aspects of the adsorption behavior will be considered: (a) the dependence of apparent standard free energy of adsorption (see below for definition of this quantity), ΔG^{o}_{ads}, on surface charge, q_M, in terms of competitive adsorption between field-oriented solvent molecules and specifically

adsorbed organic molecules[15]; (b) the dependence of ΔG^{o}_{ads} on coverage or surface concentration, Γ, with respect to interaction effects in the interphase[21,92]; and (c) the dependence of surface pressure ϕ due to adsorbed organic molecules on Γ.

In comparing methods for analysis of results in terms of adsorption isotherms, Dhar[47] in this Laboratory showed that the best approach was first to choose an appropriate configurational function, such as $(\theta/1-\theta)$ in the Langmuir case or $\theta/x(1-\theta)^{x}$ in the Flory-Huggins case (see equations 18,19,20), based on relevant statistical-mechanical lattice considerations for substitutional adsorption, taking into account the finite size of the adsorbate in relation to that of the solvent (size ratio x); the second step consisted in evaluating the coverage and charge-dependence of the formal equilibrium constant K_{ads} for a given value of q_M and temperature; finally this K_{ads} could be usefully expressed in terms of ΔG^{o}_{ads}, the corresponding "apparent standard free energy of adsorption"[92] which may vary with coverage and hence give information about interaction effects in the interphase. (This is analogous to

evaluation of a "concentration" equilibrium constant for an ionic reaction and then, from its observed dependence on ionic strength, deduction of the interaction effects in terms of activity coefficients, in such a case for the species in solution).

Dhar, Conway and Joshi[30] treated the problem of substitutional adsorption (solvent/adsorbate competitive adsorption) at the Hg electrode and derived the following isotherm related to the one derived by Zhukovitskii[29]:

$$\frac{\theta}{e^{x-1}(1-\theta)^x} = \frac{C_{org}}{55.5}_{exp} - \left[\frac{\Delta G^o_{ads}}{RT}\right] \qquad (38)$$

In the present work, ΔG^o_{ads} values were obtained both from a Langmuir function (x=1) and from the more general isotherm relation (eqn. 38), taking into account the relative sizes, x, of the adsorbate and solvent molecules.

2. Estimation of the Maximum Surface Excess Γ_m from Molecular Models

For interpretation of the results in terms of ΔG^o_{ads} from isotherms (see above), it is necessary to evaluate θ, i.e. Γ/Γ_m, for various solution concentrations and surface charges, q_M.

As was mentioned earlier, it is not possible to obtain a reliable value of the maximum surface excess Γ_m experimentally from the approach to saturation of most adsorption isotherm plots because of the limited range of concentrations over which most adsorption results can be obtained at Hg. Accordingly, estimates of Γ_m were made by measurements on space-filling Courtauld models[86], as in previous work by various authors[47,88,89]. For non-spherical molecules, assumptions have to be made about the most probable orientation of the molecule in the interphase, as discussed on p.86 . If the molecule has a strong dipole, this is usually not difficult as it will orient in the direction of the electrode field.

B. Adsorption Behavior of Urea at Hg

1. Evaluation of ΔG^o_{ads} for Urea

Γ data for urea were employed in eqn. (38) for x=1 (Langmuir case) and for x=3. The latter value was based on measurements of Courtauld models. ΔG^o_{ads} values were then calculated for various q_M. Plots of ΔG^o_{ads} as a function of q_M are shown for urea at various Γ values in Fig. 21 for x=1 and x=3, respectively. Variation of ΔG^o_{ads} with q_M is rather small, being only 1 kcal over the range of q_M. This is as expected for a rather hydrophilic molecule such as urea. In a general way, for a given Γ, ΔG^o_{ads} values become increasingly negative as Γ increases, as shown in Fig. 22. This means that apparent attractive interactions arise among the urea molecules; this effect could be produced by the $\rangle C{=}O$ function in urea which is available for intermolecular H-bonding with H_2O molecules in the interphase or with NH_2-groups of other urea molecules.

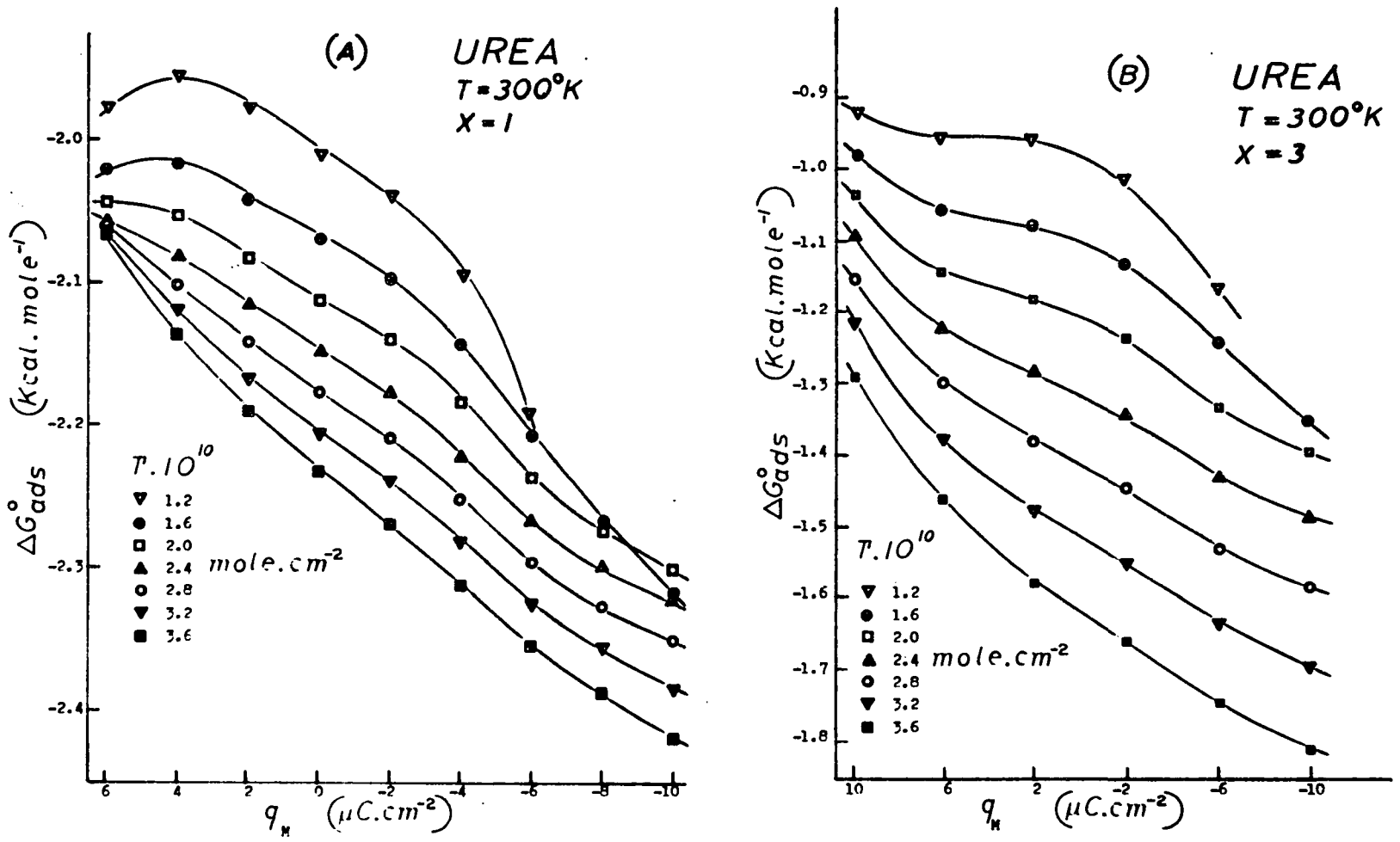

Fig. 21 Variation of ΔG^{o}_{ads} of urea as a function of q_M at various Γ values. (a) x = 1; (b) x = 3.

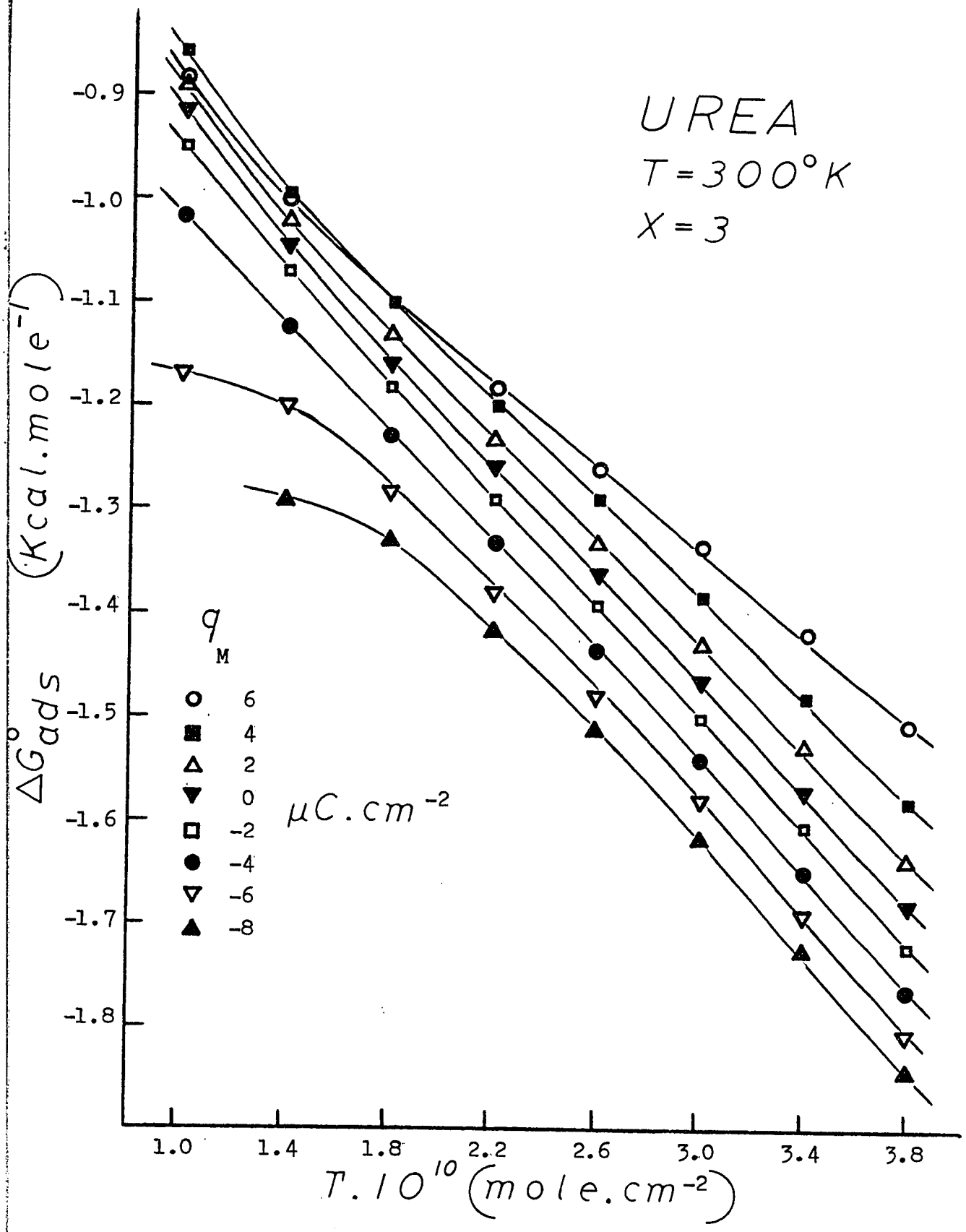

Fig. 22 Variation of ΔG°_{ads} of urea for x=3 as a function of Γ at various q_M values.

2. Surface Pressure Relations for Urea at Hg

More information on the orientation of urea in the interphase is provided by examination of the dependence of surface pressure ϕ_q on q_M or Γ and by the Esin and Markov plots (see below). ϕ_q values were calculated at various q_M's by the method described in the previous chapter.

Fig. 23 shows the relation of ϕ_q to Γ at various q_M's in relation to the ideal Henry's law type behavior (dotted line in Fig. 23); it is evident that the ϕ_q-Γ relations are only slightly dependent on q_M for urea. Deviations from ideality are most significant for the more positive q_M values but decrease to about zero as q_M becomes -10 $\mu C.cm^{-2}$. These results suggest that changes of q_M cause small but significant changes of interaction between urea molecules, an effect that is connected with their orientation (see below). All the ϕ_q vs Γ plots in Fig. 23 fall below the ideal surface pressure line ($\phi_q A = RT$) indicating that attractive interactions predominate. Presumably this is due to the H-bonding between urea molecules through the remaining water

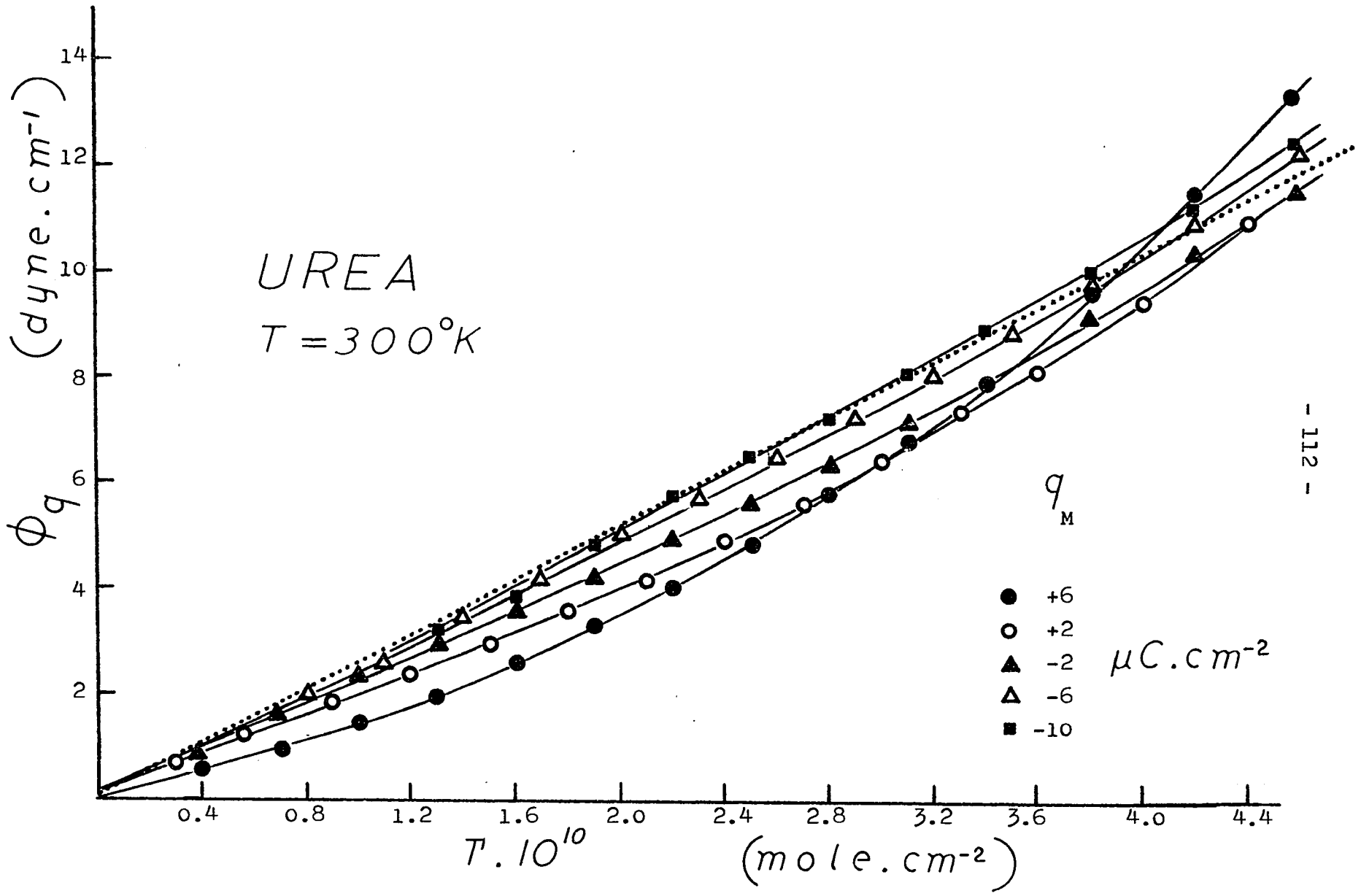

Fig. 23 Variation of surface pressure for urea as a function of Γ at various q_M values.

molecules in the interphase since the maximum coverage attained by urea in Fig. 23 is ca. 50%. Only at the highest Γ in Fig. 23 are there some indications of "repulsive" interactions.

3. Esin and Markov Effect with Urea

The Esin and Markov effect for neutral molecule adsorption has been discussed in detail previously for pyrazine and pyridine adsorption by Conway and Dhar[45]. Two principal effects are involved: (a) change of surface potential (at constant q_M) due to orientation of adsorbate dipoles and (b) change of the surface dipole contribution from previously oriented solvent dipoles due to their displacement by the organic adsorbate.

Since the orientation of adsorbate and solvent arise in a liquid interphase, it is important to note that the behaviour observed will be statistical effects involving a large population of molecular orientations of various magnitudes.

The Esin and Markov plots were shown in Fig. 11. For low coverages, $\Gamma.10^{10}$ < ca. 1.8 mol. cm^{-2}, ΔE_{q_M} increases or decreases with Γ depending on the sign and magnitude of q_M. This behaviour is consistent with initial displacement of H_2O solvent dipoles oriented to extents and in direction dependent on q_M; this effect is similar to that observed with pyrazine[47] at Hg. At larger values of Γ, ΔE_{q_M} increases at all q_M values with increasing Γ. As was shown for the case of pyridine, this is due to onset of appreciable orientation of the adsorbate dipole itself at higher coverages. This effect sets in (Fig. 11) at a coverage of ca. 25%.

The direction of the ΔE_{q_M} plots with increasing Γ at the higher Γ values indicates that the urea dipole is preferentially oriented with its NH_2-groups (the positive end of the dipole) towards the Hg surface. This seems consistent with the known donor/acceptor interactions of NH_2- with Hg despite the fact that here the NH_2- is present in an "amide" type of functionality in the molecule and hence is only a weak donor.

As was shown previously from work with pyridine[47], the extent of orientation of the adsorbate dipole itself corresponds to the differences of slopes of the two parts of each of the inflected lines of the type that arise in Fig. 11. This is shown in Fig. 24 for the series of inflected lines of Fig. 11. It is evident that there is a uniform progression of the differences of slopes of the initial and subsequent sections of the Esin and Markov plots in Fig. 11. There is thus a uniform progression of the extent of orientation of urea dipoles from $q = +6$ to $q = -8 \mu C.cm^{-2}$ (corresponding to the range of data in Fig. 11). The extent of average orientation with changing q_M is evidently somewhat larger on the positive side than on the negative, i.e. when water orientation is in the direction of O towards the metal. It is also evident that there is almost zero net orientation of urea at the potential of zero charge. This is to be contrasted with the situation with thiourea[56] which is strongly specifically oriented with the S atom lone-pairs associated with the Hg surface.

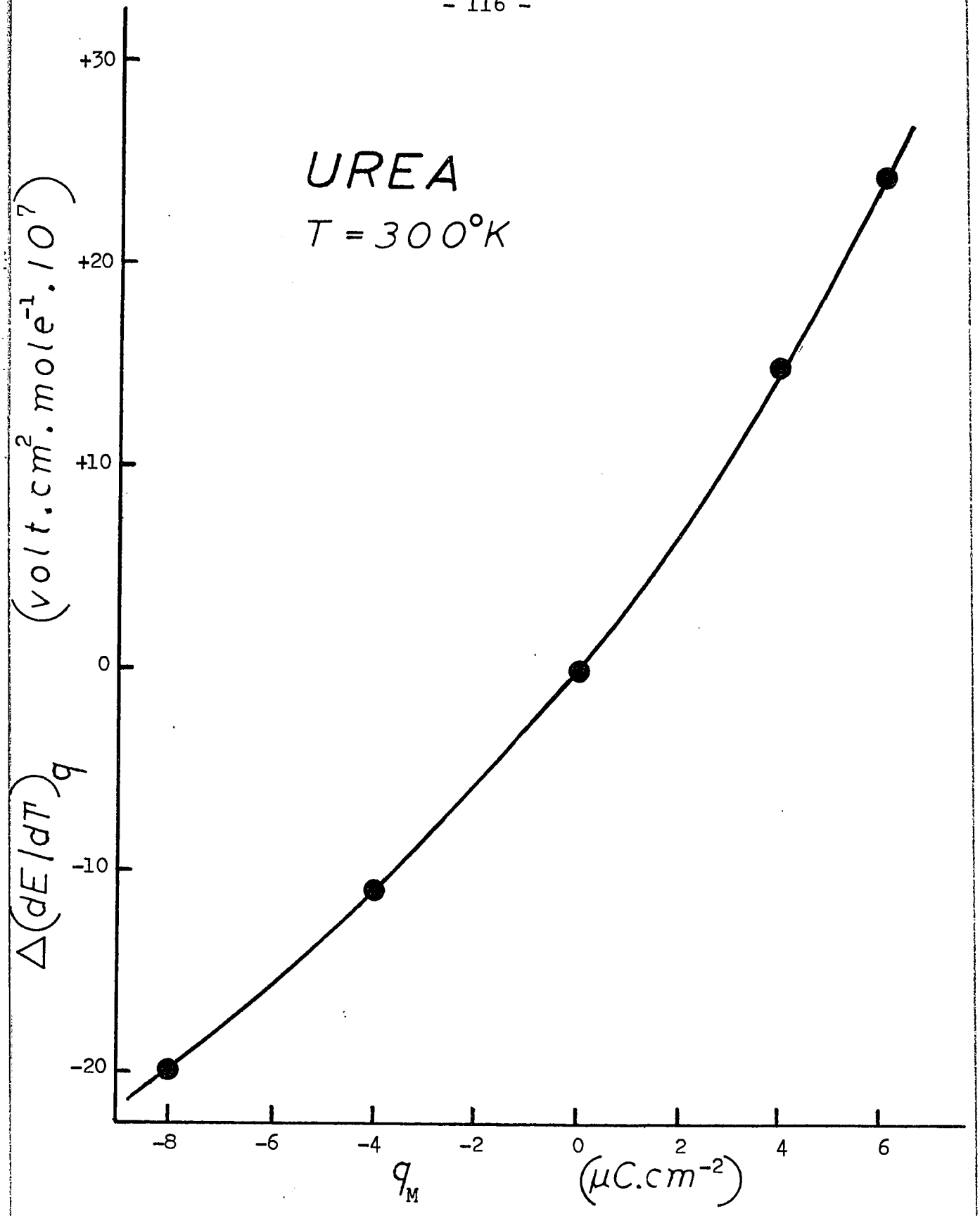

Fig. 24 Slope difference in Esin and Markov plots as a function of q_M for urea.

The behaviour indicated by the Esin and Markov plots is consistent with the surface pressure behavior in Fig. 23, if it is recognized that lateral H-bonding between the oriented $\rangle C{=}O$ groups and co-adsorbed water molecules can provide more lateral stabilization in the oriented urea layer at the Hg surface, when the urea dipole is oriented with its NH_2 groups, rather than its carbonyl O, towards the surface. Two NH_2 groups naturally provide more opportunity for intermolecular H-bonding in the interphase.

C. Adsorption of n-Pr-ammonium Cations at the Hg Electrode

1. Method of Approach

In order to evaluate the type of dependence of the interaction energy amongst adsorbed ions on their coverage at the electrode, the same method was adopted as that used for the evaluation of the adsorption behavior of urea described above.

2. Evaluations of Γ_m for Calculation of ΔG^o_{ads} Values

It was not possible to derive Γ_m for each cation from inspection of the experimental Γ *vs* log c or the Γ *vs* q_M curves for each system since $PrNH_3^+$ and $Pr_2NH_2^+$ were only weakly adsorbed (even at 0.5M in the case of $PrNH_3^+$) while Pr_4N^+ is insoluble at concentrations higher than 2.20 mM in perchloric acid; however, it was possible to approach saturation coverage for Pr_3NH^+ which appears to adopt a "parallel" orientation with the three alkyl chains straddled on the surface.

Because of these limitations which commonly arise in adsorption studies at Hg, it was necessary to make estimates of Γ_m again by means of the Courtauld models[86]. In this way, the effective areas occupied by the four different ammonium-type ions were evaluated according to their principal orientations with respect to the metal surface. The corresponding Γ_m values could then be quite accurately calculated. Table 3 shows the estimated molecular

TABLE 3

ESTIMATED AREAS ($Å^2$) OF THE SERIES OF N-PROPYLAMMONIUM IONS DERIVED FROM MEASUREMENTS ON COURTAULD MODELS

ION	PERP.	PARALLEL	EXPT.
$(n\text{-}Pr)NH_3^+$	19.2	27.2	< 57
$(n\text{-}Pr)_2NH_2^+$	18.5 (1) 33.8-40.4 (2)	40.4	< 24
$(n\text{-}Pr)_3NH^+$	39.6	56.3 (3) 66.3 (4)	70
$(n\text{-}Pr)_4N^+$	43.7	51.4	< 36

(1) linear
(2) angular(30^0-180
(3) triangular
(4) circular area swept out by rotational motion

CALCULATED MAXIMUM SURFACE EXCESS VALUES (10^{-10} mol cm^{-2})

ION	PERP.	PARALLEL	EXPT.
$(n\text{-}Pr)NH_3^+$	8.68	6.13	> 2.9
$(n\text{-}Pr)_2NH_2^+$	9.01 (1) 4.93-4.13 (2)	4.13	> 6.8
$(n\text{-}Pr)_3NH^+$	4.21	2.96 (3) 2.50 (4)	2.4
$(n\text{-}Pr)_4N^+$	3.81	3.24	> 4.6

N.B.: Very different values were estimated by Kimmerle and Menard[76] based on unspecified molecular models. It was impossible to reproduce their estimates using the Courtauld models.

areas ($\mathring{A}^2$) and the corresponding Γ_m values ($mol.cm^{-2}$), taking into account the two probable orientations which can arise with respect to the mercury surface: "parallel" or "perpendicular".

3. The Standard Free Energy of Adsorption and Surface Pressure Behaviour

(a) n-Propylammonium Perchlorate

Plots of the variation of ΔG^o_{ads} for $n\text{-}PrNH_3^+$ as a function of q_M are shown in Fig. 25 for x=1, 2, 3 and of the variation of ΔG^o_{ads} with Γ for x=2 in Fig. 26. It can be seen that in a general way ΔG^o_{ads} becomes more positive with increasing Γ for x=1: this result would suggest that repulsive interactions are predominant among the adsorbed cations in the interphase which is at first sight logical; however, if ΔG^o_{ads} values are calculated for x=2, the situation is no longer the same: the apparent repulsive interactions are limited to the region where q_M is more positive than 2 $\mu C.cm^{-2}$, while apparent attractive interactions arise when q_M is more

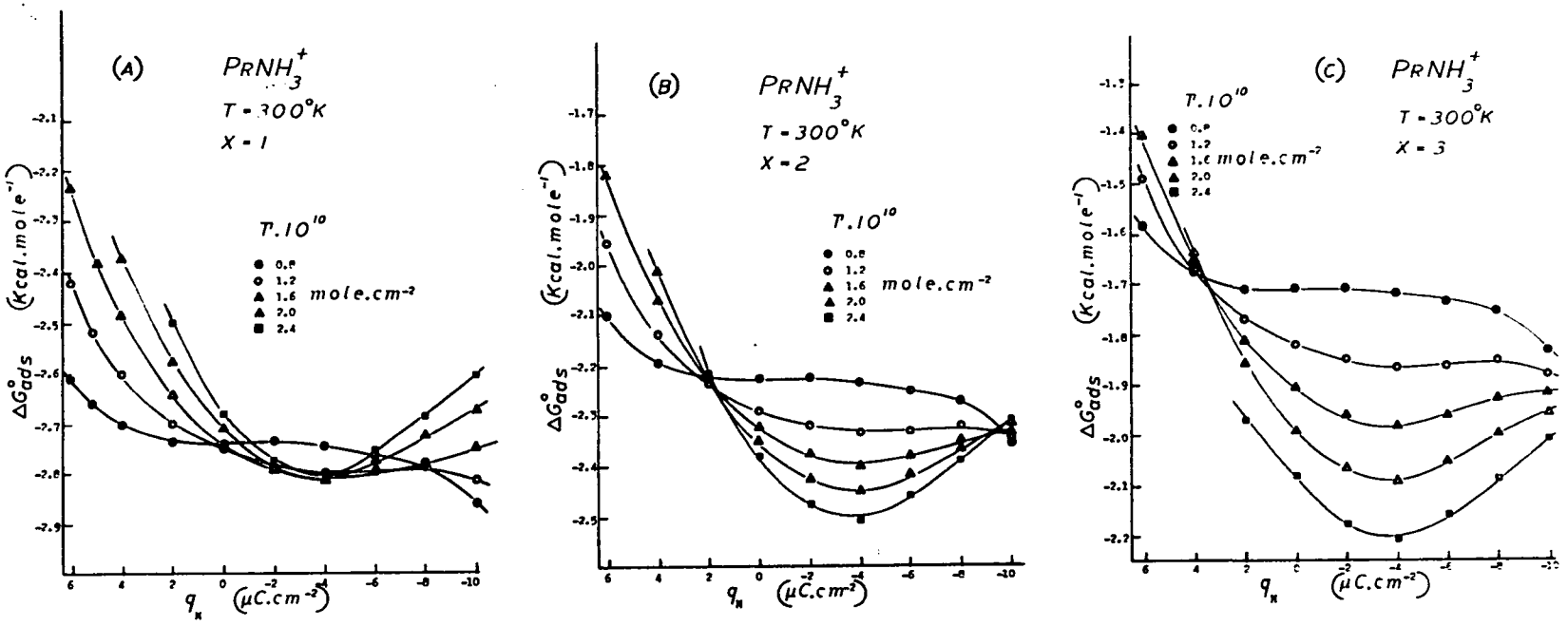

Fig. 25 Variation of ΔG^{o}_{ads} of $PrNH_3^+$ as a function of q_M at various Γ values.
(a) x = 1; (b) x = 2; (c) x = 3.

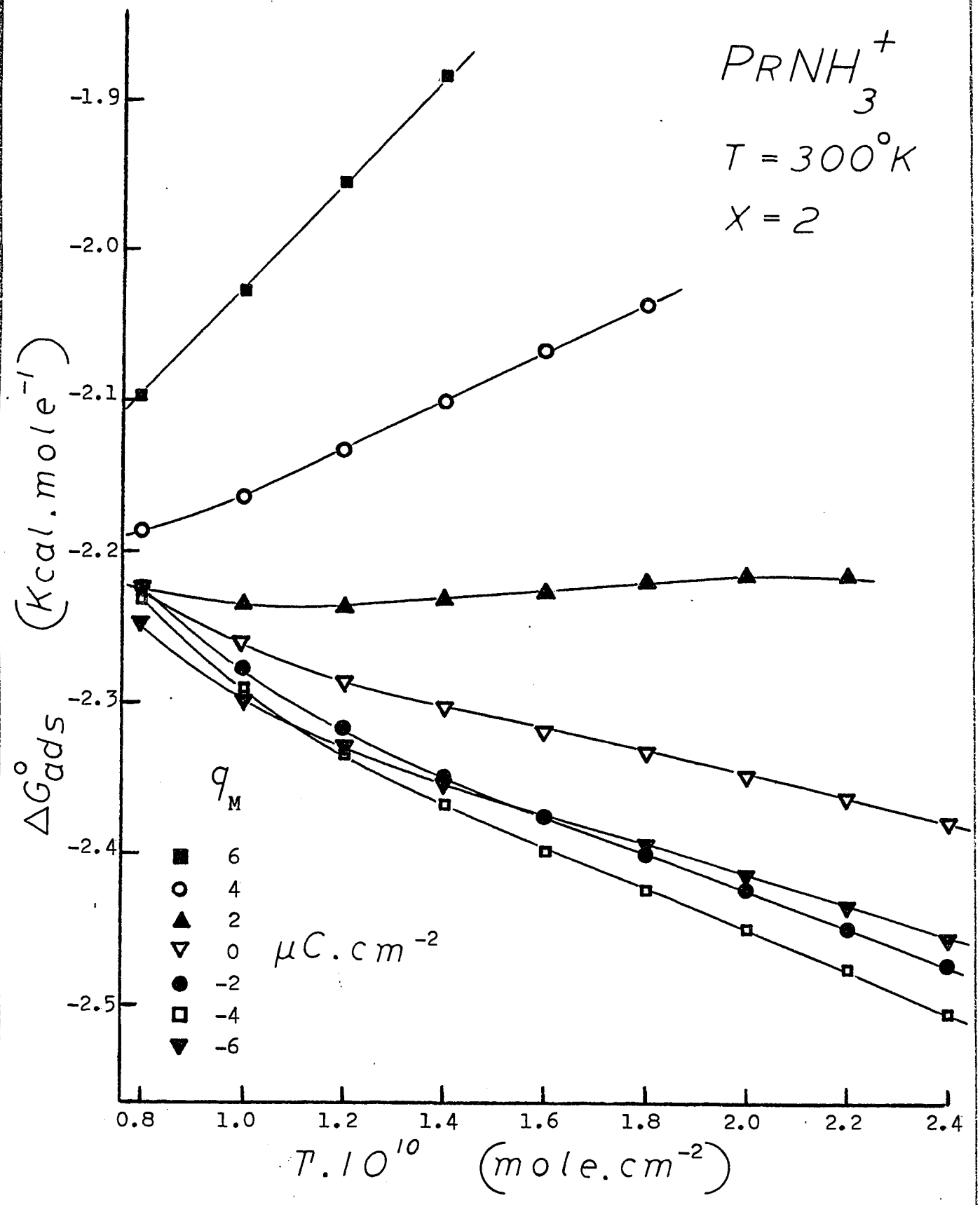

Fig. 26 Variation of ΔG^{o}_{ads} of $PrNH_3^+$ for x=2 as a function of Γ at various q_M values.

negative than 2 $\mu C.cm^{-2}$; for x=3, the cross-over point becomes 4 $\mu C.cm^{-2}$.

Examination of the plots of surface pressure ϕ_q as a function of Γ and of q_M, shown in Fig. 27, indicates that there is a significant dependence of the form of the ϕ_q vs Γ plots on q_M. This means that variations of q_M have a significant influence on the orientation of the cation in the interphase or on its interactions, or both, especially those with oriented water. This point is taken up in a general way later in relation to Gurney hydration co-sphere overlap effects in the interphase.

(b) Di-n-propylammonium Perchlorate

Plots of the variation of ΔG^o_{ads} for $(n\text{-}Pr)_2NH_2^+$ as a function of q_M are shown in Fig. 28 for x=1 and x=3 and of the variation of ΔG^o_{ads} with Γ in Fig. 29. Here it can be seen clearly that ΔG^o_{ads} becomes more negative with increasing Γ. This result suggests that apparent attractive interactions are important among the adsorbed cations in the interphase which is at first sight surprising since repulsion between ions of the same sign in an

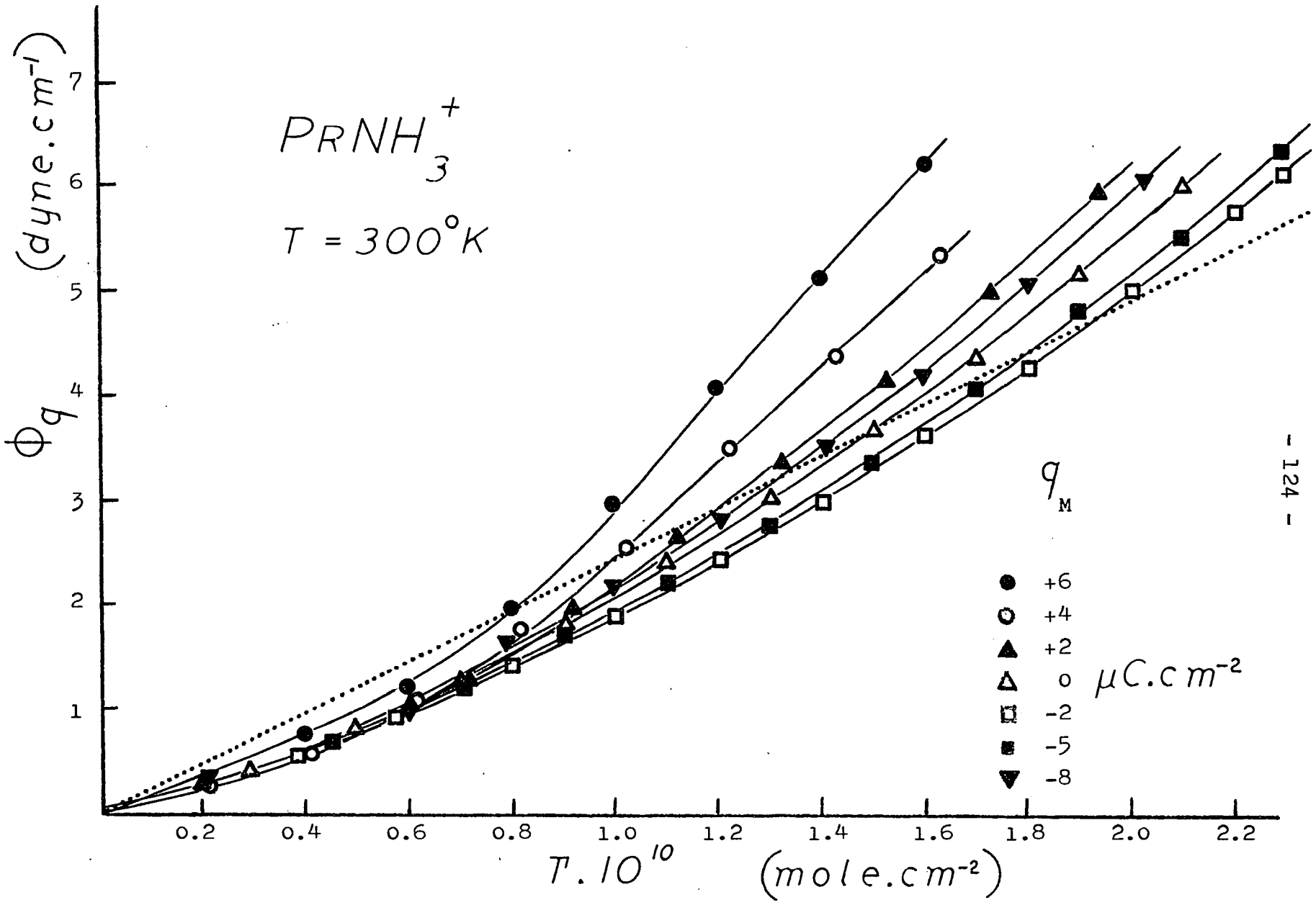

Fig. 27 Variation of surface pressure for $PrNH_3^+$ as a function of Γ at various q_M values.

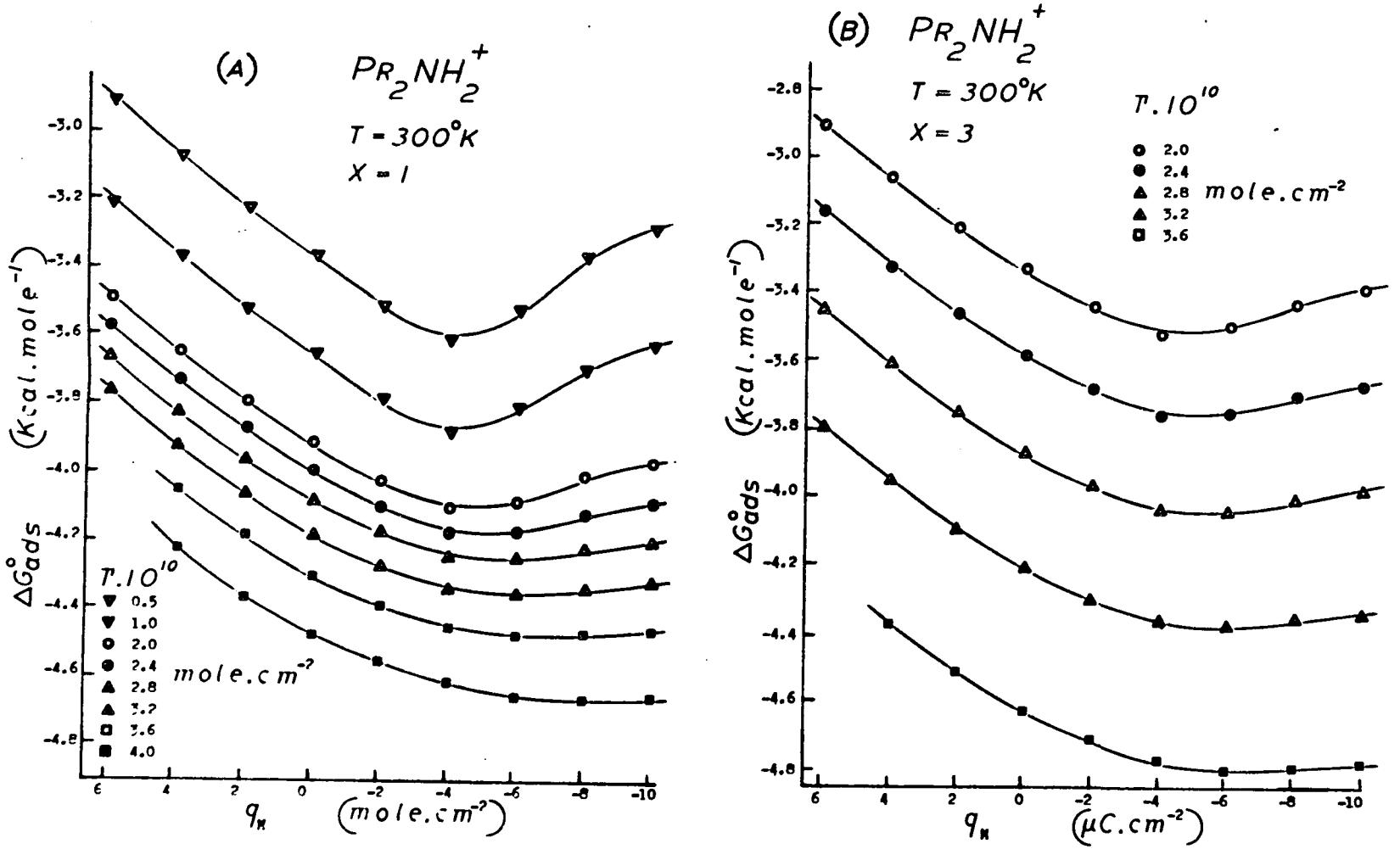

Fig. 28 Variation of ΔG^o_{ads} of $Pr_2NH_2^+$ as a function of q_M at various Γ values. (a) x = 1; (b) x = 3.

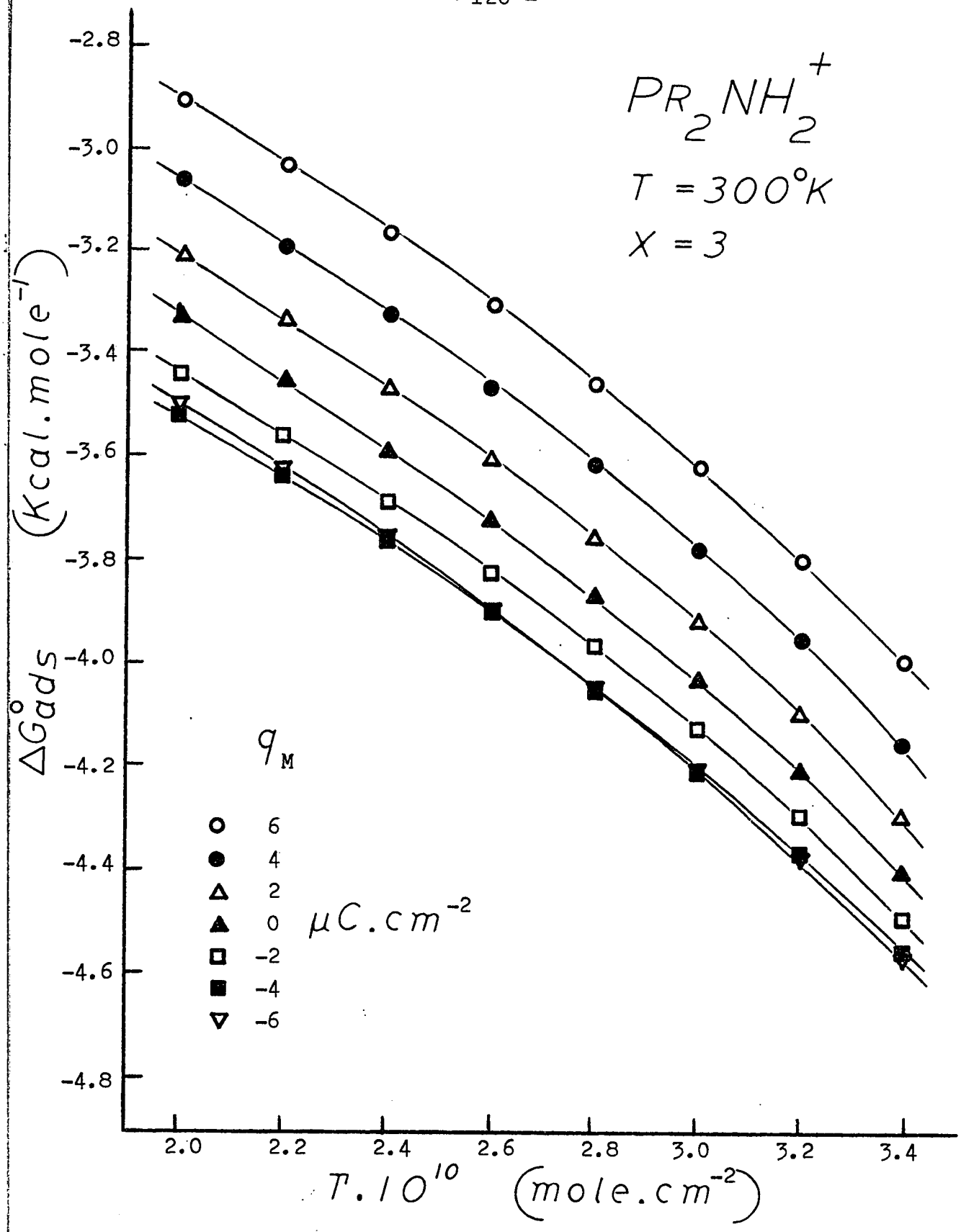

Fig. 29 Variation of ΔG°_{ads} of $Pr_2NH_2^+$ for x=3 as a function of Γ at various q_M values.

ad-layer would be the expected behaviour.

Examination of plots of surface pressure ϕ_q as a function of Γ and q_M, as shown in Fig. 30, reveals that there is only a small dependence of the form of the ϕ_q vs Γ plots on q_M. This means that variations of q_M have little influence on the orientation of the cation in the interphase or on its interactions, including those with oriented water.

(c) Tri-n-proplyammonium Perchlorate

Plots of ΔG^o_{ads} vs q_M for $(n\text{-}Pr)_3NH^+$ are shown in Fig. 31 for x=1,3,5. Plots of ΔG^o_{ads} vs Γ are shown in Fig. 32 for x=5. For q_M values more negative than +5 $\mu C.cm^{-2}$, $-\Delta G^o_{ads}$ becomes larger as Γ increases which suggests again that the principal interactions in the interphase are of an attractive kind.

The dependence of surface pressure on q_M again provides further useful information that has to be considered: plots of ϕ_q vs Γ at various

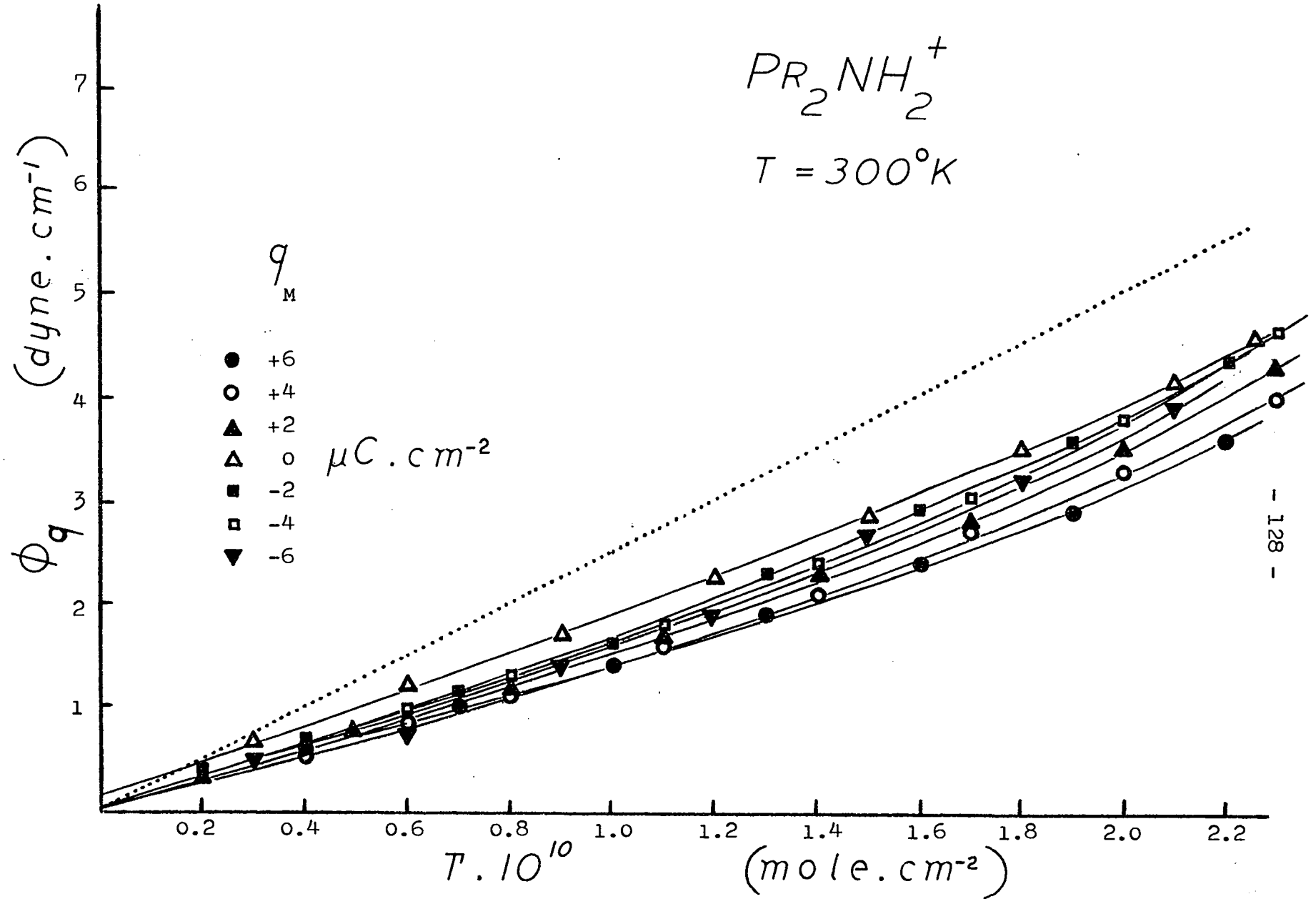

Fig. 30 Variation of surface pressure for $Pr_2NH_2^+$ as a function of Γ at various q_M values.

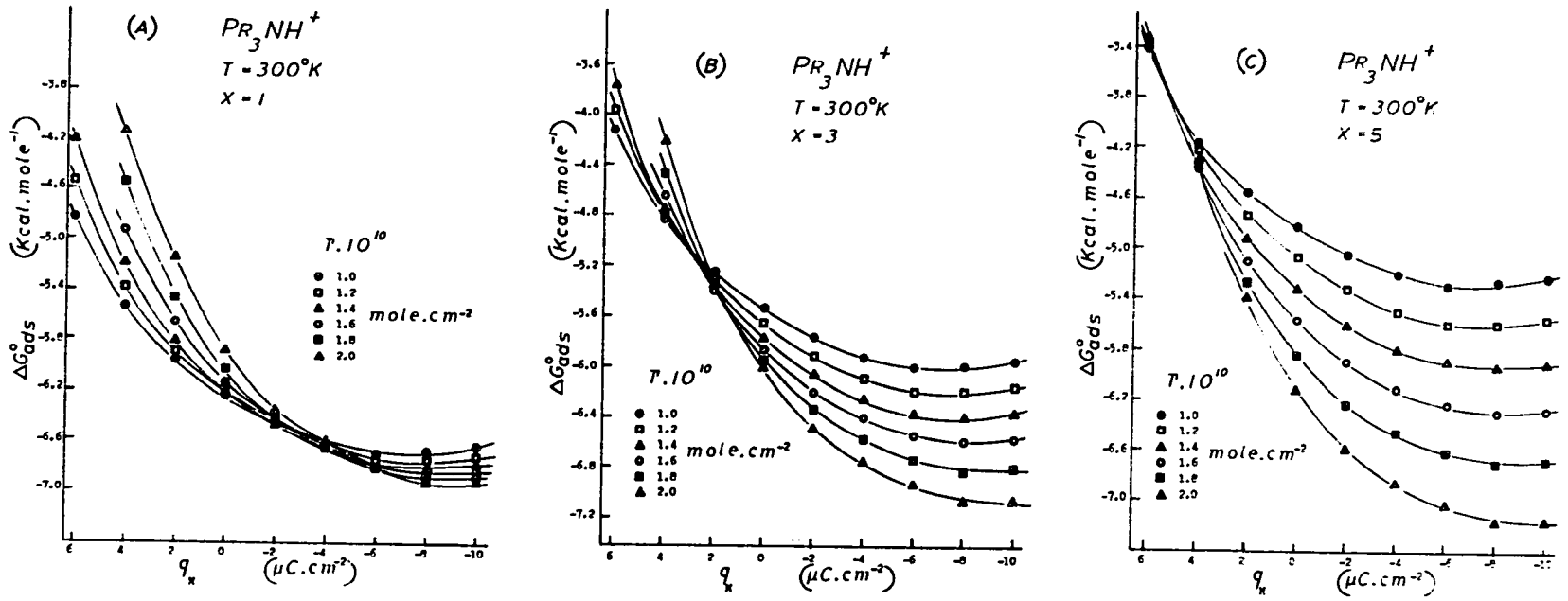

Fig. 31 Variation of ΔG^o_{ads} of Pr_3NH^+ as a function of q_M at various Γ values. (a) x = 1; (b) x = 3; (c) x = 5.

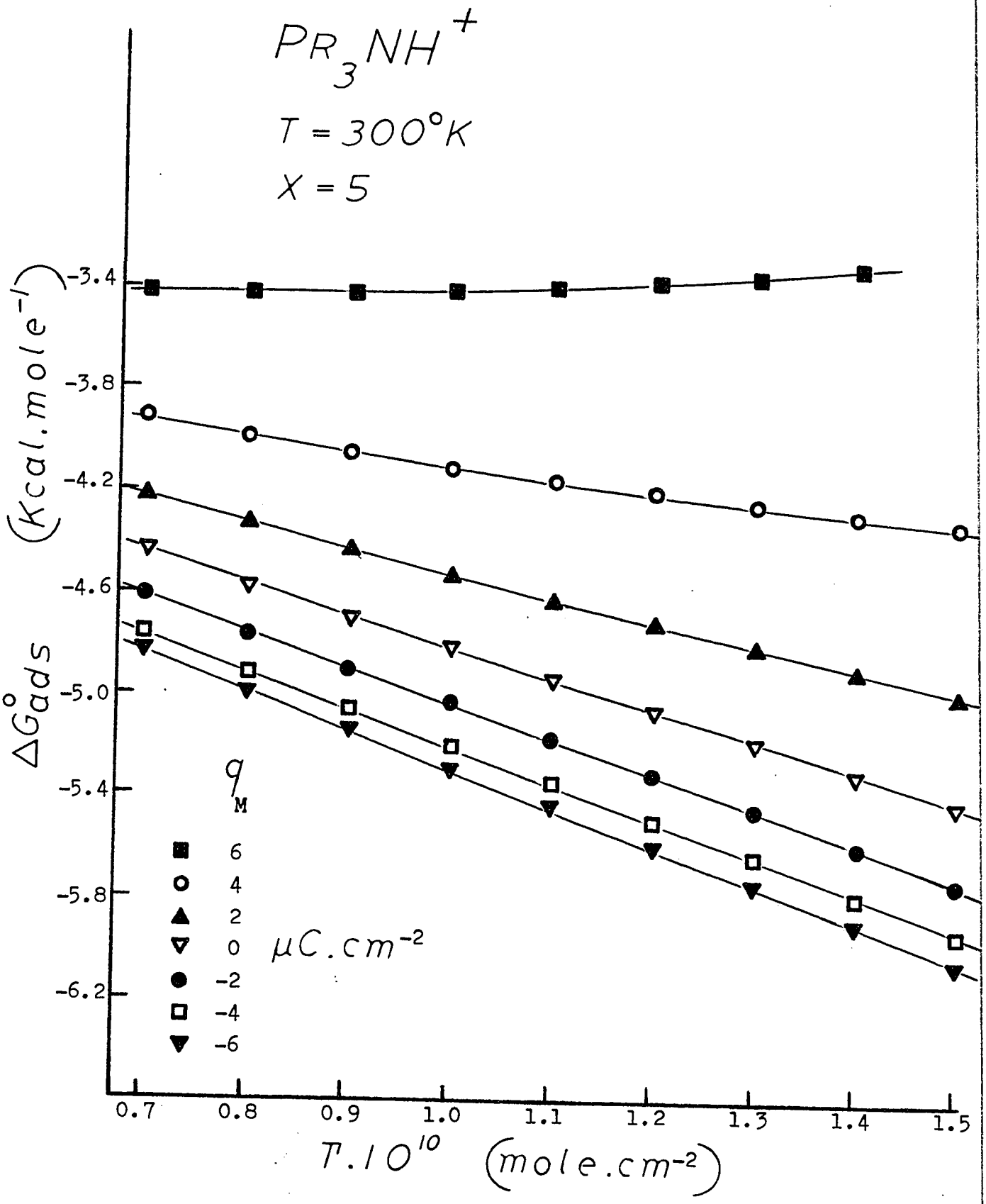

Fig. 32 Variation of ΔG°_{ads} of Pr_3NH^+ for x=5 as a function of Γ at various q_M values.

q_M values are shown in Fig. 33. It is seen that the ϕ_q-Γ relations are fairly dependent on q_M for this case.

(d) Tetra-n-propylammonium Perchlorate

Plots of ΔG^o_{ads} vs q_M for $(n\text{-}Pr)_4N^+$ are shown in Fig. 34 for x=1,3,5. The curves were not drawn to include the data for the more positive q_M values since they all crowd together into a single line. Plots of ΔG^o_{ads} vs Γ (Fig. 35) show once more the tendency for ΔG^o_{ads} to become more negative with increasing Γ indicating again the role of attractive interactions among the adsorbed cations in the interphase; this will be further discussed later.

Examination of the plots of ϕ_q vs Γ at various q_M values for $(n\text{-}Pr)_4N^+$ (Fig. 36), indicate a dissimilarity with respect to the behavior of $(n\text{-}Pr)_3NH^+$ since only a small dependence of the ϕ_q vs Γ plots on q_M is observed.

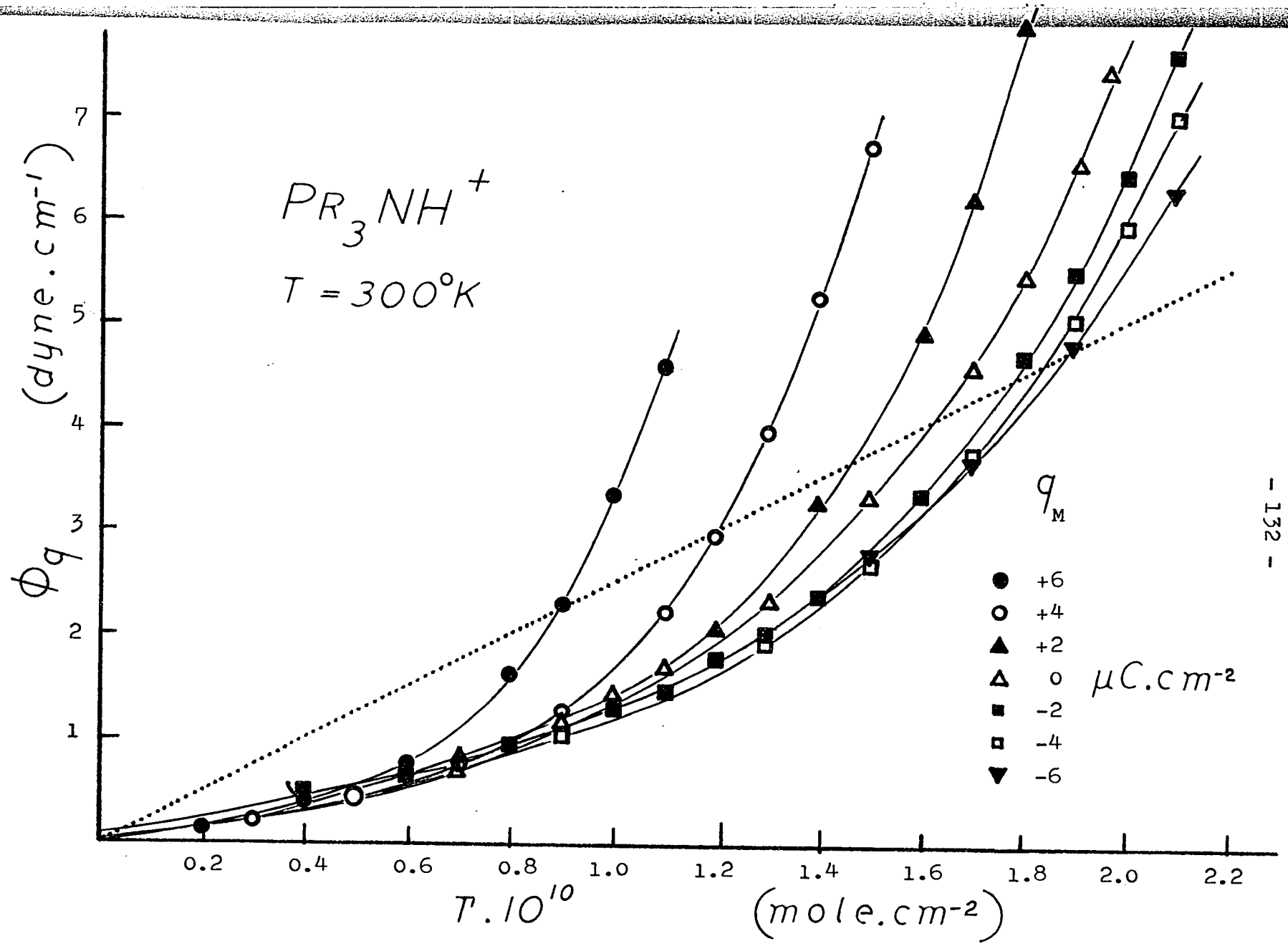

Fig. 33 Variation of surface pressure for Pr_3NH^+ as a function of Γ at various q_M values.

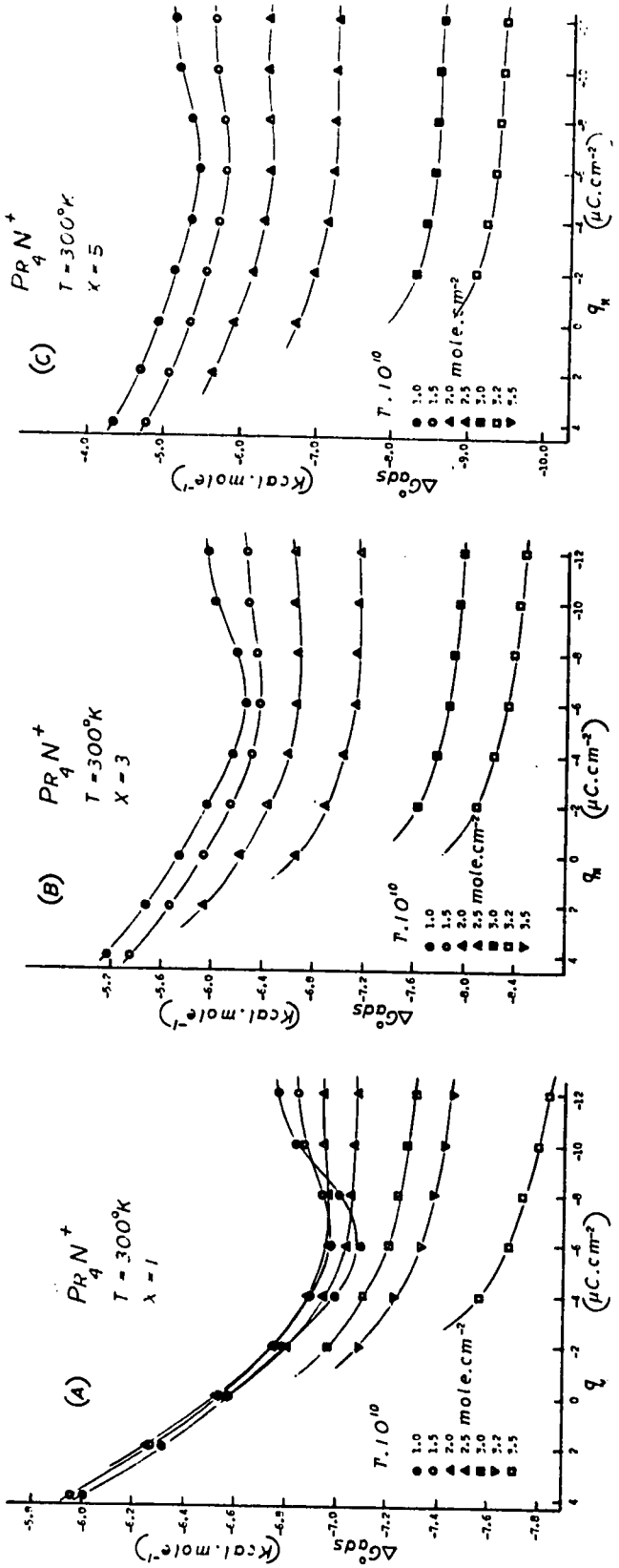

Fig. 34 Variation of ΔG^0_{ads} of Pr_4N^+ as a function of q_M at various Γ values.
(a) x=1; (b) x=3; (c) x=5.

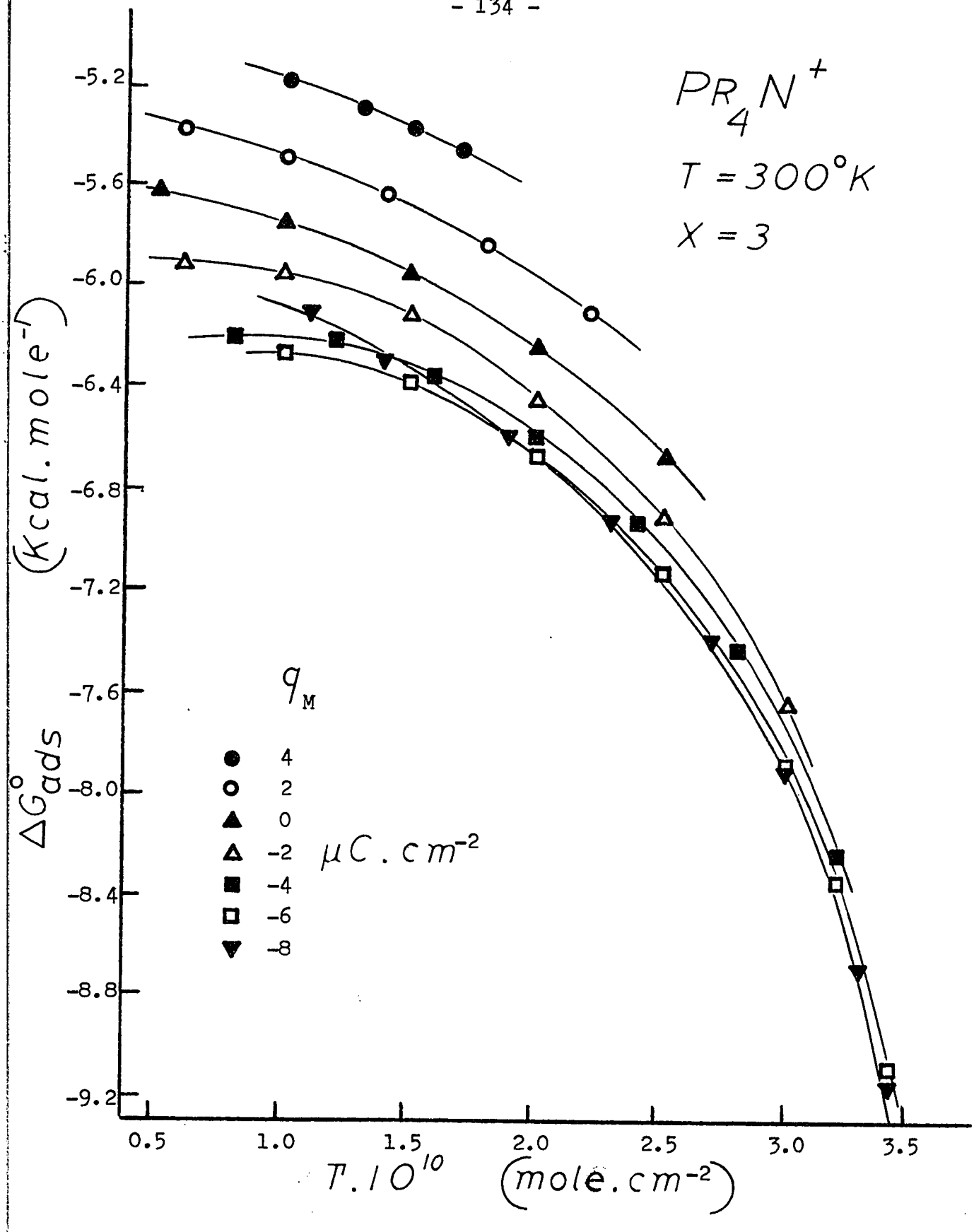

Fig. 35 Variation of ΔG^o_{ads} of Pr_4N^+ at x=3 as a function of Γ at various q_M values.

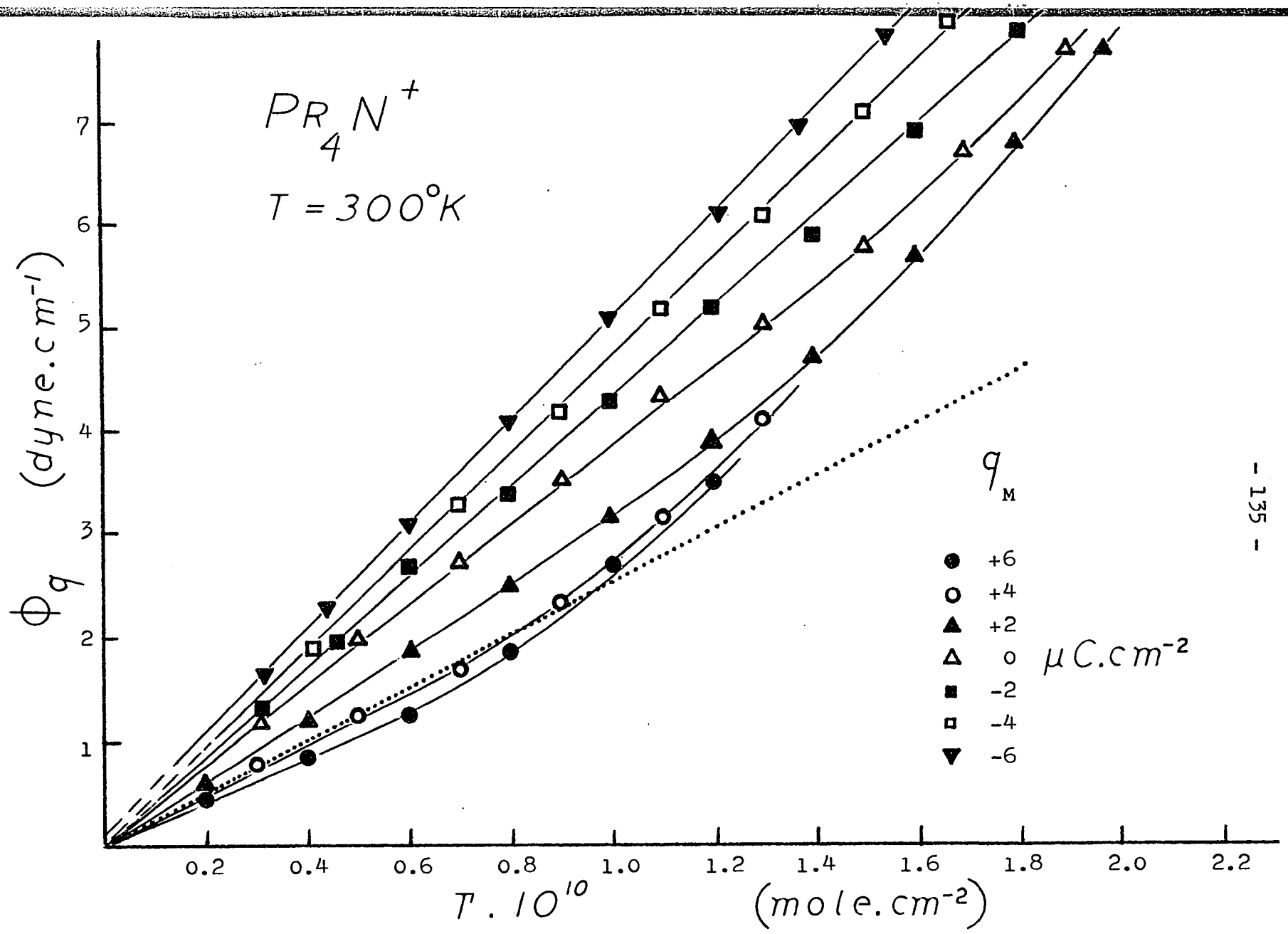

Fig. 36 Variation of surface pressure for Pr_4N^+ as a function of Γ at various q_M values.

4. Variation of Standard Free Energy of Adsorption with the Number of Carbon Atoms in the $Pr_nNH_{4-n}^+$ Series

The standard free energy of adsorption generally involves several contributions. The one due to direct electrostatic interactions with the surface can be eliminated by considering ΔG^o_{ads} values for a surface charge $q_M=0$. In Fig. 37 is shown the dependence of ΔG^o_{ads} on the number N_c of C atoms for each adsorbed cation. The data shown are taken for $\theta \simeq 0.2$ in order to include the value of ΔG^o_{ads} for $n\text{-}PrNH_3^+$. It is seen that the relation ΔG^o_{ads} **vs** N_c follows Traube's rule (1891) which recognizes that the relative strength or extent of adsorption of molecules in an homologous series of (aliphatic) organic substances depends essentially on the length and the number of alkyl chains. The applicability of this rule to the present type of ions was examined by reference to the adsorption behavior of the n-propylammonium perchlorate salts. From Fig. 37 it is seen that the decrease of free energy of adsorption per carbon atom is approximately constant

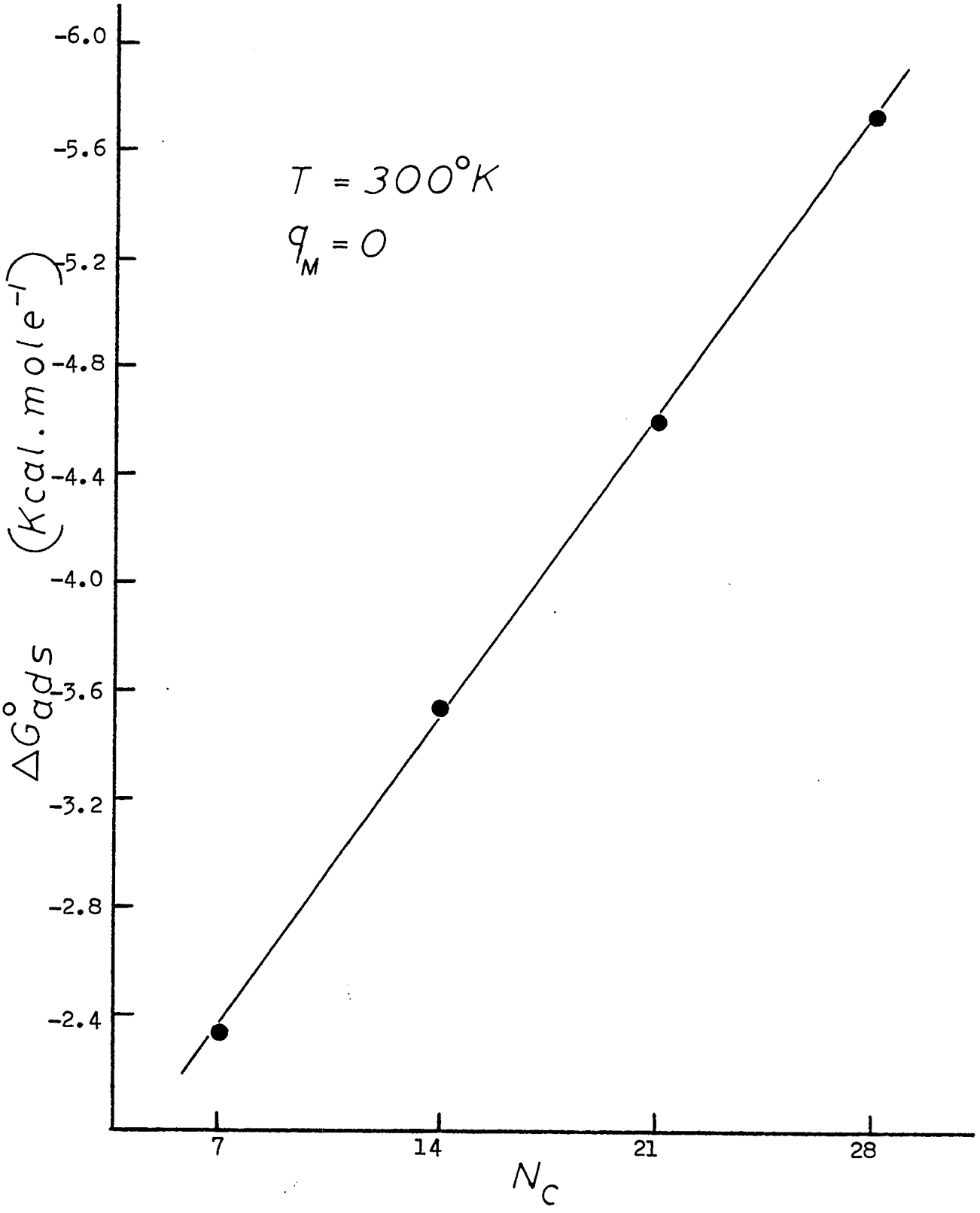

Fig. 37 Variation of ΔG°_{ads} for each alkylamine as a function of the number of carbon atoms at $q_M = 0$.

and equal to about -170 cal. mol^{-1}, a trend which reflects the increasing hydrophobicity in the series of ions.

5. Interaction Effects amongst Adsorbed Organic n-Propylammonium Cations

(a) Electrostatic and Non-electrostatic Interactions

An unscreened layer of simple ions in two-dimensions exhibits a repulsive interaction energy approximately proportional to $\theta^{\frac{1}{2}}$. For the present series of ions, with the exception of $n\text{-}PrNH_3^+$ (Fig. 26) for $q_M > 0$, all the plots of ΔG^o_{ads} vs Γ for the n-propylammonium salt series show a substantial decrease of ΔG^o_{ads} with increasing Γ, especially for the salt $(n\text{-}Pr)_4N^+ClO_4^-$ (Fig. 35) of the most hydrophobic cation. Therefore conventional ionic repulsive effects are not predominant in the ad-layer.

This, it is suggested, is due to:

(i) the large size of the organic cations which prevents their charge-centres from residing "on" the surface as is the case, relatively speaking, with smaller ions. This situation then enables anions to be present to some extent, dependent on q_M, within the organic cation layer. The cation-cation electrostatic repulsions would then be diminished and in the limiting case if cation and anion surface excesses were comparable, a net attractive energy could result (cf. the situation in 3-dimensional ionic solutions); and

(ii) hydrophobic association effects between the organic cations. This effect arises from the tendency of hydrophobic solutes to associate together in water in order to diminish their unfavorable interactions with the water structure, i.e. to minimize H-bond breaking in the water lattice. In 3-dimensional solutions, it is this effect which gives rise to formation of micelles with long-chain organic electrolytes. Such hydrophobic association

effects will be strongest with the $(n\text{-}Pr)_4N^+$ ion and could explain the appreciable decrease of ΔG^o_{ads} in Fig. 35 with increasing Γ.

The interaction effects amongst hydrated ions at fairly high concentrations (> 1-≃2M) must be considered not only in terms of their electrostatic repulsions or attractions but also in terms of interactions between their hydration co-spheres [factor (ii) above] in the sense of Gurney[95]. For ions of like sign, this can give rise to an attractive or repulsive energy dependent on the type of co-sphere sharing involved. Hydrophobic ions can have attractive Gurney co-sphere sharing interactions.

Conway and Dhar[96], and more recently Conway[97], gave a calculation of Gurney co-sphere interactions that can arise electrostatically from ions sharing the same co-volumes of polarized solvent. This type of interaction can give rise only to a repulsive energy increasing with concentration. It is much more difficult to make a similar a priori calculation for the case where H-bonding structural

interactions predominate. However, by using the empirically evaluated Gurney "A_{ij}" free-energy or "E_{ij}" energy parameters for 3-dimensional interactions in the interphase at an electrode, some progress can be made. An outline of this approach is given below but unfortunately the full required data for ClO_4^- salts are not available.

(b) Evaluation of Co-sphere Overlap Effects from Empirical Gurney A_{ij} Parameters

The basis of this evaluation of hydration co-sphere interaction effects is the model shown in Fig. 38 where two solvated ions, i and j, upon close approach, e.g. due to increase of concentration (or here, ion accumulation at an interface in the double-layer), are regarded[98,99] as releasing a certain co-volume, V_c, of ion-influenced solvent to the bulk, with a resulting free energy change GUR_{ij} given[98,100] by

$$GUR_{ij} = A_{ij} V_{H_2O}^{-1} \quad V_c(r_i + r_{c,i}, r_j + r_{c,j}, r) \qquad (39)$$

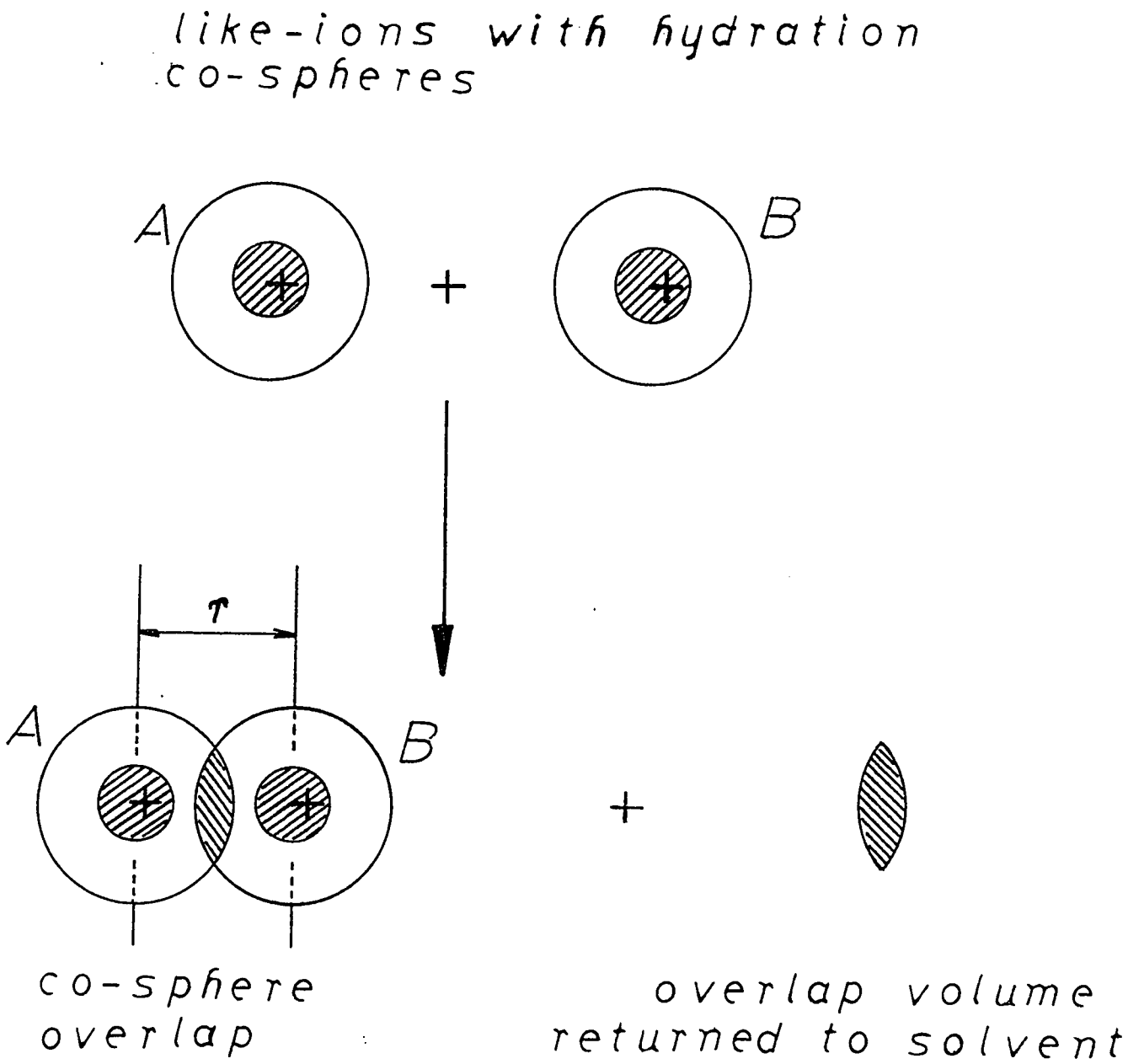

Fig. 38 Gurney hydration co-sphere overlap between ions in solution illustrating the volume of ion-influenced water returned to the bulk (after Ramanathan and Friedman[99]).

where $r_{c,i}$ or $r_{c,j}$ are the thicknesses of the co-spheres around ions i or j, and r_i and r_j are the ionic radii. V_c is the co-sphere volume arising when a solvated ion of radius $r_i + r_{c,i}$ approaches another ion of radius $r_j + r_{c,j}$ at a mean center-to-center distance of r and is a function of these parameters, as indicated in eqn. 39. The co-sphere thickness $r_{c,i}$ is often taken[98,99] for either cation or anion as the diameter of a water molecule* but, in reality, this quantity must be ion-specific[74],

---

*Overlap between co-spheres of ions at distances greater than $r_i + r_j + (2 \times 2.78\text{Å})$ has not been considered in present treatments[98,99] of electrolyte solutions since the co-sphere thickness is normally taken as the diameter of a water molecule (2.78Å). This probably underestimates the co-sphere thickness in relation to the important region of structure-modified water[90] beyond the primary hydration shells and certainly in relation to the region of non-specific, long-range Born polarization. The presently available systems of A_{ij} parameters are, however, based on a co-sphere thickness of 1 H_2O molecule diameter. A scheme of different values would be required if $r_{c,i}$ and $r_{c,j}$ were taken > 2.78Å.

depending on the strength and structural features[90] of the ion-solvent interactions. V_{H_2O} is the molar volume of solvent water and A_{ij} is the empirical Gurney parameter[95,98] assumed[98,99] independent of ionic concentration. The concentration dependence of GUR arises from that of V_c and of r. The overlap volume V_c is given geometrically by the formula for the volume of spherical segments:

$$V_c = \pi\left[-(a^2-b^2)^2/4r + \frac{2}{3}(a^3+b^3) - \frac{1}{2}r(a^2+b^2) + r^3/12\right] \quad (40)$$

where a and b are the co-sphere radii $r_i + r_{c,i}$ and $r_j + r_{c,j}$ of the two ions. For cation-cation interaction in the case of interest here, obviously a=b so that $V_c = \pi(\frac{4}{3}a^3 - ra^2 + r^3/12)$.

Some values of the A_{ij} parameters for various pairs of ions have been given from the calculations of Ramanathan and Friedman[99] for aqueous electrolyte solutions. The overlap volumes V_c are shown in Fig. 39 as a function of interionic separation r (=AB) expressed in terms of Γ or q through the following equation:

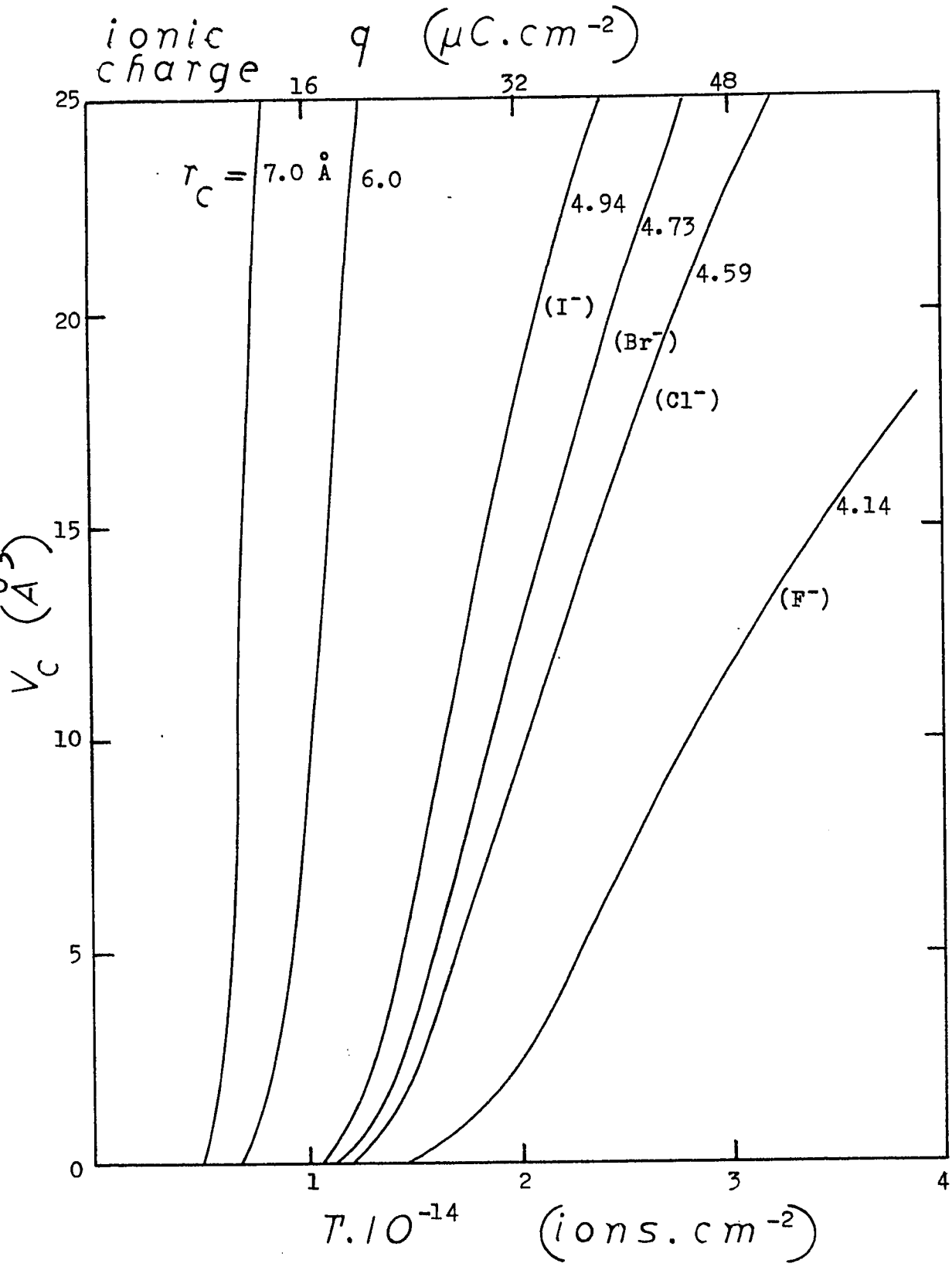

Fig. 39 Co-sphere overlap volumes, V_c as a function of interionic distance r for various values of the total co-sphere radius $r_i + r_{i,c}$, and as a function of surface ionic charge density q or surface excess Γ.

$$AB = (1/N_A\Gamma)^{\frac{1}{2}} = r \qquad (41)$$

where N_A is Avogadro's number.

Unfortunately, the set of data of Ramanathan and Friedman do not exhibit realistic or expected signs and trends for the do-sphere overlap energies for like anions where, e.g., the F^-/F^- hydration shell interaction would be expected to give a larger positive energy change than that for I^-/I^-. The problem with the A_{ij} data are that they are "catch-all" parameters which reflect not only hydration shell interaction energy but any errors in the evaluation of CAVity polarization[91] and CORE repulsion contributions to ionic interaction energy.

For the R_4N^+ ions in aq. solution, attractive cation-cation interactions arise which can be represented by data given by Streng and Wen[100]. These A_{ij} parameters (A_{++} for cations) can be used to estimate the (attractive) interaction effects that can arise in the double-layer (as in bulk

water solution) due to sharing of structure-enforced regions of the solvent about such cations.

The volume of the water molecule to be taken in eqn. 40 is ca. 30 $(\text{Å})^3$ so that an attractive energy of the order of -85 to -300 cal. mol^{-1} arises with increasing coverage of an electrode surface by R_4N^+ ions due to hydration shell sharing in the Gurney co-sphere. This energy adds[96,98] to the coulombic repulsion and Van der Waals attraction contributions[89]. Co-sphere "contact" for 1-H_2O thickness occurs at the following mean ionic charge densities in the double-layer for R_4N^+ ions: Me 13.1, Et 10.6, n-Pr 9.1 and n-Bu, 8.15 $\mu C.cm^{-2}$. Significant contacts will, of course, arise statistically below these limiting surface concentrations due to thermal motions and be determined by the two-dimensional pair (++) distribution function for cation-cation encounters.

Figs. 32 and 35 showed the experimentally determined standard free energies of adsorption of $(n\text{-Pr})_4N^+$ and $(n\text{-Pr})_3NH^+$ ions in excess (1M) $HClO_4$

from aqueous solution at Hg at 27°C as a function of surface excess Γ. The $-\Delta G^{o}$ values were shown to increase with increasing coverage, i.e., attractive interactions are predominant, and the effect is greater with the tetra than with the tri-n-propyl ammonium ion. Normally[89], coulombic ionic repulsions lead, in the first order approximation, to $-\Delta G^{o}$ decreasing with coverage. The $-\Delta G^{o}$ values actually increase by ca. 2.5 kcal $mole^{-1}$ which is of the correct order of magnitude for the quasi-attractive interaction effects which can evidently arise in this case (Fig. 35) due to the co-sphere overlap effects determined by the A_{ij} values. In Table 4 are shown free energy changes, GUR_{ij}, for $(n\text{-}Pr)_4N^+$, as calculated from eqn. 39 for $A_{++} = -0.12$ kcal mol^{-1}, $V_{H_2O} = 30$ $(\text{Å})^3$ and $r_c = 6.76$ Å (for 1 H_2O) for various surface excess values. Also tabulated are the relative experimental free energy values, $(\Delta G^{o}_{ads})_{\Gamma_i} - (\Delta G^{o}_{ads})_{\Gamma} = 0$, using plots shown in Fig. 35. The experimental relative free energy values and the calculated GUR_{++} values for $(n\text{-}Pr)_4N^+$ were plotted against the surface excess, Γ, as shown in Fig. 40.

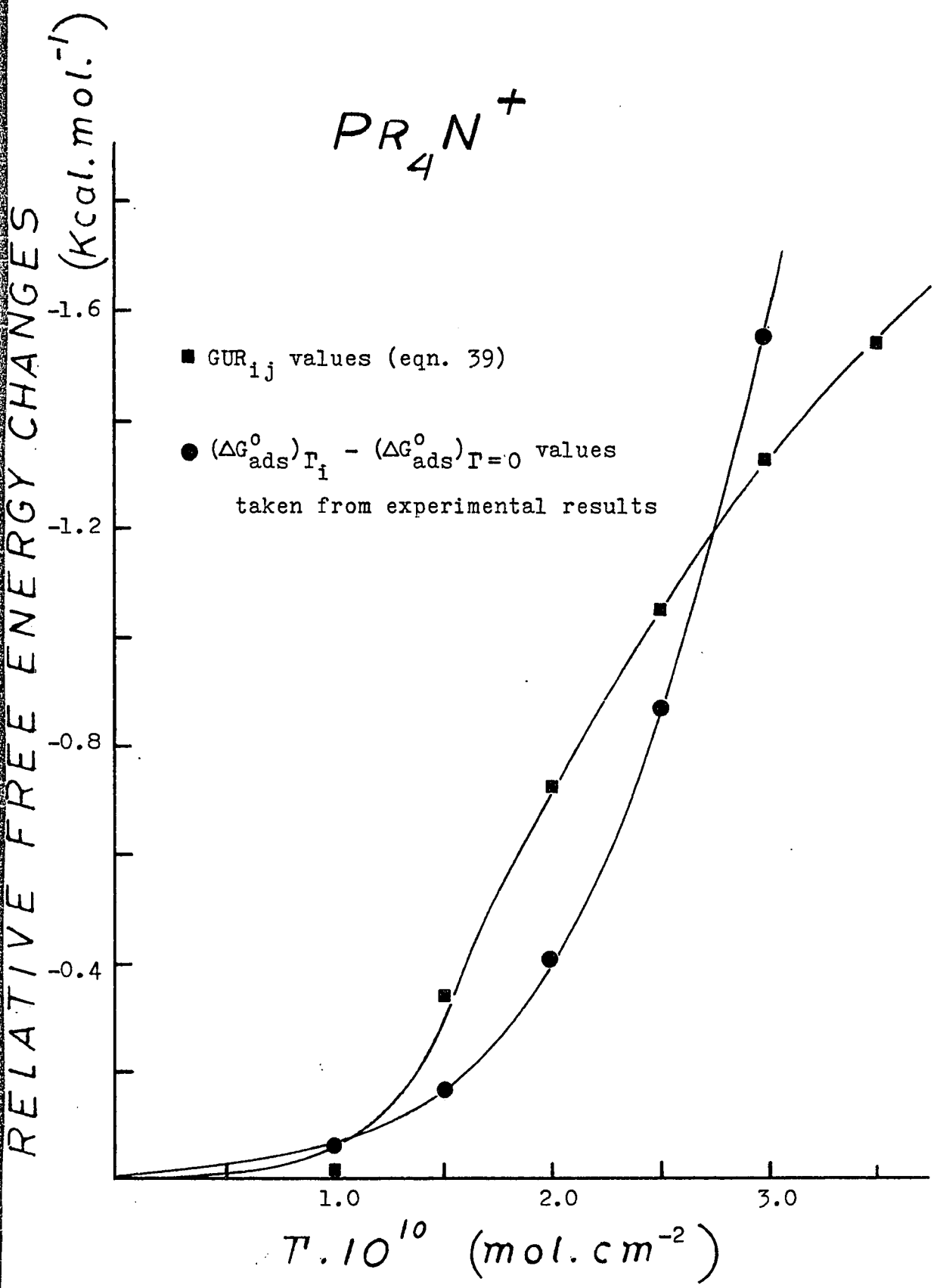

Fig. 40 Experimental free energy values and calculated Gurney free energy changes as a function of surface excess.

Quite good agreement with experiment is evidently obtained indicating that the co-sphere overlap effect is a major factor in the attractive interactions for this case. By contrast, for $(n\text{-}Pr)_3NH^+$, the effects are smaller owing to the greater hydrophilic character of this ion in comparison with $(n\text{-}Pr)_4N^+$, and the anticipated co-sphere repulsion contribution due to solvent polarization at the NH^+ centre. The coulombic repulsion effect will be almost the same at a given coverage (depending on the local dielectric properties of the interphase) and the Van der Waals interaction approximately 25% smaller.

Table 4

COMPARISON BETWEEN RELATIVE VALUES OF EXPERIMENTAL FREE ENERGIES OF ADSORPTION OF $(n\text{-}Pr)_4N^+$ AND CALCULATED GURNEY CO-SPHERE OVERLAP ENERGIES AT VARIOUS SURFACE CONCENTRATIONS

$\Gamma.10^{10}$ mol cm^{-2}	r Å	V_c (Å)^3	GUR_{++} Kcal mol^{-1}	ΔG^o_{ads} Kcal mol^{-1}
1.0	12.9	0.97	~0	-0.06
1.5	10.5	83.6	-0.33	-0.16
2.0	9.10	181.6	-0.72	-0.40
2.5	8.19	260	-1.04	-0.86
3.0	7.46	329	-1.32	-1.54
3.5	6.93	383	-1.53	-3.32

CLAIMS TO ORIGINAL RESEARCH

1. Electrochemical studies of adsorption of urea from its aqueous solution at the Hg electrode interface were made. This system provides an interesting aqueous "mixed solvent" for adsorption studies in relation to the special solution properties of urea in water.

2. Urea was found to adsorb in a predominantly perpendicular orientation to the mercury surface with its $\rangle C{=}O$ group oriented towards the solution. The experimental maximum surface excess value, Γ_m, corresponds fairly well with the value that can be calculated from Courtauld space-filling molecular models for this particular orientation.

3. The $(n\text{-}Pr)_3NH^+$ ion probably adsorbs in the "flat" orientation with its three alkyl chains straddled on the surface as indicated from the experimental Γ_m value.

4. The standard free energy of adsorption of the

alkylammonium ions varies with the number of carbon atoms (Traube's rule) for the series $(n\text{-}Pr)_n N^+H_{4-n}$ with n=1 to n=4. The decrease of free energy of adsorption per carbon atom is equal to about -170 cal. mol^{-1}, reflecting the increasing hydrophobicity in the series of ions as n is increased.

5. The variation of free energy of adsorption with coverage for each of the series of organic cations shows that attractive lateral interactions become predominant as $n \longrightarrow 4$ which is unexpected since repulsion (coulombic forces) between ions of the same sign would be the more expected behaviour. The anomalous behaviour is rationalized in terms of Gurney co-sphere interactions.

6. Co-sphere overlap effects were evaluated from empirical Gurney A_{ij} parameters for $(n\text{-}Pr)_4N^+$. Comparison between the relative experimental ΔG^o_{ads} values for $(n\text{-}Pr)_4N^+$ as a function of coverage and calculated Gurney co-sphere overlap energies at various surface concentrations showed that the co-sphere overlap effect is a major factor in the predominantly attractive interactions which are observed in this case. Solution

properties of organic ions can thus be usefully used in interpretations of the thermodynamics of their adsorption at the charged Hg electrode interface.

REFERENCES

1. H.L.F. Helmholtz, Ann. Physik., 7, 337 (1879).
2. G. Gouy, J. Phys., 9, 457 (1910); Compt. Rend., 149, 654 (1909).
3. G. Gouy, Ann. Phys., 7, 129 (1917).
4. D.L. Chapman, Phil. Mag., 25, 470 (1913).
5. O. Stern, Z. Electrochem., 30, 508 (1924).
6. D.C. Grahame, Chem. Rev., 41, 441 (1947).
7. G. Lippmann, Ann. Chim. Phys., 5, 494 (1875).
8. F.O. Koenig, Z. Physik. Chem., 154, 421, 454 (1931); 156, 38 (1931); 157, 96 (1931); J. Phys. Chem., 38, 111, 339 (1934).
9. A.N. Frumkin, Z. Phys. Chem., 116, 466 (1925).
10. A.N. Frumkin, Z. Physik., 35, 792 (1926).
11. J.A.V. Butler, Proc. Roy. Soc. (London), A113, 594 (1927); A122, 399 (1929).
12. R.J. Watts-Tobin, Phil. Mag., 6, 133 (1961).
13. N.F. Mott and R.J. Watts-Tobin, Electrochim. Acta, 4, 79 (1961).
14. N.F. Mott, R. Parsons and R.J. Watts-Tobin, Phil. Mag., 7, 483 (1962)
15. J.O'M. Bockris, M.A.V. Devanathan and K. Müller, Proc. Roy. Soc. (London), A274, 55 (1963).
16. B.B. Damaskin, O.A. Petrii and V.V. Batrakov, Adsorption of Organic Compounds on Electrodes, Plenum Press, New York, 1971.
17. C. Giomini and L. Rampazzo, J. Phys. Chem., 76, 707 (1972).
18. R. Parsons, J. Electroanal. Chem., 8, 93 (1964).
19. J. Lawrence and R. Parsons, J. Phys. Chem., 73, 3577 (1969).
20. R. Payne, J. Electrochem. Soc., 113, 999 (1966).
21. B.E. Conway and L.G.M. Gordon, J. Phys. Chem., 73, 3609 (1969).
22. B.E. Conway, H.P. Dhar and S. Gottesfeld, J. Colloid and Interface Science, Vol. 43, No. 2, 303 (1973).
23. D.C. Grahame and R.W. Whitney, J. Am. Chem. Soc., 64, 1548 (1942).
24. M. Proskurnin and A.N. Frumkin, Trans. Far. Soc., 31, 110 (1935).
25. B.E. Conway, Adv. Colloid and Interface Science, 8, (2,3), 91 (1977).
26. E. Bou Karam, Ph.D. thesis, Université des Sciences et Techniques du Languedoc, 1975.
27. R. Parsons, Pure and Appl. Chem., 18, 91 (1958).

28. I. Langmuir, J. Am. Chem. Soc., 38, 2221 (1916); 39, 1848 (1917).
29. A. Zhukovitskii, Acta Physicochem. URSS, 19, 176 (1944).
30. H.P. Dhar, B.E. Conway and K.M. Joshi, Electrochimica Acta, 18, 789 (1973).
31. S. Levine, R. Bell and M. Calvert, Can. J. Chem., 40, 518 (1962).
32. H. Wroblowa, J.O'M. Bockris and B. Piersma, J. Electroanal. Chem., 6, 401 (1963).
33. J.O'M. Bockris and D.A.J. Swinkells, J. Electrochem. Soc., 111, 736 (1964).
34. B.E. Conway and L.G.M. Gordon, J. Phys. Chem., 73, 3609 (1969).
35. J.O'M. Bockris and M. Habib, J. Electroanal. Chem., 65, 473 (1975).
36. D. Eisenberg and W. Kauzmann, The Structure and Properties of Water, Oxford at the Clarendon Press, 1969.
37. H.S. Frank and W.Y. Wen, Disc. Far. Soc., 24, 133 (1957).
38. G. Nemethy and H.A. Scheraga, J. Chem. Phys., 36, 3382 (1962).
39. B. Kamb, Structural Chemistry and Molecular Biology, Eds. A. Rich and N. Davidson, Freeman, San Francisco, 1968.
40. O.Y. Samoilov, Structure of Aqueous Electrolyte Solutions and the Hydration of Ions, Consultant Bureau, N.Y., 1965.
41. J.A. Pople, Proc. Roy. Soc. (London), A205, 163 (1951).
42. H.S. Frank, Science, 169, 635 (1970).
43. B.B. Damaskin and A.N. Frumkin, Electrochim. Acta, 19, 173 (1974).
44. R. Parsons, J. Electroanal. Chem., 59, 229 (1975).
45. B.E. Conway and H.P. Dhar, Croatica Chem. Acta, 45, 109 (1973).
46. A.N. Frumkin, Z. Physik Chem., 103, 55 (1923).
47. H.P. Dhar, Ph.D. thesis, Un. of Ottawa, 1973.
48. A.I. Popov and D.H. Geske, J. Am. Chem. Soc., 80, 1340, 5346 (1958).
49. W.P. Jencks, Catalysis in Chemistry and Enzymology, McGraw-Hill, N.Y., 1969.
50. J. Wyman, J. Am. Chem. Soc., 55, 4116 (1933).
51. D.V. Beauregard and R.E. Barrett, J. Chem. Phys., 49, 5241 (1962).
52. J.C. MacDonald, J. Serphillips and J.J. Guerrera, J. Phys. Chem., 77, 370 (1973).
53. E.G. Finer, F. Franks and M.J. Tait, J. Am. Chem. Soc., 94, 4424 (1972).
54. J.G. Mathieson and B.E. Conway, J. Solution Chem., 3, 781 (1974).

55. A.N. Frumkin, Ergebn. Exact. Naturwiss., 7, 258 (1928).
56. R. Parsons, Proc. Roy. Soc. (London), A79, 261 (1961).
57. F.W. Shapink, M. Oudeman, K.W. Leu and J.N. Helle, Trans. Far. Soc., 56, 415 (1960).
58. D.H. Everett and W.F.K. Wynne-Jones, Trans. Far. Soc., 35, 1383 (1939); Proc. Roy. Soc. (London), A177, 499 (1940).
59. R. Bennes and B.E. Conway, in course of publication.
60. D.N. Hume, Anal. Chem., 38, 261R (1966).
61. B. Kastening and L. Holleck, Talanta, 12, 1259 (1965).
62. C.N. Reilley and W. Stumm, In Progress in Polarography, Vol. 1, Edited by P. Zuman, Interscience Publishers Inc., New York, 1960, p. 241.
63. R.G. Barradas and P.G. Hamilton, Can. J. Chem., 43, 2468 (1965).
64. R.G. Barradas, P.G. Hamilton and B.E. Conway, Coll. Czech. Chem. Commun., 32, 1790 (1967).
65. R.G. Barradas and F.M. Kimmerle, J. Electroanal. Chem., 9, 483 (1965).
66. R.G. Barradas and F.M. Kimmerle, J. Electroanal. Chem., 11, 128 (1966).
67. R. Parsons, In Modern Aspects of Electrochemistry, Vol. 1, Edited by J.O'M. Bockris and B.E. Conway, Butterworths, London, 1954, Chap. 3, p. 103ff.
68. R.G. Barradas and F.M. Kimmerle, Can. J. Chem., 45, 109 (1967).
69. B.B. Damaskin, Russ. Chem. Rev., Engl. Trans., 30, 78 (1961).
70. F.M. Kimmerle, H. Ménard, B.E. Conway and H.P. Dhar, Electrochimica Acta, 19, 883 (1974).
71. N.K. Adam, Physics and Chemistry of Surfaces, 3rd ed., Oxford University Press, Oxford, 1941, p. 376.
72. P. Corbusier and L. Gierst, Anal. Chim. Acta, 15, 254 (1956).
73. S. Sathyanarayana, Indian J. Chem., 2, 474 (1964).
74. R.H. Stokes and R.A. Robinson, J. Am. Chem. Soc., 70, 1870 (1948).
75. I. Smoler, Electroanal. Chem. and Interfacial Electrochem., 51, 452 (1974).
76. H. Ménard and F.M. Kimmerle, Electroanal. Chem. and Interfacial Electrochem., 47, 375 (1973).
77. B.E. Conway and L.G.M. Gordon, J. Electroanal. Chem., 15, 7 (1967).

78. D.J.G. Ives and G.J. Janz, Reference Electrodes, Ch. 3, p. 133.
79. J.F. O'Donnell, J.T. Ayres and C.K. Mann, Anal. Chem., Vol. 37, 9, 1161 (1965).
80. M.A.V. Devanathan and P. Peries, Trans. Far. Soc., 50, 1236 (1954).
81. P. Champion, Ph.D. thesis, Univ. de Paris, p. 48, 1969.
82. D.J.G. Ives and G.J. Janz, Reference Electrodes, Ch. 4, p. 179.
83. D.C. Grahame, R.P. Larsen and M.A. Poth, J. Am. Chem. Soc., 71, 2975 (1949).
84. E. Verdier, R. Grand and P. Vanel, J. Chim. Phys., 66, 376 (1969).
85. R.H. Stokes, Austr. J. Chem., 20, 2087 (1967).
86. G.S. Hartley and C. Robinson, Trans. Far. Soc., 48, 847 (1952).
87. J. Lawrence, R. Parsons and R. Payne, J. Electroanal. Chem., 16, 193 (1968).
88. E. Blomgren and J.O'M. Bockris, J. Phys. Chem., 63, 1475 (1959).
89. B.E. Conway and R.G. Barradas, Electrochim. Acta., 5, 319 (1961); 5, 349 (1961).
90. H.S. Frank, Zeit. Phys. Chem., Leipzig, 228, 364 (1965).
91. F.P. Buff and F.H. Stillinger, J. Chem. Phys., 39, 1911 (1963).
92. B.E. Conway and E. Gileadi, Trans. Far. Soc., 58, 2493 (1962).
93. P. Champion, C. R. Acad. Sc. Paris, t. 269, 545 (1969).
94. P. Champion, C. R. Acad. Sc. Paris, t. 272, 987 (1971).
95. R.W. Gurney, Ionic Processes in Solution, Dover, N.Y., 1953.
96. B.E. Conway and H.P. Dhar, J. Coll. Interface Sci., 48, 73 (1974).
97. B.E. Conway, Elektrokhimiya, 12 (6), 822 (1977).
98. P.S. Ramanathan, C.V. Krishnan and H.L. Friedman, J. Solution Chem., 1, 237 (1972).
99. P.S. Ramanathan and H.L. Friedman, J. Chem. Phys., 54, 1086 (1971).
100. W.H. Streng and W.Y. Wen, J. Solution Chem., 3, 865 (1974).